

**CHARACTERIZATION OF SELECTED PHOTONIC  
MATERIALS AND SYSTEMS USING  
PHOTOACOUSTIC TECHNIQUE**



**ANNIETA PHILIP K.**

THESIS SUBMITTED  
IN PARTIAL FULFILMENT OF THE REQUIREMENTS  
FOR THE AWARD OF THE DEGREE OF  
**DOCTOR OF PHILOSOPHY**



INTERNATIONAL SCHOOL OF PHOTONICS  
COCHIN UNIVERSITY OF SCIENCE AND TECHNOLOGY  
KOCHI - 682 022, INDIA.

OCTOBER 2004

***Characterization of Selected Photonics Materials and Systems Using Photoacoustic technique***

Ph.D Thesis in the field of Photonics

**Author:**

Annieta Philip K.

Research Fellow, International School of Photonics,

Cochin University of Science & Technology,

Kochi – 682 022, India.

E – mail: [annietaphilip@yahoo.co.in](mailto:annietaphilip@yahoo.co.in)

**Permanent affiliation:**

Department of Physics, The Cochin College, Kochi-2, India.

**Research advisor:**

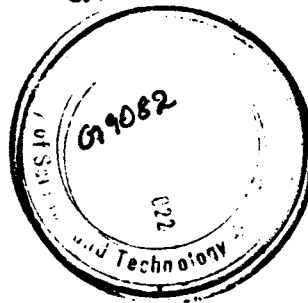
Dr. P. Radhakrishnan

Professor, International School of Photonics,

Cochin University of Science & Technology,

Kochi – 682 022, India.

E – mail: [radhak@cusat.ac.in](mailto:radhak@cusat.ac.in)



International School of Photonics,

Cochin University of Science & Technology,

Kochi – 682 022, India.

[www.photonics.cusat.edu](http://www.photonics.cusat.edu)

October 2004

R  
585.14  
ANN

## CERTIFICATE

Certified that the research work presented in the thesis entitled "*Characterization of Selected Photonic Materials and Systems using Photoacoustic Technique*" is based on the original work done by Mrs. Annieta PhilipK. under my guidance and supervision in the International School of Photonics, Cochin University of Science & Technology, Kochi 682 022 and has not been included in any other thesis submitted previously for the award of any degree.

Kochi  
29-10-2004



**Dr. P. Radhakrishnan**  
(Supervising Guide)  
International School of Photonics  
CUSAT

## DECLARATION

Certified that the work presented in the thesis entitled “*Characterization of Selected Photonic Materials and Systems using Photoacoustic Technique*” is based on the original work done by me under the guidance and supervision of Dr. P Radhakrishnan, Professor, International School of Photonics, Cochin University of Science & Technology, Kochi 682 022, India and has not been included in any other thesis submitted previously for award of any degree.

Kochi  
29 -10-2004

  
**Annieta Philip K.**

## Preface

Spectroscopy is the measurement and interpretation of absorption and emission of electromagnetic radiation when atoms or molecules or ions move from one energy level to another. Because of its versatility, range and non-destructive nature, optical spectroscopy remains a widely used and most important tool for investigating and characterizing the properties of matter. The photoacoustic (PA) effect originally discovered by Alexander Graham Bell in 1880 has been developed into an elegant, sensitive and nondestructive method for measuring the optical and thermal properties of materials due to the availability of coherent optical sources and advancement in signal processing and data acquisition systems. In the simplest terms laser photoacoustic spectroscopy (PAS) involves the absorption of light energy by a molecule or atom and the subsequent detection of heat energy released by the molecule upon return to the ground state where as in conventional optical absorption spectroscopy the optical absorption properties of the sample are studied by measuring the light transmitted by it. Since PAS measures the internal heating of the sample, it is clearly a form of calorimetry as well as a form of optical spectroscopy. The sensitivity of laser photoacoustic spectroscopy arises from the inherently high efficiency of thermal conversion that occurs in most of these light absorption processes coupled with the efficiency of the sensing device that converts the pressure waves into a voltage pulse. One of the great advantages of the PA measurements is that it is a direct monitoring of the non-radiative relaxation channel and therefore the PA technique may complement the absorption and luminescence spectroscopic techniques.

The basic physical process in the PA effect is that, a medium converts part of the intensity modulated light energy absorbed by it into heat. Such heat can be detected either by measuring the time dependent pressure fluctuations induced in a coupling gas or

by measuring the thermal stresses or strains in the absorbing medium. The pressure fluctuations can be detected using a microphone and the thermal stress can be detected using a piezoelectric transducer. The technique can be used to measure optical absorption coefficient in extremely wide range of frequencies, to get information on thermal properties of a material and as a tool for investigating nonradiative processes in matter. The sample can be in the form of gas, liquid or solid. It can be either bulk solid or in thin film form. The main advantage of this technique is that only a small volume of the sample is required and the detection mechanism is sensitive to weak absorptions.

In the studies reported here the gas microphone detection scheme is employed and the samples are mainly in the form of thin films. The thin film samples selected for investigations find several scientific and industrial applications.

The thesis is divided into seven chapters and the chapter-wise summary of the same is given below.

**Chapter 1** gives a general introduction to photothermal phenomena giving emphasis to photoacoustics. A review of the history of photoacoustics and the development of photoacoustic technique is given. The photoacoustic spectroscopy can be used in the investigation of optical and thermal properties of materials and for non-destructive testing. This chapter gives an idea of the various branches of science and technology where PA technique can be used for material characterization. A review of the work done by various researchers using PA technique is also presented.

The **second chapter** describes in detail the absorption of radiation by matter and the subsequent generation of photoacoustic signal in condensed matter. A general theory for the photoacoustic effect in condensed media was formulated by Rosencwaig and Gersho. Later on many improvements were made to the theory by McDonald and Wetzel and others. However, all such modifications are valid only in certain specific cases and these refinements have not changed the basic results of RG theory in most of the

experimental situations. The theoretical model of photoacoustic signal generation in condensed media formulated by Rosencwaig and Gersho (RG theory) is presented in this chapter.

**Chapter 3** deals with the PA studies on certain ceramic materials. Details of the experimental setup and the open photoacoustic cell used for the studies are discussed in this chapter. PA technique has been used for the thermal characterization of Silicon carbide, alumina-zirconia, zirconia, barium titanate, barium tin titanate, lead magnesium niobate titanate(PMNPT) and lead zirconate titanate(PZT) tapes. Significance and uses of the materials selected for investigations and the details of the tape casting process are discussed. Both reflection and transmission geometry have been used for the evaluation of thermal parameters of the sample and the experimental details are given. The thermal diffusivity, thermal conductivity, thermal capacity and effusivity of the ceramic tapes have been evaluated and the results are reported.

**Chapter 4** describes the use of laser induced photoacoustic technique in the study of photobleaching of Rhodamine 6G and Rhodamine B mixture doped in polymethyl methacrylate (PMMA). Dye mixtures find application as laser media. Thin films are prepared by incorporating Rhodamine 6G and Rhodamine B mixtures into polymethyl methacrylate matrix. Energy transfer from a donor molecule to an acceptor molecule in a dye mixture affects the output of the dye. Details of investigations on the role of laser power, concentration of the dye, modulation frequency and the irradiation wavelength on the photosensitivity of dye mixture film are presented in this chapter. Photosensitivity is found to change with changes in donor acceptor concentrations. Dye mixture doped PMMA samples are found to be more photosensitive when the dyes are mixed in same proportion.

**Chapter 5** deals with the non-destructive testing of multilayer coatings. Multilayer dielectric coatings are used as laser mirrors and antireflection coatings. PA

technique finds application as an effective tool for nondestructive testing of materials. The feasibility of the PA technique for the characterization of weakly absorbing samples like reflection coatings is demonstrated. Details of the PA cell developed and its calibration are also discussed. Sample can be directly mounted on the cell and from the measurement of PA signal amplitude and phase as a function of modulation frequency of the excitation source; thermal parameters of the sample can be evaluated. Details of the optical sources used and the actual experimental setup used for the PA measurements are given. Photoacoustic signal is found to be sensitive to the presence of a boundary in a layered structure. PA signal generation in highly reflecting multilayer structure is very complicated and hence calculation of thickness and thermal parameters from the PA signal data is not possible. Since phase of PA signal is sensitive to the presence of interphases, an attempt was made on depth profiling. The number of layers present in the multilayer stack and the defective structure present in it are clearly brought out. Through the detection of transmitted and absorbed radiation, reflectance of the film is calculated. The average reflectance value calculated from PA measurement is in close agreement with the value measured using conventional techniques. Experimental details and results are presented.

**Chapter 6** discusses the investigations carried out on cresyl violet (CV) incorporated in polymer film. Thin film samples are prepared by incorporating a laser dye- cresyl violet- into polyvinyl alcohol and gelatin matrices. Film preparation method and experimental details are presented in this chapter. Photostability of these samples are investigated using photoacoustic technique. Introductory studies are carried out on CV-gelatin film and detailed studies are carried out on CV-PVA film. Chopping frequency dependence of bleaching of cresyl violet in polyvinyl alcohol due to irradiation by laser light is investigated. The results indicate that photo degradation rates can be controlled by

adjusting the modulation frequency. The influences of dye concentration and laser power on photo degradation rate are also discussed.

**Chapter 7** gives general conclusions of the present investigations and future prospects of the work.

### **Papers published**

- Photoacoustic study of periodic dielectric multilayer stack. (*Int. J. Optoelectronics*, 8,4,493-499,1993)
- Photoacoustic study on bleaching of cresyl violet in polyvinyl alcohol by laser light. (*Int. J. Optoelectronics*, 8,4,501-503,1993)
- Monitoring the photoinduced bleaching of CV in PVA by PA technique. (*Spl. Issue of Optical Engineering*,. 33,6,1963,1994)
- Photoacoustic studies on multilayer dielectric coatings (*J. Physics D. Appl. Phys.*,836-838,1993)
- Photoacoustic studies on multilayer dielectric coatings (Reply to comment) (*J. Physics D, Appl. Phys.*,1387-1388,29(1996)

### **Conference Papers**

- Photoacoustic studies on bleaching of cresyl violet in gelatin by laser light, APSYM, CUSAT, Kochi, 1992
- Photoacoustic Studies on multilayer dielectric coatings, National symposium on Photonics and Integrated Optics, SAMEER, Mumbai,1992.
- Photoacoustic studies on bleaching of cresyl violet in polyvinyl alcohol by laser light, National laser symposium, IIT, Madras, 1993.

### **Papers communicated**

- Studies on Photostability of organic dye pairs in PMMA matrix using PA technique. (Communicated to PHOTONICS 2004)

## **Acknowledgements**

I express my gratitude and heartfelt thanks to Dr.P.Radhakrishnan for the supervision, guidance and support, without which I could not have completed this work.

I am grateful to Dr.C.P.Girijavallabhan for encouraging me through out the period of my research. His vast knowledge in all aspects of physics including electronic equipments was a real help to me.

I sincerely thank Dr.V.P.N.Nampoori for his valuable support and inspiration without which it would not have been possible for me to complete the research work.

I also thank Dr.V.M.Nandakumaran for his valuable suggestions and encouragement.

The moral support and encouragement rendered by Dr.Deepthy Menon was a great help. I thank her with all my heart.

Dr.Edwin Xavier, Dr.V.Vidyalal and Dr.K.Rajasree helped me a lot in the early stages of my work. I thank them for their support and encouragement. I acknowledge with gratitude the help and cooperation extended to me by all the research scholars of ISP. I am extremely thankful to my young friends Litty and Lyjo for their invaluable help and support during the final stages of my work. Without their help it would not have been possible for me to complete the work in time.

I convey my indebtedness and sincere thanks to Dr.Raghu Natarajan, Mr.Denny Alappat and Ms.Bindu Venu of CMET, Trichur for providing me with samples and its technical details at the right time.

I extend my sincere thanks to the non-teaching staff of ISP, USIC, staff of physics department and various libraries for their timely help and co-operation.

I extend my sincere thanks to the Principal and manager of The Cochin College, Kochi for their cooperation and help. I also thank the teaching and non-teaching staff of The Cochin College, especially those in the Physics department, whose support and encouragement helped me a lot.

Financial assistance from DST during the early stages of my work is gratefully acknowledged.

Thanks to Mr. Peter for converting this report to the book form.

I have no words to express my gratitude to my family whose encouragement and support helped me in the successful completion of this work. I bow my head to my mother, the real source of inspiration.

Superior to all, I bow my head before the power that controls everything and everybody, without whose blessings and mercy we cannot achieve anything in this world.

**Thanks to Almighty God.**

Annieta Philip K.

# Contents

## Chapter 1. INTRODUCTION

Abstract	1
1.1 Interaction of radiation with matter	2
1.2 Photothermal methods	4
1.3 Photoacoustic technique	8
1.4 Photonic materials	10
References	11

## Chapter 2. PHOTOACOUSTICS : GENERAL THEORY

Abstract	17
2.1 Introduction	18
2.2 Photoacoustic effect in condensed media	19
2.3 Rosencwaig-Gersho theory	19
2.3.1. Temperature distribution in the cell	23
2.3.2. Production of the acoustic signal	27
2.3.3. Special cases	
2.3.3.1. Optically transparent solids	30
2.3.3.2. Optically opaque solids	33
2.4 Heat transmission configuration	34
References	37

## Chapter 3. THERMAL CHARACTERIZATION OF CERAMIC TAPES

Abstract	39
3.1 Introduction	40
3.2 Ceramics	41
3.2.1 Ceramic processing	41
3.2.2 Tape casting	43

3.3 Significance of thermal parameters	
3.3.1 Thermal diffusivity	44
3.3.2 Thermal effusivity	45
3.4 Theoretical background	
3.4.1 Thermal diffusivity measurement	46
3.4.2 Thermal effusivity measurement	48
3.5 Experimental details	
3.5.1 Experimental setup	50
3.5.2 Open photoacoustic cell	51
3.5.3 Sample specifications	52
3.5.4 Thermal diffusivity measurements	53
3.5.5 Thermal effusivity measurements	55
3.6 Results and discussion	56
3.7 Conclusions	66
References	66

## **Chapter 4. PHOTOACOUSTIC STUDIES ON DYE MIXTURES**

Abstract	69
4.1 Introduction	70
4.2 Materials	
4.2.1 Rhodamine 6G-Rhodamine B systems	73
4.2.2 Preparation of dye-doped polymer samples	75
4.3 Experimental details	76
4.4 Results and discussions	78
4.5 Conclusions	89
References	90

**Chapter 5. PHOTOACOUSTIC MEASUREMENTS ON MULTILAYER DIELECTRIC SYSTEMS**

Abstract	93
5.1 Introduction	94
5.2 Theoretical background	95
5.3 Multilayer dielectric films	97
5.4 Design and fabrication of a photoacoustic cell	99
5.5 Experimental	102
5.6 Results and discussions	103
5.7 Conclusions	109
References	110

**Chapter 6. INVESTIGATIONS ON PHOTOBLEACHING OF CRESYL VIOLET IN POLYVINYL ALCOHOL**

Abstract	112
6.1 Introduction	113
6.2 Methods to measure dye photodegradation	115
6.3 Experimental details	
6.3.1. Preparation of the sample	117
6.3.1a. Cresyl violet dye	117
6.3.1b. Film deposition	118
6.3.2. Experimental setup used for the photoacoustic study	119
6.4 Results and discussions	121
6.5 Conclusions	126
References	127

**Chapter 7. SUMMARY AND CONCLUSIONS** 130

## *Chapter 1*

### **Introduction**

#### **Abstract**

This chapter gives a general introduction to the different processes resulting from light matter interaction. Different non-radiative relaxation processes that lead to photo-thermal phenomena in general, giving emphasis to photoacoustic effect, is discussed in detail. A review of the work done by various researchers and the applicability of photoacoustic technique for the characterization of photonic materials are also included.

## 1.1. Interaction of radiation with matter

Everything we know about light comes from its interaction with matter. As the radiation falls on matter, the electrical vector of radiation interacts with the atoms and molecules of the medium. The nature of interaction depends on the properties of the material. There are a number of processes by which radiation may interact with matter. Some of the phenomena that are likely to occur when electromagnetic radiation passes through matter are dispersion, reflection, refraction, scattering, absorption, polarization etc. The radiations passing through matter are not essentially completely absorbed and it is possible that some of them may pass into matter and undergo scattering or reflection. Sometimes the radiations are neither absorbed nor scattered. In such cases they only undergo changes in orientation or polarization. In some cases the excited molecules formed due to absorption do not de-excite quickly but lose the excess energy only after some time. In such cases, the energy is re-emitted in the form of electromagnetic radiations mostly of larger wavelength than the wavelength of the absorbed radiation. This happens in the case of fluorescence and phosphorescence. When the energy of the radiation corresponds to appropriate values they may be absorbed by matter, electronic, vibrational or rotational energy changes occur. Sometimes a combination of these changes may take place. The absorption of photons by atoms or molecules will result in a series of processes or effects in a material (1-6). When atoms or molecules absorb energy they go to excited states, which are unstable, and give out the excess energy quickly through radiative processes such as spontaneous emission and stimulated emission or through non-radiative relaxation processes. The non-radiative relaxation processes mainly

results in heat generation. Depending on the strength of the interacting electric field of the electromagnetic radiation, materials exhibit several linear and non-linear phenomena (7,8).

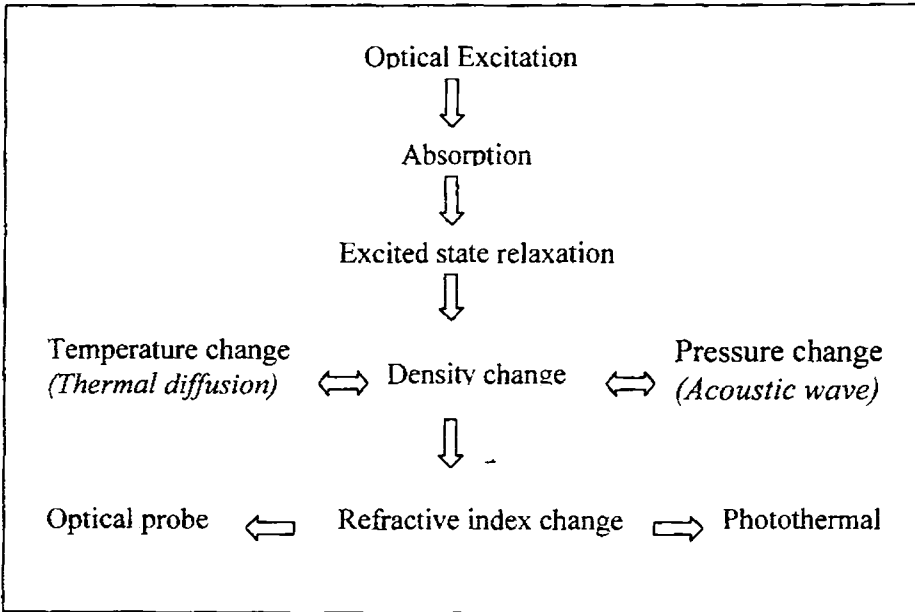


Figure 1. Basic processes responsible for the photothermal signal generation.

Destructive changes such as vaporization of the material and plasma generation may take place as a result of photon-matter interaction at very high power densities of the incident light (9-15). When the strength of interacting field is of the order of atomic field, materials show different nonlinear optical properties such as harmonic generation, hyper polarizability, higher order susceptibility etc.(16). If the photon energy is high enough, photochemical changes such as photo-decomposition, photo-ionization etc. may take place (17). Chemical changes may be irreversible or reversible. Measurement of the

energy absorbed or released through any of the relaxation channels facilitates the study of various properties and parameters of the sample. During the last two decades, many researchers have explored the non-radiative path of de-excitation of specimen after irradiating with a chopped optical radiation to investigate the thermal, optical, transport and structural properties of materials (18-30).

## **1.2. Photothermal methods**

Thermo optic spectroscopy is a branch of spectroscopy, which has been developed to study those materials that cannot be studied using conventional spectroscopic techniques. The peculiarity of this technique over the conventional spectroscopy is that even though the incident energy is in the form of photons, the interaction of these photons with the material is studied not through subsequent detection and analysis of photons, but through a direct measure of the energy absorbed by the material as a result of its interaction with the light beam. Direct consequence of the non-radiative relaxation is a change in temperature of the sample or the coupling fluid, which is in contact with the sample. If the temperature change occurs in a faster time scale than the time required for the fluid to expand, the rapid temperature change will result in a pressure change in the sample. The non-destructive or non-intrusive photothermal methods are based on the detection of a transient temperature change that characterizes the thermal waves generated in the sample after illumination with pulsed or chopped optical radiation.

Since absorption of electromagnetic radiation is required for the generation of photothermal signal, light that is scattered or transmitted is not

detected and hence does not interfere with the photothermal techniques. Another advantage is the capability of obtaining optical absorption spectra of materials that are completely opaque (31, 32). It is a photo-calorimetric method that measures how much of the electromagnetic radiation absorbed by a sample is converted into heat. It can be used to obtain the absorption or excitation spectrum, the lifetime of excited states and the energy yield of radiative processes. It can also be used to measure the thermal and elastic properties of materials, study chemical reactions, measure thickness of thin films and for non-destructive testing of materials (33-43). The magnitude of photothermal signal depends on the specific method used to detect the photothermal effect and on the type of the sample analyzed.

The common detection techniques that are employed in photothermal methods are shown in table.1 Even though all these techniques are based on the same principle, the detected parameter changes from one technique to other.

In photothermal calorimetry, the change in temperature of the sample due to non-radiative magnitude of the photothermal signal depends on the specific method used to relaxation processes is directly measured.(45-50).The temperature change is measured directly by monitoring the infrared emission and it can be used in situations where a large temperature change has occurred. This technique can be used for non-destructive testing and analysis of materials. Thermal imaging of samples can also be carried out using this technique. The major advantage of this technique is that remote sensing of the signal is possible and investigations can be carried out on samples of any shape.

Thermodynamic parameter	Measured property	Detection technique
Temperature	Temperature	Calorimetry
	Infrared emission	Photothermal radiometry
Pressure	Acoustic wave	Photoacoustic spectroscopy
Density	Refractive index	Photothermal lens Photothermal Interferometry Photothermal deflection Photothermal refraction Photothermal diffraction
	Surface deformation	Surface deflection
Pressure	Acoustic wave	Photoacoustic spectroscopy

Table 1. Common detection techniques used in photothermal spectroscopy.

In the photopyroelectric method (51-53), simultaneous measurement of different thermal parameters is possible. In this case a pyroelectric sensor is used. When thermal waves reach the pyroelectric sensor, it detects an electric current, which contains information about the structure, thermal and optical properties of the sample. Calibration of the detector is necessary for the accurate measurement of data.

The temperature change due to non-radiative de-excitation can produce changes in the volume and density of the specimen. Photothermal interferometry directly measures the refractive index changes through the

If the pressure change produced in the coupling gas due to the transient temperature change in the sample is measured, the detection scheme is known as opto-acoustic or photo-acoustic technique (68-70).

Two types of pumping mechanisms can be used for the excitation of the sample. They are the pulsed laser excitation and modulated continuous wave (cw) laser excitation. Pulsed excitation produces transient signals of large amplitude immediately after the excitation and it decays as the sample approaches thermal equilibrium through heat diffusion. Usually the transient signals last for few microseconds in gas phase and several milliseconds in condensed matter. By performing the transient waveform analysis, one can obtain a variety of sample properties. If the excitation is carried out using a periodically modulated cw laser, the signal will be periodic and its magnitude and phase will be functions of modulation frequency. The frequency dependent phase-shift information is essentially equivalent to that contained in the time dependent signal transients obtained from pulsed excitation.

### 1.3. Photoacoustic technique

The term opto-acoustics (OA) or photo-acoustics (PA) usually refers to the generation of acoustic waves by modulated optical radiation. In its broader sense, photoacoustics can mean the generation of acoustic waves or other thermo-elastic effects by any type of energetic radiation, including electromagnetic radiation from radio frequency to X-ray, electrons, protons, ions and other particles. Intensity modulation of the light source is a necessary requirement for the production of PA signal as it is the periodic heating and cooling of the sample, following absorption, which induces the measurable

acoustic signal. The absorbed optical energy, which ultimately causes the photoacoustic signal, is that fraction of the total absorbed energy, which is converted to heat via non-radiative de-excitation processes in the sample. It is Alexander Graham Bell who discovered the PA effect in 1880 (71). Later on many theories are developed by several others and the technique has been effectively used by many others in diverse areas of physics, chemistry and medicine (72-81). With the advent of high power lasers, sensitive detection schemes and data acquisition systems, the versatility of PA technique has paved way to several innovative experiments.

The PA generation can be classified as direct or indirect. In direct PA signal generation, the acoustic wave is produced in the sample whereas in the indirect PA signal generation, the acoustic wave is generated in the coupling medium adjacent to the sample. In the direct PA signal generation, acoustic wave generated due to transient temperature change is measured using a piezoelectric transducer kept in contact with the specimen. Since the volume expansion of solids and liquids is less than that of gases, microphone detection scheme is more sensitive for these types of samples. In the case of powdered sample or gels, the piezoelectric detection is not applicable. In such cases, the microphone detection scheme is used. The simple and elegant microphone version of the PA technique can measure a temperature rise of  $10^{-6}$  to  $10^{-5}$  °C . Different versions of microphone based photoacoustic technique are used for the characterization of condensed matter (83-85). Depending on the position of the microphone in the PA cell cavity, the PA technique can be employed in two configurations viz., reflection configuration and transmission configuration, details of which are given in later chapters. The transmission configuration is found to be more useful in evaluating the thermal properties of material (86). The disadvantage of the microphone version of the PA

technique is that the response time of the detector is limited by the transit time of the acoustic wave in the PA cell cavity and the low frequency response of the microphone.

#### 1.4. Photonic materials

The advent of advanced lasers has led to significant break-through in basic science and the emergence of key technologies. These serve as the foundation for the development of new photonic materials and devices, as well as novel concepts for storage, display, communication and sensing. Photonic materials are used for generation, guiding, amplification and switching of light. Semiconductors, dielectrics, organic dyes, ceramics etc. are the commonly used materials in photonics industry.

Some of the potential applications of nonlinear optics include quantum computing, quantum communications, quantum imaging, all-optical switching, optical power limiting, and nonlinear optical image processing. However, the implementation of these applications has historically been held back by the limited availability of materials with the required properties of large optical non-linearity combined with high optical transparency and high resistance to laser damage. Several strategies have traditionally been exploited in an attempt to create new materials with more desirable optical properties. These strategies include the synthesis of new chemical compounds with intrinsically large optical response and the creation of composite materials that can combine the desirable characteristics of two or more constituent materials to create a new material with tailored optical properties. Of particular interest is the hope of developing artificial materials and structures with optical properties fundamentally different from those of naturally occurring materials.

Nanocomposite materials are especially well suited for photonics applications because they can be constructed in such a manner as to produce enhanced nonlinear optical response. Some of these materials are formed by the random association constituents, whereas others are formed with deterministic properties through various fabrication methods. But, mere development of a new material with some specific features will not be sufficient for its effective use in any of the applications. A complete characterization of materials is necessary for a comparative study of different materials to identify the most appropriate one. Photonic materials, being directly related to the generation or detection of photons, optical techniques are the most suitable for their characterization. Because of the high sensitivity, photothermal methods can be effectively employed for the characterization of photonic materials.

## References

1. D.S.Kliger (Edit.), *Ultrasensitive laser spectroscopy*, (Academic Press, New York), (1983)
2. K.K.R.Mukherjee, *Fundamentals of photochemistry*, (New Age International Publishers, New Delhi) (1978)
3. J.D.Winefordner(Edit.), *Chemical Analysis: A series of monographs on analytical chemistry and its applications* (John Wiley & Sons, Inc.)(1996)
4. G.M.Hieftje, J.C.Travis and F.E.Lytle, *Lasers in chemical analysis*, (Humana: Clifton, New Jersey) (1981)
5. C.V.Bindu, *Studies on laser induced photothermal phenomena in selected organic compounds and fullerenes*, (Ph.D Thesis, Cochin University of Science and Technology)(1998)

6. *A.V.R.Kumar, Applications of laser induced photoacoustic effect for the study of gases and solids, (Ph.D Thesis, Cochin University of Science and Technology) (1992)*
7. *P.Sathy, Studies on two photon absorption in certain dyes using photoacoustic ad fluorescene technique (Ph.D Thesis, Cochin University of Science and Technology) (1994)*
8. *G.K.Varrier, Investigations on nonlinear and radiative properties of certain photonic materials (Ph.D Thesis, Cochin University of Science and Technology) (1998)*
9. *R.C.Issac, Evolution and dynamics of plasma generated from solid targets by strong laser field (Ph.D Thesis, Cochin University of Science and Technology) (1998)*
10. *S.S.Harilal, Optical emission diagnostics of laser induced plasma from carbon and  $YBa_2Cu_3O_7$  (Ph.D Thesis, Cochin University of Science and Technology) (1998)*
11. *J.D.Winefordner, S.G.Schulman and T.C.O'Haver, Luminescence spectroscopy in analytical chemistry (Wiley Interscience, New York), (1972).*
12. *P.Hess (Edit.), Photoacoustic, photothermal and photochemical processes in gases, (Springer-Verlag, Berlin) (1988).*
13. *S.E.Bialkoswski, Photothermal Spectroscopy Method Chemical Analysis (Wiley, New York) (1996).*
14. *G.Chen, Phys.Rev.B, 57, 14958 (1998)*
15. *A.Kurian, K.P.Unnikrishnan, S.D.George, P.Gopinath, V.P.N.Nampoori and C.P.G.Vallabhan, Spectrochemica Acta part A, 59, 487 (2003)*

16. K.P.Unnikrishnan, *Z Scan and degenerate four wave mixing studies in certain photonic materials (Ph.D Thesis, Cochin University of Science and Technology) (2003)*
17. A.Kurian, *Characterization of photonic materials using thermal lens technique, (Ph.D Thesis, Cochin University of Science and Technology) (2002)*
18. Sajan D George, P. Radhakrishnan, V. P. N. Nampoory and C. P. G. Vallabhan, *J. of Phys. D: Appl. Phys.* **36** (8), 990 (2003)
19. S. D George, S. Augustine, E. Mathai, P.Radhakrishnan, V. P. N. Nampoory and C. P. G. Vallabhan, *Phys. Stat. Sol. (a)* **196** (2) 384-389 (2003)
20. J. Ptruzzelo, J. Gaines, P. Van der Sluis, D. Olego and C. Ponzoni, *Appl. Phys. Lett.* **62**, 1496 (1993)
21. Albert Feldman and Naira M Valzeretti, *J. Res. Natl. Inst. Stand. Technol.* **130**, 107 (1998);
22. D. G. Chill, *J. Vac. Sci. Technol. A* **7**, 1259 (1990)
23. L. Hatta, *Int. J. Thermophysics* **11**, 293 (1990);
24. K. E Goodson and M. I. Flik, *Appl. Mech. Rev.* **47**, 101 (1994)
25. C. L. Tien and G. Chen, *J. Heat Transf.* **116**, 799 (1994)
26. I. Riech, P. Diaz and E. Marin *Phys.status.solidi (b)*, **220**, 305 (2000).
27. G. Chen and M. Naegu, *Appl. Phys. Lett.* **71**, 2761 (1997)
28. J. A. Sell (Edit), *Photothermal investigations of solids and fluids, (Academic Press, Boston) 1989.*
29. A. Mandelis Ed. *Photoacoustic and Thermal Wave Phenomena in Semiconductors, Elsevier Scientific, North-Holland, New York (1987)*
30. H. Vargas and L. C. M. Miranda "Photoacoustic and related photothermal techniques" *Phys.Rep.* **161**, 43 (1988).

- 
31. A.Fukuyama, T.Ikari, K.Maeda and K.Futagami, *Jpn.J.Appl.Phys. Part1*, **32**, 2567 (1993)
  32. A.Fukuyama, T.Ikari, K.Miyazaki, K.Maeda and K.Futagami, *Jpn.J.Appl.Phys.Suppl.* **31**, 20 (1992)
  33. J.A.Balderas lopez, A.Mandelis and J.A.Garcia, *J.Appl.Phys.*, **92**, 6 (2002)
  34. A.Fukuyama, Y.Akashi, K.Yoshino, K.Maeda and T.Ikari, *Phys.Rev.B*, **58**, 12868 (1998)
  35. W.Y.Zhou, S.S.Xie, S.F.Qian, G.Wang, L.X.Qian, D.S.Tang and Z.Q.Liu, *J.Phys. Chem. Of solids*, **61**, 1165 (2000)
  36. B.X.Shi, C.W.Ong and K.L.Tam, *J.Mater.Sci.*, **34**, 5169 (1999)
  37. Q.E.Khuen, W.Faubel and H.J.Ache, *J.de.Physique*, **4**(C7), 361(1994)
  38. Z.Bozoki, J.Sneider and A.Mikols, *Acoustica*, **82**, 118(1996)
  39. Z.D.Ristovski and M.D.Dramicanin, *Appl.Opt.*, **36**, 648(1997)
  40. M.Bertolotti, G.L.Likahou, A.Ferrari, V.Ralchenko, A.A.Smolin, E.Obrazsova, K.G.Korotoushenko, S.M.Pimenov and V.I.Konov, *J.Appl.Phys.*, **75**, 7795(1994)
  41. S.D.George, C.P.G.vallabhan, M.Heck, P.Radhakrishnan and V.P.N.Nampoori, *J. Non-destructive testing an devaluation*, **18**, 75(2002)
  42. A.Mandelis, *Non-destructive evaluation (PTR Prentice Hall, Englewood Cliffs, New jersey)*(1994)
  43. J.C.Krapez, *J.Appl.Phys.* **87**, 9 (2000)
  44. A.Mandelis and M.M.Zver, *J.Appl.Phys.*, **57**, 4421 (1985)
  45. C.W.Garland, *Thermochemica Acta*, **8**, 127(1985)
  46. I.Hatta, Y.Sasuga, R.Kato and A.Maesono, *Rev.Sci.Instru.*, **56**, 1643(1985)
  47. I.Hatta, *Pure and Applied Chem.*, **64**, 79(1992)
  48. R.Geer, T.Stobe, T.ptchford and C.C.huang, *Rev.Sci.Instru.*, **62**, 415(1991)

- 
49. *Christofides, A.Mandelis, A.Engel, M.Bison and G.Harling, Can.J.Phys., 69,317 (1991)*
  50. *A.Mandelis, J.Vanniasinkam, S.Budhudhu, A.Orthonos and M.Kokta, Phys.Rev.B, 48, 6808(1993)*
  51. *J.Shen and A.Mandelis, Rev.SciInstru., 66,4999(1995)*
  52. *J.Philip,R.Rajesh and P.S.Menon, Anal.Sci.,17,April(2001)*
  53. *D.Bicanic, M.Chirtoc, V.Tosa and P.torfs, Phys.Chem., 95, 766(1991)*
  54. *J.Stone, Appl.Opt., 12, 1828(1973)*
  55. *A.Hordvick, Appl.Opt.,16, 2827(1977)*
  56. *Y.Ohsuka and K.Itoh, Appl.Opt., 18, 219(1979)*
  57. *S.Ameri, E.A.Ash, V.Neuman and C.R.Petts, Electro.Lett.,17, 357(1981)*
  58. *L.C.M.Miranda, Appl.Opt., 22, 2882(1983)*
  59. *M.A.Olmstead, N.M.Amer, S.Kohn, D.Fournier and A.C.Boccara, Appl.Phys.A,32,141(1983)*
  60. *J.P.Gordon, R.C.C.Leite, R.S.moore, S.P.S.Portoand J.R.Whinery, J.Appl.Phys.,36,3(1965)*
  61. *S.O.Kanstad and P.E.Nordal, Can.Phys., 64, 1155(1986)*
  62. *M.L.Baesso, J.Shen and R.D.Snook, Chem.Phys.Lett., 197, 255 (1992)*
  63. *M.L.Baesso,A.C.Bento, A.A.Andrade, T.Catunda, E.Pecararo, L.A.O.Nunes, J.A.Sampaio and S.Agma, Phys.Rev.B, 57,10545 (1998)*
  64. *S.M.Lima, T.Catunda, R.Lebullenger, A.C.Hernandes, M.L.Baesso, A.C.Bento and L.C.M.Miranda, Phys.Rev.B, 60, 15173(1999)*
  65. *J.H.Rohling, A.M.F.Caldeira, J.R.D.Pereira, A.F.Rubira, A.N.Medina, A.C.Bento, M.L.Baesso and L.C.M.Miranda, J.Appl.Phys., 89, 2220(2001)*
  66. *A.C.Boccara,D.Fournierand J.Baloz, Apl.Phys.lett.,36,130(1980)*
  67. *R.Charpentier, F.Lepoutre, and L.Bertrand, J.Appl.Phys., 53, 608 (1982)*
  68. *N.F.Leite and L.C.M.Miranda, Rev.Sci.Instru., 63, 4398(1992)*

69. K.Yoshino, A.Fukuyama, H.Yokoyama, K.Meada, P.J.Fones, A.Yamada, S.Niki and T.Ikari, *This Solid Films*, **33**, 591(1995)
70. K.Song, H.Cha, J.Lee and I.A.Veselovskii, *Appl.Phys.B*, **61**, 547(1995)
71. A.G.Bell, *Am.J.Sci.*, **20**, 385 (1880)
72. A.G.Bell, *Philoss.Mag.*, **11**, 510(1881)
73. A.Rosencwaig, *Science*, **181**, 657 (1973)
74. A.Rosencwaig, *Phys.Today*, **29**, 23(1975)
75. A.Rosencwaig and A.Gersho, *J.Appl.Phys.*, **47**, 64(1975)
76. A.Rosencwaig, *Anal.Chem.*, **47**, 502(1975)
77. A.Rosencwaig, *Rev.Sci.Instru.*, **48**, 1133(1977)
78. A.Rosencwaig, *Opt.Comm.*, **7**, 305 (1973)
79. A.Rosencwaig, *Anal.Chem.*, **47**, 592(1975)
80. A.Rosencwaig, *Advances in Electronics and Electron Physics*, **46**(1978)
81. R.L.Thomas, *Anal.Sci.*, **17**, 1(2001)
82. W.Faubel, S.Heissler, U.Pyelland N.Ragozina, *Rev.Sci.Instrum.*, **74**, 491(2003)
83. S.S.Raman, V.P.N.Nampoore, C.P.G.Vallabhan, G.Ambadas and S.Sugunan, *Appl.Phys.lett.*, **67**, 2939(1995)
84. V.A.Aablikov and V.B.Sandomirski, *Phys.Stat.Solidi(a)*, **120**, 471,(1983)
85. N.A.George, V.P.N.Nampoore, P.Radhakrishnan and C.P.G.Vallabhan, *Opt.Engg.*, **41**, 251(2002)
86. L.F.Perondi and L.C.M.Miranda, *J.Appl.Phys.*, **62**, 2955(1987)

## *Chapter 2*

# **Photoacoustics : General Theory**

### **Abstract**

During the past decade, there has been substantial development in instrumentation and experimental methodologies related to photoacoustic technique mainly due to the availability of high-energy sources, sensitive detectors and equipment for data collection and processing. With its various spectroscopic and non-spectroscopic attributes, photoacoustics has already found many important applications in research and characterization of materials. The photoacoustic technique is based on strong theoretical background. Since the formulation of one-dimensional heat flow model by Rosencwaig and Gersho to explain the photoacoustic signal generation, a number of modifications and extended models have been reported. Eventhough several modifications are proposed, the basic result of Rosencwaig and Gersho (R-G) is valid for most of the experimental conditions. The R-G theory for reflection configuration and its extension to transmission configuration are presented in this chapter.

## 2.1. Introduction

One of the important photothermal phenomena, the photoacoustic effect was first observed in 1880 by Alexander Graham Bell (1). The term photoacoustic effect (PA) usually refers to the generation of acoustic waves by a sample as a result of interaction with modulated electromagnetic radiation. Eventhough the PA effect was discovered more than a century ago, Veingerov experimentally observed it in gaseous samples (2) only after the advent of microphones in 1938. Emergence of lasers in 60's gave a boost to the photoacoustic studies in gaseous samples. A general theoretical formulation for the photoacoustic effect in solids was given by Rosencwaig and Gersho in mid seventies (4) and is known as Rosencwaig-Gersho (RG) theory. Later on many scientists made modifications to the RG theory. Bennet and Forman (5) in 1976 and Aamodt et.al in 1977 (6) have modified the basic theoretical model by treating the acoustic wave transport in the gas using Navier-Stokes equations. McDonald and Wetsel (7) made modifications on the RG theory by taking into consideration the mechanical vibrations of the sample. Quimby (8) made additional changes to the theory by making use of the three-dimensional heat flow model. In 1982, Guli (9) formulated a theory based on thermo-elastic considerations in the sample. Eventhough several modifications were made and new theories were proposed, basic results of RG theory remains the same for most of the experimental conditions and the predictions of R-G theory have been experimentally verified by others (10-18).

---

## 2.2. Photoacoustic effect in condensed media

The photoacoustic technique is essentially a closed cavity detection of energy liberated by atoms or molecules through non-radiative de-excitation mechanism, subsequent to light absorption by a sample. When a solid sample placed inside an air-tight cavity is irradiated with a modulated optical radiation, the energy liberated through non-radiative channels will result in the generation of thermal waves within the sample. The thermal waves diffuse through the sample to the gas in the cavity and will produce periodic pressure fluctuations in the cavity. This pressure variation can be detected using a microphone kept inside the cavity. If the sample to be analysed is in gaseous form, then the sample itself can act as the source of signal generation and the acoustic coupler to the microphone. In order to investigate liquid samples, a piezoelectric transducer is used. The piezoelectric transducer kept in contact with the liquid sample will detect the acoustic pulse propagating through the medium.

## 2.3. Rosencwaig –Gersho Theory

Rosencwaig-Gersho (RG) theory is sufficient to describe the photoacoustic signal generation in condensed media. It is a one-dimensional analysis of the production and flow of heat from a sample on irradiation. The theory which is being presented is for the reflection ( front side illumination) configuration. According to this theory, for a gas-microphone detection scheme, the signal depends on the generation of acoustic pressure disturbance at the sample-gas interface, which in turn depends on the periodic temperature change at the gas-sample surface.

RG theory is formulated by considering the generation of photoacoustic signal in a simple configuration as in figure 1. The sample is considered to be in the form of a disc having diameter  $D$  and thickness  $l$  and it is mounted so that its back surface is against a poor thermal conductor of thickness  $l'$ . The length  $l'$  of the gas column in the cell is then given by  $l' = L - l - l''$ . It is also assumed that the gas and the backing material are not light absorbing.

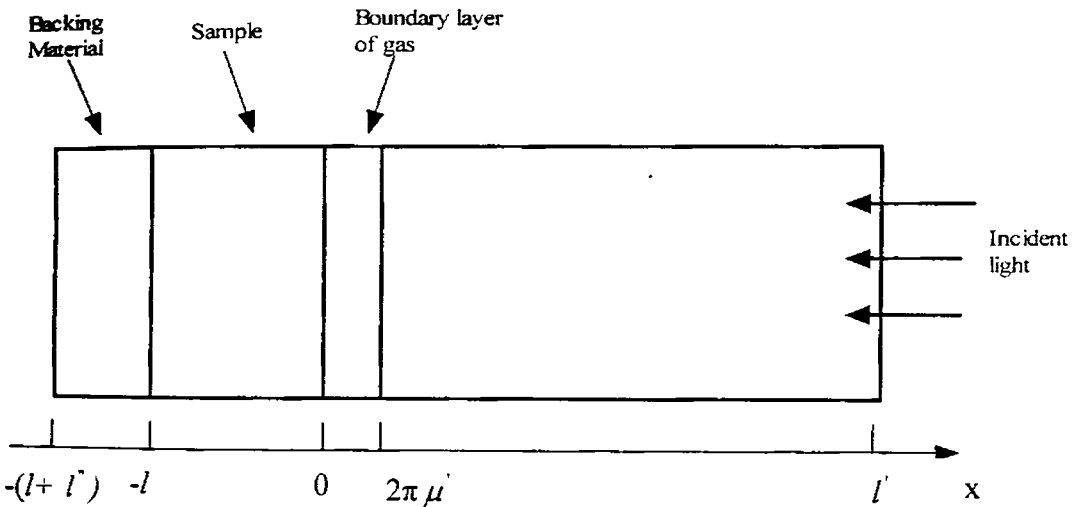


Figure 1. Schematic representation of the photoacoustic cell configuration

The parameters used in the theory are :

$\kappa$  : the thermal conductivity (cal/cm-sec- $^{\circ}$ C)

$\rho$  : the density (g/cm $^3$ )

$C$  : the specific heat (cal/g- $^{\circ}$ C)

$\alpha = \kappa / \rho C$  : the thermal diffusivity ( $\text{cm}^2/\text{sec}$ )

$a = (\omega/2 \alpha)^{1/2}$  : the thermal diffusion coefficient ( $\text{cm}^{-1}$ )

$\mu = \frac{1}{a}$  , the thermal diffusion length (cm)

$\omega = 2\pi f$  where 'f' denotes the chopping frequency of the incident light beam. Sample parameters are denoted by unprimed symbols, gas(air) parameters by singly primed symbols and backing material parameters by doubly primed symbols.

Assume a sinusoidally chopped monochromatic light source with wavelength  $\lambda$  incident on the solid with intensity

$$I = \left(\frac{1}{2}\right) I_0 (1 + \cos \omega t) \quad (1)$$

where  $I_0$  is the incident monochromatic light flux ( $\text{W}/\text{cm}^2$ ) and  $\beta$  denotes the optical absorption coefficient of the solid sample (in reciprocal centimeters) for the wavelength  $\lambda$ . The heat density produced at any point  $x$  due to light absorbed at that point in the solid is then given by

$$\frac{1}{2} \beta I_0 e^{\beta x} (1 + \cos \omega t) \quad (2)$$

where  $x$  takes on negative values since the solid extends from  $x = 0$  to  $x = -l$ , with the light incident at  $x = 0$ . The air column extends from  $x=0$  to  $x=l'$  and the backing material from  $x = -l$  to  $x = -(l+l')$ .

The thermal diffusion equation in the solid, taking into account the distributed heat source, can be written as

$$\frac{\partial^2 \theta}{\partial x^2} = \frac{1}{\alpha} \frac{\partial \theta}{\partial t} - A e^{\beta x} (1 + e^{i\omega t}) \quad \text{for } -l \leq x \leq 0 \quad (3)$$

with

$$A = \frac{\beta I_0 \eta}{2k} \quad (4)$$

where  $\theta$  is the temperature and  $\eta$  is the efficiency at which the absorbed light at wavelength  $\lambda$  is converted to heat by the nonradiative deexcitation processes. For most solids at room temperature,  $\eta = 1$ . For the backing and the gas, the heat diffusion equations are respectively given by

$$\frac{\partial^2 \theta}{\partial x^2} = \frac{1}{\alpha''} \frac{\partial \theta}{\partial t} \quad -l'' - l < x < -l \quad (5)$$

$$\frac{\partial^2 \theta}{\partial x^2} = \frac{1}{\alpha''} \frac{\partial \theta}{\partial t} \quad 0 < x < l \quad (6)$$

The real part of the complex valued solution  $\theta(x, t)$  of equations(3) –(6) represents the temperature in the cell relative to ambient temperature as a function of position and time. Thus the actual temperature field in the cell is given by

$$T(x, t) = \text{Re} \theta(x, t) + \varphi_0 \quad (7)$$

where Re denotes the “real part of ” and  $\varphi_0$  is the ambient (room) temperature.

To completely specify the solution of (3), (5), and (6), the appropriate boundary conditions are obtained from the requirement of temperature and heat flux continuity at the boundaries  $x=0$  and  $x=-l$ , and from the constraint that the temperature at the cell walls  $x=+l$  and  $x=-l-l''$  is at ambient. It is assumed that the dimensions of the cell are small enough to ignore convective heat flow in the gas at steady state conditions.

### 2.3.1. Temperature distribution in the cell

The general solution for  $\theta(x,t)$  in the cell, neglecting transients, can be written as

$$\theta(x,t) = \begin{cases} \frac{1}{l}(x+l+l'')W_0 + We^{\sigma''(x+l)}e^{i\omega t} & \dots\dots\dots 8(a) \\ b_1 + b_2x + b_3e^{\beta x} + (Ue^{-\sigma x} + Ve^{\sigma x} - Ee^{\beta x})e^{i\omega t} & \dots\dots\dots 8(b) \\ (1 - \frac{x}{l'})F + \theta_0 e^{-\sigma'x}e^{i\omega t} & \dots\dots\dots 8(c) \end{cases}$$

For 8(a),  $-l-l'' \leq x \leq -l$   
 For 8(b),  $-l \leq x \leq 0$   
 For 8(c),  $0 \leq x \leq l'$

where  $W, U, V, E,$  and  $\theta_0$  are complex valued constants,  $b_1, b_2, b_3, W_0,$  and  $F$  are real valued constants, and  $\sigma = (1+i) a$  with  $a = (\frac{\omega}{2\alpha})^{1/2}$ .  $\theta_0$  and  $W$  represent the complex amplitudes of the periodic temperatures at the sample – gas boundary ( $x = 0$ ) and the sample – backing boundary ( $x = -l$ ) respectively. The d.c. solution in the backing and air make use of the assumption that the temperature (relative to ambient) is zero at the ends of the cell. The quantities

$W_0$  and  $F$  denote the d.c components of the temperature (relative to ambient) at the sample surfaces  $x = -l$  and  $x = 0$  respectively. The quantities  $E$  and  $b_3$ , determined by the forcing function in (3), are given by

$$b_3 = \frac{-A}{\beta^2} \quad (9)$$

$$E = \frac{A}{\beta^2 - \sigma^2} = \frac{\beta I_0}{2k(\beta^2 - \sigma^2)} \quad (10)$$

Since for all frequencies of interest, the thermal diffusion length is small compared to the length of the material in both the gas and the backing, the growing exponential component of the solutions to the gas and backing material are omitted in the general solution (8). That is,  $\mu' < l'$  and  $\mu' < l'$ , and hence the sinusoidal components of these solutions are sufficiently damped so that they are effectively zero at the cell walls. Therefore, to satisfy the temperature constraint at the cell walls, the growing exponential components of the solutions would have coefficients that are essentially zero.

The temperature and flux continuity conditions at the sample surfaces are explicitly given by the following set of relations.

$$\theta'(0, t) = \theta(0, t)$$

$$\theta'(-l, t) = \theta(-l, t) \quad (11)$$

$$k' \frac{\partial \theta''}{\partial x}(0, t) = k \frac{\partial \theta}{\partial x}(0, t)$$

$$k' \frac{\partial \theta}{\partial X}(-l, t) = k \frac{\partial \theta}{\partial X}(-l, t)$$

These constraints apply separately to the d.c. component and to the sinusoidal component of the solution. From ( 11 ), the d.c components of the solution can be obtained as

$$F_0 = b_1 + b_3$$

$$W_0 = b_1 - b_2 l + b_3 e^{-\beta l} \quad (12)$$

$$\frac{-k'}{l''} f_0 = kb_2 + k\beta b_3$$

$$\frac{-k'}{l''} w_0 = kb_2 + k\beta b_3 e^{-\beta f}$$

These equations determine the coefficients  $b_1$ ,  $b_2$ ,  $b_3$ ,  $W_0$ , and  $F_0$  for the time-independent (d.c.) components of the solution. Applying (11) to the sinusoidal component of the solution yields:

$$\theta_0 = U + V - E$$

$$W = e^{-\sigma^1 U} + e^{\sigma^1 V} - e^{-\beta^1 E} \quad (13)$$

$$-k' \sigma' \theta_0 = k\sigma U - k\sigma V - k\beta E$$

$$k'' \sigma'' W = k\sigma e^{-\sigma^1 U} - k\sigma e^{\sigma^1 V} - k\beta e^{-\beta^1 E}$$

These quantities together with the expression for E in (10) determine the coefficients U, V, W, and  $\theta_0$ . Hence the solutions to (12) and (13) allow us to evaluate the temperature distribution (8) in the cell in terms of the optical, thermal, and geometric parameters of the system. The explicit solution of  $\theta_0$ , the complex amplitude of the periodic temperature at the solid-gas boundary ( $x = 0$ ) is given by

$$\theta_0 = \frac{\beta I_0}{2k(\beta^2 - \sigma^2)} \left[ \frac{(r-1)(b+1)e^{\sigma l} - (r+1)(b-1)e^{-\sigma l} + 2(b-r)e^{-\beta l}}{(g+1)(b+1)e^{\sigma l} - (g-1)(b-1)e^{-\sigma l}} \right] \quad (14)$$

where

$$b = \frac{k'' a''}{ka} \quad (15)$$

$$g = \frac{k' a'}{ka} \quad (16)$$

$$r = (1-i) \frac{\beta}{2a} \quad (17)$$

and  $\sigma = (1+i)a$ . Thus equation (14) can be evaluated for specific parameter values, yielding a complex number whose real and imaginary parts,  $\theta_1$  and  $\theta_2$  respectively determine the in-phase and quadrature components of the periodic temperature variation at the surface ( $x=0$ ) for the sample. The actual temperature at  $x = 0$  is given by

$$T(0,t) = \varphi_0 + F_0 + \theta_1 \cos \omega t - \theta_2 \sin \omega t \quad (18)$$

where  $\varphi_0$  is the ambient temperature at the cell walls and  $F_0$  is the increase in temperature due to the steady-state component of the absorbed heat.

### 2.3.2. Production of the acoustic signal

The main source of the acoustic signal arises from the periodic heat flow from the solid to the surrounding gas. The periodic diffusion process produces a periodic temperature variation in the gas as given by the sinusoidal (a. c.) component of the solution

$$\theta_{a.c.}(x,t) = \theta_0 e^{-\sigma' x} e^{i\omega t} \quad (19)$$

Taking the real part of (19), we see that the actual physical temperature variation in the gas is

$$T_{a.c.}(x,t) = e^{-a'x} \left[ \theta_1 \cos(\omega t - a'x) - \theta_2 \sin(\omega t - a'x) \right] \quad (20)$$

where  $\theta_1$  and  $\theta_2$  are the real and imaginary parts of  $\theta_0$ , given by (14). The time-dependent component of the temperature in the gas attenuates rapidly to zero with increasing distance from the surface of the solid. At a distance of

$\frac{2\pi}{a} = 2\pi\mu'$ , where  $\mu'$  is the thermal diffusion length in the gas, the periodic

temperature variation in the gas is effectively fully damped out. Thus we can define a boundary layer with thickness  $2\pi\mu'$  ( $\sim 0.1$  cm at  $\omega/2\pi = 100$  Hz) and maintain to a good approximation that only this thickness of air is capable of responding thermally to the periodic temperature at the surface of the sample.

The spatially averaged temperature of the gas within this boundary layer as a function of time can be determined by evaluating.

$$\bar{\theta}(t) = \frac{1}{2\pi\mu'} \int_0^{2\pi\mu'} \theta_{a.c}(x, t) dx \quad (21)$$

$$\bar{\theta}(t) = \frac{1}{2\sqrt{2\pi}} \theta_0 e^{i(\omega t - \pi/4)} \quad (22)$$

using the approximation  $e^{-2\pi} \ll 1$ .

Because of the periodic heating of the boundary layer, this layer of gas expands and contracts periodically and thus can be thought of as acting as an acoustic piston on the rest of the air column, producing an acoustic pressure signal that travels through the entire air column.

The displacement of this gas piston due to the periodic heating can be simply estimated by using ideal gas law,

$$\delta x(t) = 2\pi\mu' \frac{\bar{\theta}(t)}{T_0} = \frac{\theta_0 \mu'}{\sqrt{2} T_0} e^{i(\omega t - \pi/4)} \quad (23)$$

Here, the average d.c. temperature of the gas boundary layer, equal to the d.c. temperature at the solid surface is  $T_0 = \varphi_0 + F_0$ .

If it is assumed that the rest of the gas responds to the action of this piston adiabatically, then the acoustic pressure in the cell due to the displacement of this gas piston is derived from the adiabatic gas law

$$PV^\gamma = \text{constant} \quad (24)$$

where P is the pressure, V is the gas volume in the cell, and  $\gamma$  is the ratio of the specific heats. Thus the incremental pressure is

$$\delta p(t) = \frac{\gamma P_0}{V_0} \delta V = \frac{\gamma P_0}{l'} \delta x(t) \quad (25)$$

where  $P_0$  and  $V_0$  are the ambient pressure and volume, respectively, and  $-\delta V$  is the incremental volume. Then from ( 23 ),

$$\delta p(t) = Q e^{i(\omega t - \pi/4)} \tag{26}$$

where,

$$Q = \frac{\gamma P_0 \theta_0}{\sqrt{2l' a' T_0}} \tag{27}$$

Thus the actual physical pressure variation,  $\Delta p(t)$ , is given by the real part of  $\delta p(t)$  as

$$\Delta p(t) = Q_1 \cos(\omega t - \frac{\pi}{4}) - Q_2 \sin(\omega t - \frac{\pi}{4}) \tag{28}$$

or

$$\Delta p(t) = q \cos(\omega t - \psi - \frac{\pi}{4}) \tag{29}$$

where  $Q_1$  and  $Q_2$  are the real and imaginary parts of  $Q$ , and  $q$  and  $-\psi$  are the magnitude and phase of  $Q$ , that is,

$$Q = Q_1 + iQ_2 = q e^{-i\psi} \tag{30}$$

Thus  $Q$  specifies the complex envelope of the sinusoidal pressure variation.

Combining (14) and (27) we get the explicit formula (31),

$$Q = \frac{\beta l_0 \gamma P_0}{2\sqrt{2} T_0 k l' a' (\beta^2 - \sigma^2)} \times \left[ \frac{(r-1)(b+1)e^{\sigma t} - (r+1)(b-1)e^{-\sigma t} + 2(b-r)e^{-\beta t}}{(g+1)(b+1)e^{\sigma t} - (g-1)(b-1)e^{-\sigma t}} \right]$$

where  $b = \kappa'' a'' / \kappa a$ ,  $g = \kappa' a' / \kappa a$ ,  $r = (1-i)\beta/2a$ , and  $\sigma = (1+i)a$ . At ordinary temperatures  $T_0 \cong \varphi_0$  so that the d.c component of the temperature distribution need not be evaluated.

Equation (31) can be used to evaluate the magnitude and phase of the acoustic pressure wave produced in the cell by the photoacoustic effect. It is difficult to interpret the full expression for  $\Delta p(t)$  because of the complicated expression of  $Q$  as given by equation(31). Hence, some special cases, according to experimental conditions, have to be considered to get a clear physical insight. Different cases can be categorised according to the optical opaqueness of the solid. For each category of optical opaqueness, there are three different cases according to the relative magnitude of the thermal diffusion length  $\mu$ , as compared to the physical length  $l$  and the optical absorption length  $l_\beta = 1/\beta$  where  $\beta$  is the optical absorption coefficient. For all the cases, it is assumed that  $g < b$  and  $b \sim 1$ . *i.e.*,  $\kappa' a' < \kappa'' a''$  and  $\kappa a \approx \kappa'' a''$ . Depending on the experimental conditions, sample can be classified mainly into two groups. Samples are optically transparent when the absorption length exceeds the sample thickness and are optically opaque when the optical absorption length is less than the physical thickness. The sample can be again divided into two categories by considering its thermal properties. Samples are considered to be thermally thin when the thermal diffusion length exceeds the sample thickness and thermally thick when it is less than the sample thickness.

### 2.3.3 Special cases.

#### 2.3.3.1 Optically transparent solids ( $l_\beta > l$ )

When the sample is optically transparent, the light is absorbed through out the length of the sample, and some light is transmitted through the sample.

**Case 1(a): Thermally Thin Solids ( $\mu \gg l; \mu > l_\beta$ )**

Setting  $e^{-\beta l} \cong 1 - \beta l$ ,  $e^{\pm \sigma l} \cong 1$ , and  $|r| > 1$  in equation (31), we get

$$Q = \frac{Yl(\beta - 2ab - i\beta)}{2a' a'' \kappa''} \cong \frac{(1-i)\beta l}{2a'} \left( \frac{\mu''}{\kappa''} \right) Y \quad (32)$$

with

$$Y = \frac{\gamma^P I_o}{2\sqrt{2T_0} l'} \quad (33)$$

where  $\mu = \sqrt{2\alpha/\omega}$  and  $a = \frac{1}{\mu}$ . The acoustic signal is thus proportional to  $\beta l$

and has an  $\omega^{-1}$  dependence. Moreover, the signal is now determined by the thermal properties of the backing material.

**Case 1(b): Thermally Thin Solids ( $\mu > l; \mu \ll l_\beta$ )**

Setting  $e^{-\beta l} \cong 1 - \beta l$ ,  $e^{\pm \sigma l} \cong (1 \pm \sigma l)$ , and  $|r| < 1$  in equation (31) we get,

$$Q = \frac{\beta l Y}{4ka' a^3 b} [(\beta^2 + 2a^2) + i(\beta^2 - 2a^2)] Y \cong \frac{(1-i)\beta l}{2a'} \left( \frac{\mu''}{\kappa''} \right) Y \quad (34)$$

In this case also, the acoustic signal is proportional to  $\beta l$ , varies as  $\omega^{-1}$ , and depends on the thermal properties of the backing material. Equation (34) is identical to (32).

**Case 1(c) Thermally Thick Solids ( $\mu < l$ ;  $\mu \ll l_\beta$ )**

Setting  $e^{-\beta l} \cong 1 - \beta l$ ,  $e^{-\sigma l} \cong 0$ , and  $|r| \ll 1$  in equation (31), the acoustic signal becomes,

$$Q \cong -i \frac{\beta \mu}{2a'} \left(\frac{\mu}{k}\right) Y \quad (35)$$

Here, the signal is proportional to  $\beta\mu$  rather than  $\beta l$ . That is, only the light absorbed within the first thermal diffusion length contributes to the signal, in spite of the fact that light is being absorbed throughout the length  $l$  of the solid. Also, since  $\mu < l$ , the thermal properties of the backing material present in (32) are replaced by those of the sample and hence backing material does not have any contribution to the signal. The photoacoustic signal has a frequency dependence of  $\omega^{-3/2}$ .

Cases 1a, 1b, and 1c for the so-called optically transparent sample demonstrate a unique capability of photo acoustic spectroscopy, the capability of obtaining a depth profile of optical absorption within a sample. By starting at a high chopping frequency we can obtain optical absorption information from a layer of material near the surface of the solid. For materials with low thermal diffusivity this layer can be as small as  $0.1 \mu\text{m}$  at chopping frequencies of  $10,000 - 100,000 \text{ Hz}$ . Then by decreasing the chopping frequency, we increase the thermal diffusion length and obtain optical absorption data further within the material, until at  $\sim 5 \text{ Hz}$  we can obtain data down to  $10-100 \mu\text{m}$  for materials with low thermal diffusivities. This capability for depth-profile analysis is unique and opens up exciting possibilities in studying layered and amorphous materials and in determining thin film thicknesses.

### 2.3.3.2 Optically opaque solids ( $l_\beta \ll l$ )

In these cases, most of the light is absorbed within a distance that is small compared to  $l$ , and essentially no light is transmitted.

#### Case 2(a): Thermally thin Solids ( $\mu \gg l; \mu \gg l_\beta$ )

Setting  $e^{-\beta l} \cong 0, e^{\pm \sigma l} \cong 1$ , and  $|r| \gg 1$  in equation (31) we get,

$$Q \cong \frac{(1-i)}{2a'} \left( \frac{\mu''}{k''} \right) Y \quad (36)$$

Now the acoustic signal is independent of  $\beta$ , which is characteristic of a black absorber such as carbon black. The signal is  $1/\beta l$  times as strong as that in case 1(a) and depends on the thermal properties of the backing material. The signal varies as  $\omega^{-1}$ .

#### Case 2(b): Thermally thick solids ( $\mu < l; \mu > l_\beta$ )

Setting  $e^{-\beta l} \simeq 0, e^{\pm \sigma l} \simeq 0$ , and  $|r| > 1$  in equation (31), we get,

$$Q \simeq \frac{Y}{2a' ak\beta} (\beta - 2a - i\beta) \simeq \frac{(1-i)}{2a'} \left( \frac{\mu}{k} \right) Y \quad (37)$$

Equation (37) is analogous to (36), but the thermal parameters of the backing are now replaced by those of the sample. Again the acoustic signal is independent of  $\beta$  and varies as  $\omega^{-1}$ .

**Case 2(c): Thermally Thick Solids ( $\mu \ll l$ ;  $\mu \ll l_\beta$ )**

Setting  $e^{-\beta l} \approx e^{\sigma l} \approx 0$ , and  $|r| < 1$  in equation (31) we get,

$$Q = \frac{-i\beta Y}{4a'a^3k} (2a - \beta + i\beta) \approx \frac{-i\beta Y}{2a'} \left( \frac{\mu}{k} \right) Y \quad (38)$$

In this case, even though the solid is optically opaque ( $\beta l \ll l$ ), as long as  $\beta \mu \ll l$  (i.e.,  $\mu \ll l_\beta$ ), it is not photo-acoustically opaque. The light absorbed within the first thermal diffusion length  $\mu$  alone will contribute to the acoustic signal. Thus even though this solid is optically opaque, the photoacoustic signal is proportional to  $\beta$ . The signal is also dependent on the thermal properties of the sample and varies as  $\omega^{-3/2}$ .

The different cases discussed so far can be made use of in the photoacoustic study of any type of sample. One of the important predictions of the R-G theory is that the photoacoustic signal is always linearly proportional to the incident light intensity, irrespective of the sample properties and cell geometry.

**2.4. Heat transmission configuration**

The heat transmission (rear side illumination) geometry used in the open cell configuration is a modified form of conventional photoacoustic cell. In this configuration the sample is mounted on the cell leaving a small volume of air in between the sample and the microphone (18-33). The back surface of the sample is free and is open to the ambient. The sample is illuminated from the rear side and the microphone detects the pressure variation from the front

side. The major advantage of this configuration is that samples having large area can be studied, whereas in conventional PA cells sample size should be small enough to be enclosed within the cell cavity.

The R-G theory can be used to derive an expression for the periodic pressure variation produced in the air column inside the PA cell.

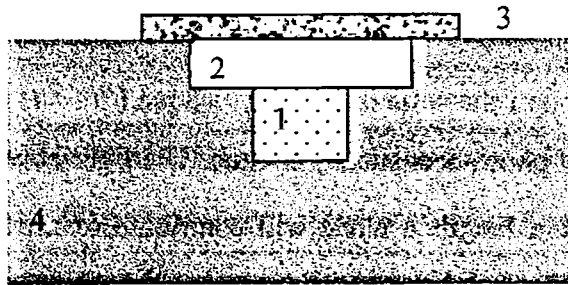


Figure2. General schematic representation of open photoacoustic cell (OPC)

1. Microphone 2. Air chamber 3. Sample 4. Cell body

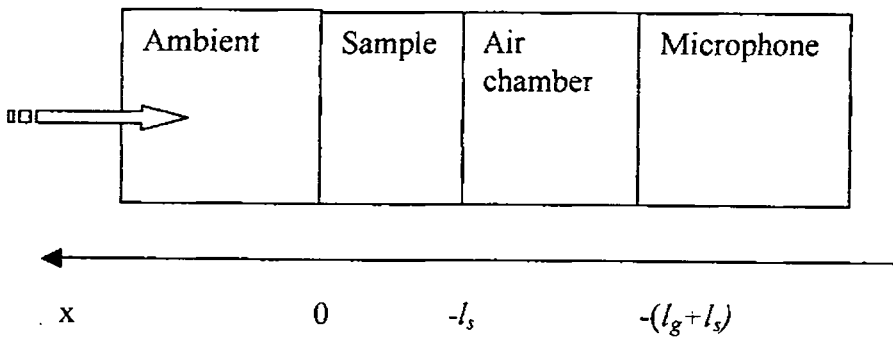


Figure 3. Schematic representation of the OPC geometry

Consider the OPC geometry as shown in figure 3. Assume that the sample is optically opaque and the incident energy is fully absorbed at the sample surface itself. Then according to R-G theory, we can show that the periodic pressure variation in the air chamber is given by,

$$Q = \frac{\gamma P_0 I_0 (\alpha_g \alpha_s)^{1/2} e^{j(\omega t - \pi/2)}}{2\pi T_0 l_g k_s f \sinh(l_s \sigma_s)} \quad (39)$$

Now, if the sample is thermally thin (*i.e.*,  $l_s \alpha_s \ll 1$ ), the equation (39) reduces to

$$Q \cong \frac{\gamma P_0 I_0 \alpha_g^{1/2} \alpha_s e^{j(\omega t - 3\pi/4)}}{(2\pi)^{3/2} T_0 l_g l_s k_s f^{3/2}} \quad (40)$$

Here, the amplitude of the PA signal varies as  $f^{-3/2}$ . At high chopping frequencies, sample is thermally thick (*i.e.*,  $l_s \alpha_s \gg 1$ ) and the pressure variation in the air chamber is given by,

$$Q \cong \frac{\gamma P_0 I_0 (\alpha_g \alpha_s)^{1/2} e^{-l_s \sqrt{\pi f / \alpha_s}}}{\pi T_0 l_g k_s f} e^{j(\omega t - \pi/2 - l_s \alpha_s)} \quad (41)$$

For a thermally thick sample, the amplitude of the OPC signal varies exponentially with the modulation frequency as  $\left(\frac{1}{f}\right) \exp(-b\sqrt{f})$ , where

$b = l_s \sqrt{\frac{\pi}{\alpha_s}}$  and the phase decreases linearly with  $\sqrt{f}$  with a slope of  $b$ .

Hence, the thermal diffusivity  $\alpha_s$  of the sample can be easily evaluated either from the signal amplitude plot or from the phase plot. However, a necessary

condition to employ the OPC configuration is that the sample should be optically opaque at the incident wavelength.

Investigations discussed in the subsequent chapters are based on the theoretical models described in this chapter.

## References

1. A.G.Bell, *Am.J.Sci.*, **20**, 305 (1880)
2. M.L.Veingorov, *Dokl. Akad. NaukSSSR*, **19**, 687(1938)
3. A.G.Bell, *Philos. Mag.*, **11**, 510 (1881)
4. A.Rosencwaig and A. Gersho, *J.Appl.Phys.*, **47**, 64,(1976)
5. H.S.Bennet and R.A.Forman, *Appl.Opt.*, **15**, 2405 (1976)
6. L.C.Aamodt, J.C.Murphy and J.G.Parker, *J.Appl.Phys.*, **48**, 927 (1977)
7. F.A. McDonald and G.C.Wetsel, *J.Appl.Phys.*, **49**, 2313 (1978)
8. A.Rosencwaig , *Photoacoustics and photoacoustic spectroscopy*, ( John Wiley 7 Sons, New York) (1980)
9. R.S.Quimby and W.m.yen, *Appl.Phys.lett.*, **95**, 43 (1979).
10. Guli, *Appl.Opt.*, **5**, 955 (1982)
11. S.K.Vikram Singhe, R.C.Bray, V.Gipson, C.F.Quate and H.R.Saludo, *Appl.Phys.Lett.*, **33**, 923 (1978)
12. A.Rosencwaig and G.Busse, *Appl.Phys.Lett.*, **36**, 725 (1980)
13. A.Rosencwaig and A. Gersho, *science*, **190**,556 (1975)
14. M.J.Adams, G.F.Kirkbright and K.R.Menon, *Anl.Chem.* **51**, 508(1979)
15. J.F.McClrell and R.N.Knisely, *Appl.Phys.Lett.*, **28**, 467 (1976)
16. G.C.Wetsel and F.A. McDonald, *Appl.Phys.lett.*, **30**, 252(1977)
17. E.M.Monahan Jr. and A.W.Nolle, *J.Appl.Phys.*, **48**, 3519(1977)

18. S.O.Kanstad and P.E.Nordal, *Opt.Comm.*, **26**, 367 (1978)
19. L.F.Perondi and L.C.M.Miranda, *J.Appl.Phys.*, **62**, 2955 (1987)
20. M.V.Marquezini, N.Cell, A.M.mansanares, H.Vergas and L.C.M.Miranda, *Meas. Sci.Technol.*, **2**, 396 (1991)
21. A.P.Neto, H.Vergas, N.F.Leote and L.C.M.Miranda, *Phys.Rev.B*, **40**, 3924 (1989)
22. A.P.Neto, H.Vergas, N.F.Leote and L.C.M.Miranda, *Phys.Rev.B*, **41**, 9971 (1990)
23. A.M.Mansanares, H.Vergas, F. Galembeck, J.Buijjs and D.Bicanic, *J.Appl.Phys.*, **70**, 7046 (1991)
24. P.M.Nikolic, D.M.Trodorovic, A.J.Bojicic, K.T.Radulovic, D.Urosevic, J.Elzar, V.Bлагоjevic, P.Mihajlovic and M.Miletic, *J.Phys;Condens.Matter*, **8**, 5673, (1996)
25. C.G.Segundo, M.V.Muniz and S.Muhl, *J.Phys.D :Appl.Phys.*, **31**, 165, (1998)
26. E.Marin, H.Vergas, P.Diaz and I.Riech, *Phys.Stat. Sol(a)*, **179**, 387 (2000)
27. O.D.Vasallo, A.C.Valdes, E.Merin, J.A.P.lima, M.G.Silva, M.Sthel, H.Vergas and S.L.Cardoso, *meas.Sci.Technol.*, **11**, 412 (2000)
28. O.D.Vasallo and E.Merin, *J.Phys.D:Appl.Phys.*, **32**, 593 (2000)
29. Qing Shen and Taro Toyoda, *Jpn.J.Appl.Phys.*, **39**, 511 (2000)
30. N.A.George, *Smart.Mater.Struct.* **11**, 561 (2002)
31. N.A.George, C.P.G.Vallabhan, V.P.N.Nampoori, A.K.George and P.Radhakrishnan, *Appl.Phys.B*, **73**, 145 (2001)
32. N.A.George, C.P.G.Vallabhan, V.P.N.Nampoori, A.K.George and P.Radhakrishnan, *Opt.Eng.*, **40**, 1343 (2001)
33. S.D.George, P.Radhakrishnan, V.P.N.Nampoori and C.P.G.Vallabhan, *Phys.Rev.B*, **68**, 165319 (2003)

## *Chapter 3*

### **Thermal characterization of ceramic tapes**

#### **Abstract**

Thermal characterization of ceramic tapes is presented in this chapter. The evaluation is carried out using photoacoustic technique. Transmission mode geometry is employed for the measurement of thermal diffusivity and reflection mode geometry is used for the measurement of thermal effusivity. In both these geometries, same open photoacoustic cell is used. From the measured values of thermal diffusivity and thermal effusivity, thermal conductivity value has also been evaluated. Investigations carried out on seven different materials and the results obtained are presented.

---

### 3.1. Introduction

During the last decade, several methods have been developed for the non-destructive characterization of thermal, optical and structural properties of materials (1-8). The laser induced photoacoustic (PA) method has gained more popularity due to its simple, elegant experimental scheme as well as due to its versatility in employing different configurations to measure the required thermo-physical parameters with great accuracy (9-11). The principle of the effect is that a sample in a closed cell illuminated by modulated light at audio frequencies produces an acoustic signal.

Photoacoustic technique has been made use of by many scientists for the measurement of thermal parameters of thin films and solid samples (12-21). In the heat transmission configuration of PA cell geometry, when the sample is illuminated with the chopped light beam, heat oscillations generated at the illuminated surface, facing the ambient, propagate through the sample to the sample-air boundary in the microphone chamber of the cell. Pressure oscillations of the same frequency are induced in the air chamber by the temperature variations at the surface interface between the sample and the air and a microphone can detect them. The photoacoustic signals obtained have a certain phase shift relative to the signal detected in the case of reflection geometry. Since the phase shift of the signal does not depend on the optical properties of the sample, it is simpler to extract information on the thermal diffusivity from the experimental results. Phase measurements are most suitable for determining the thermal parameters of the material.

Ceramics are considered to be one of the most suitable components for the fabrication of many of the devices used in electronic and optoelectronic

---

industry. In the case of ceramics, thermal accumulation causes thermally induced stresses in the sample, which in turn causes failure and deterioration in ceramic-based devices. Since ceramic tapes are used for microelectronic device fabrication, a thorough knowledge of the thermal parameters is essential.

## **3.2. Ceramics**

Ceramics, one of the three major material families, are crystalline compounds of metallic and nonmetallic elements. The ceramic family is large and varied, and includes such materials as refractories, glass, brick, cement and plaster, abrasives, ferroelectrics, ferrites, dielectric insulators etc (22, 23). Eventhough ceramics are crystalline materials like metals, they have little or essentially no electrical conductivity at room temperature because of fewer free electrons. They have high stability and, on an average, higher melting points and greater chemical resistance than metals and organic materials. These materials typically exhibit excellent corrosion resistance, high hardness, good wear resistance and low thermal conductivity. Ceramic materials find applications in electronics and optical hardware. They are used as substrates for fiber optic waveguides in integrated optics and for the manufacture of components in microelectronics.

### **3.2.1. Ceramic processing**

Ceramic processing is the sequence of operations that purposely and systematically change the chemical and physical aspects of the structure. The processing commonly begins with one or more ceramic materials, liquids, and special additives called processing aids (24). The forming technique used will

depend on the consistency (slurry, paste, plastic body or granular material) of the system and will produce a particular un-fired shape with a particular composition and microstructure. The finished material is then commonly heat-treated to produce a sintered microstructure. The sintered product may have a single component or a multicomponent composite structure.

In processing ceramic materials, several processing additives must be incorporated in a batch to produce the flow behavior and properties requisite for forming. Although most of these substances are added in relatively small amounts and some may be eliminated at a later stage of processing and do not appear in the final product, they are essential materials for processing. Polymer molecules and coagulated colloidal particles that are absorbed and bridge between ceramic particles may provide inter-particle flocculation, and are commonly called flocculants or binders. In condensed systems, such as cast bodies and unfired ceramic coatings, the binder may improve the plasticity green strength. Different types of binders are needed for different processes. In tape casting it is necessary for the binder to be a film former as it comes out of solution. Decomposition of the binder during firing commonly produces gas and pores, which are eliminated during sintering to obtain dense ceramic. In addition to the binders, a plasticizer is also added to modify the viscoelastic properties of a condensed binder-phase film on the particles. Binders used in ceramic processing must be plasticized to produce a moldable composition. Casting processes are used to produce a self-supporting shape called a cast from specially formulated slurry. Tape casting process is employed for the preparation of thin ceramic tiles that are used in the fabrication of microelectronic components.

### 3.2.2. Tape casting

Doctor-blade processing or tape casting is a specialized method of producing thin, flat uniform strip, which can subsequently be cut into rectangular tiles. This process is a low cost process for the manufacture of large areas of thin ceramic sheets of controlled thickness and high quality (25-28). In this process inorganic powders are mixed with a solvent and dispersant in a ball mill. A binder and plasticizer are added to the suspension in a second milling step. The homogeneous, well-dispersed and concentrated slurry is degassed and spread on a flat moving carrier surface using the doctor blade process. A thin sheet of high uniformity is formed. The solvents are evaporated leaving the dried tape with sufficient strength and flexibility to be cut to the proper shape.

The thickness of the tape is a function of the height of the blade, the viscosity of the slurry, the speed of the carrier film and the drying shrinkage. The casting speed is dependent on the thickness of the tape, the evaporation rate and the length of the machine, all of which control the drying time. In the first stage of the firing process the binder and other organic additives are burned out carefully and the resulting inorganic structure is sintered at higher temperatures to a dense thin ceramic product with the desired properties. Green sheets can be laminated to create multilayer systems that are transformed to a monolithic structure by firing. The method is used almost exclusively for the production of thin electronic substrates where the control of surface finish and flatness is of overriding importance (29, 30). These include multilayer ceramic electronic packaging, multiyear titanate capacitors, piezoelectric devices, thick and thin insulators, ferrite memories and catalyst supports. In producing

---

electronic packaging, metal circuit patterns and film resistors are commonly printed on the green sheet and co-fired.

### 3.3 Significance of thermal parameters

#### 3.3.1 Thermal diffusivity

Centuries before, Jean Fourier (1768-1830) derived a basic law defining the propagation of heat in a one-dimensional homogeneous solid as (31-33)

$$\frac{\partial Q}{\partial t} = -kA \frac{\partial T}{\partial x} \quad (1)$$

The above equation is known as Fourier equation. Equation (1) implies that the quantity of heat  $dQ$  conducted in the x-direction of a uniform solid in time  $dt$  is equal to the product of the conducting area  $A$  normal to the flow path, the temperature gradient  $dT/dx$  along this path, and the thermal conductivity  $k$  of the conducting material. Formal definition of thermal diffusivity arises when deriving an expression for a transient temperature field in a conducting solid from the Fourier equation. The equation describing the temperature field in a homogeneous, linear conducting solid with no internal heat source is,

$$\nabla^2 T = \frac{1}{\alpha} \frac{\partial T}{\partial t} \quad (2)$$

where the thermal diffusivity  $\alpha$  is given by

$$\alpha = \frac{k}{\rho C} \quad (3)$$

---

where  $k$  is the thermal conductivity,  $\rho$  is the density and  $C$  is the specific heat capacity of the material. The thermal diffusivity  $\alpha$  is usually expressed in  $\text{m}^2/\text{s}$ . Thermal diffusivity is thus an important thermo physical parameter, which essentially determines the diffusion of heat through a sample. The inverse of thermal diffusivity is a measure of time required to establish thermal equilibrium in a system for which a transient temperature change has occurred (34, 35).

### 3.3.2. Thermal effusivity

Another important and unique thermal parameter, thermal effusivity, measures the thermal impedance of the material. It is the ability of the sample to exchange heat with the environment and hence it is an important parameter for surface heating and cooling processes. The major difference between thermal diffusivity and thermal effusivity is that diffusivity is a bulk property of the sample where as the effusivity is a surface property. The thermal effusivity is defined as  $e_s = \sqrt{k\rho C}$  with dimension  $\text{W s}^{1/2} \text{cm}^{-2} \text{K}^{-1}$ , where  $k$  is the thermal conductivity,  $\rho$  is the density and  $C$  is the specific heat capacity. Knowing the values of thermal diffusivity ( $\alpha$ ) and thermal effusivity, thermal conductivity ( $k$ ) value can be evaluated. The feasibility of photoacoustic technique for the simultaneous measurement of thermal conductivity and heat capacity has already been established (36). Thermal effusivity value of ceramic tapes has great importance when they are used for microelectronic device fabrication or used as thermal barriers in integrated optics.

---

### 3.4. Theoretical background

#### 3.4.1. Thermal diffusivity measurement

The heat transmission configuration is depicted in figure1. For an optically opaque solid, the entire light is absorbed by the sample at  $x = 0$  and the periodic heat is generated at the same place. Assuming that the heat flow into the air (ambient) in contact with the front surface of the solid is negligibly small, the thermal waves generated at  $x=0$  will penetrate through the sample to its rear surface. The heat thus reaching the sample-air interface at  $x=-l_s$  will get attenuated after traveling a very small distance called the first thermal diffusion length in air. Thermal diffusion length is given by  $\mu = \left(2\alpha/\omega\right)^{1/2}$ , where  $\alpha$  and  $\omega$  are the thermal diffusivity of air and modulation frequency of the incident light respectively. Consequently, this periodic heating process arising as a result of the periodic absorption of light at the interface at  $x = 0$  results in an acoustic piston effect in the air column in between the sample and the microphone.

According to the one-dimensional heat flow model of Rosencwaig and Gersho, for the arrangement schematically shown in figure1, the pressure fluctuation in the air inside the chamber is given by (37-40),

$$Q = \frac{\gamma P_0 I_0 (\alpha / \sigma_s)^{1/2}}{(2\pi) l_g T_0 k_s f \sinh(l_s \sigma_s)} e^{j(\omega t - \pi/2)}$$

where  $\gamma$  is the ratio of specific heat capacities of air,  $P_0$  and  $T_0$  are the ambient pressure and temperature,  $I_0$  is the radiation intensity,  $f$  is the modulation frequency, and  $l$ ,  $k$ , and  $\alpha$ , are the length, thermal conductivity and the thermal

diffusivity of the medium.  $i = g$  refers to the air and  $i = s$  refers to the solid sample. Also  $\sigma_i = (1+j) a_i$  where  $a_i = (\pi f / \alpha_i)^{1/2}$  is the thermal diffusion coefficient of the medium  $i$ . In arriving at the above expression it is assumed that the sample is optically opaque.

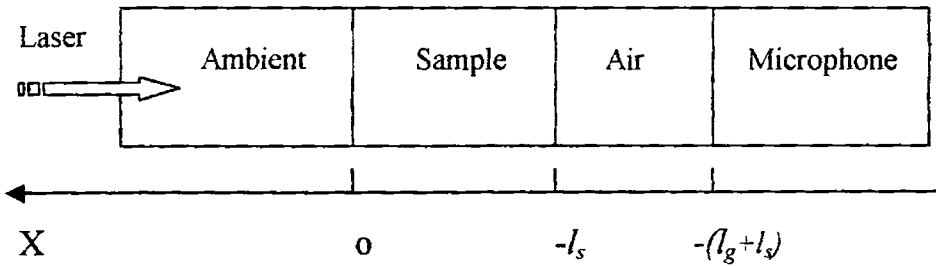


Figure 1. Schematic representation of the open cell geometry

For thermally thin sample (ie.  $l_s a_s \ll 1$ ), the expression for  $Q$  reduces to

$$Q = \frac{\gamma P_0 I_0 \alpha_g^{1/2} \alpha_s e^{j(\omega t - 3\pi/4)}}{(2\pi)^{3/2} T_0 l_g l_s k_s f^{3/2}}$$

Above expression implies that the PA signal amplitude from a thermally thin sample under the heat transmission configuration varies as  $f^{3/2}$  and the phase is insensitive to the variation in the modulation frequency.

When the sample is thermally thick (ie.  $l_s a_s \gg 1$ ), the expression for  $Q$  becomes

$$Q = \frac{\gamma P_0 I_0 (\alpha_g \alpha_s)^{1/2} \exp\left[-l_s (\pi f / \alpha_s)^{1/2}\right]}{\pi T_0 l_g k_s f} e^{j(\omega t - \pi/2 - l_s a_s)}$$

The amplitude of the PA signal decreases with the modulation frequency as  $\left(\frac{1}{f}\right) \exp(-b\sqrt{f})$  with  $b = l_s \sqrt{\pi/\alpha_s}$ , while the phase  $\phi$  decreases linearly with  $b\sqrt{f}$ . Hence, the thermal diffusivity  $\alpha_s$  can be evaluated either from the amplitude data or from the phase data, provided the sample is optically opaque and thermally thick in the frequency region of interest. Though the phase and amplitude of the PA signal contains clear signature of the thermal properties of the specimen, phase data is more reliable for open cell configuration since the amplitude data depends on many external parameters such as sample surface quality and detector response at different wavelengths. Experimental results reported here are derived from the phase data.

### 3.4.2 Thermal effusivity measurement.

According to Rosencwaig and Gersho theory (37,38) for the heat reflection configuration, when the sample is kept in contact with a thermally thin absorbing layer, the acoustic pressure in the microphone chamber is given by the equation,

$$\delta Q_1 = \frac{\gamma P_0 I_0 (\alpha_g \alpha_s)^{1/2}}{(2\pi) l_g T_0 k_s f} e^{j(\omega t - \pi/2)}$$

where  $k_i$  and  $\alpha_i$  are the thermal conductivity and thermal diffusivity.  $i = s$  corresponds to the sample,  $i = 0$  corresponds to the absorbing layer and  $i = g$  corresponds to the air in the microphone chamber.  $\gamma$  is the ratio of specific heats for air,  $P_0$  is the pressure,  $I_0$  is the incident intensity,  $l_g$  is the length of the gas column in the cavity,  $T_0$  is the temperature of the gas inside the chamber.

Here,  $\omega = 2\pi f$  and  $b = \left( \frac{k_s \sigma_s}{k_0 \sigma_0} \right)$ . The acoustic signal varies as  $\frac{1}{f}$  and

is proportional to the ratio  $\frac{\sqrt{\alpha_s}}{k_s}$ , the inverse of the thermal effusivity of the

sample.

In the absence of the sample (i.e., only the absorbing layer is present) the pressure fluctuation inside the cavity is given by,

$$\delta Q_2 = \frac{\gamma P_0 I_0 \alpha_g^{1/2} \alpha_0}{(2\pi)^{3/2} T_0 l_g l_0 k_0} \frac{e^{j(\omega t - 3\pi/4)}}{f^{3/2}}$$

The PA signal varies as  $f^{-3/2}$  and depends on the ratio  $\frac{\alpha_0}{k_0}$ .

Now,

$$\frac{\delta Q_1}{\delta Q_2} \propto \frac{l_0 k_0 \sqrt{\alpha_s}}{\alpha_0 k_s} f^{1/2}$$

Thermal effusivity of the sample ( $e_s = k_s / \sqrt{\alpha_s}$ ) can be evaluated by measuring the signal amplitude as a function of modulation frequency from the

---

absorbing layer-sample composite and that from the absorbing layer alone, provided the thickness, density and specific heat capacity of thin absorbing layer are known.

## **3.5 Experimental details**

### **3.5.1 Experimental setup**

The experimental setup consists of an Argon ion laser (Liconix 5000 series), a mechanical chopper (Stanford Research Systems SR540) and the open photoacoustic cell. The schematic of the experimental set-up is given in figure 2. The open photoacoustic cell (figure 3) has provisions for both rear side and front side illumination.

The intensity modulated optical radiation from the Argon ion laser is allowed to fall on the sample kept inside the open photoacoustic cell. The PA signal generated in the cell is detected using a sensitive electret microphone (BT 1834) and is amplified using a lock-in amplifier. The phase and amplitude of the PA signal are recorded using a digital lock-in amplifier SR 830. Samples in the form of free-standing ceramic tapes are pasted on aluminium foils using thermal paste to avoid mechanical vibrations of the samples due to its periodic dilation (drum effect) during irradiation (41).

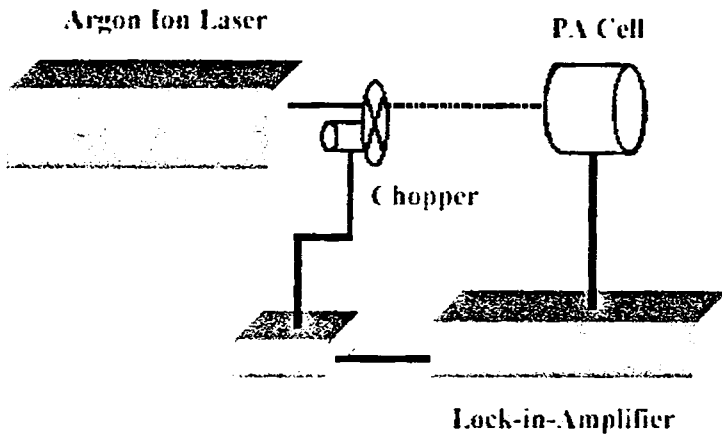


Figure 2. Schematic diagram of the experimental setup

### 3.5.2 Open photoacoustic cell

The major building block of the cell is an acrylic (perspex) disk of thickness 1cm and diameter 5.5cm. The acoustic chamber is made by drilling a bore of diameter 3mm across the thickness at the centre of the disk. One end of this cylindrical hole is closed with an optical quality glass slide of thickness 1.4mm and the other end is kept open. Another fine bore of diameter 1.5mm pierced at the middle of the main chamber and perpendicular to it serves as the acoustic coupler between the main chamber and the microphone. At a distance of 8mm from the main chamber the microphone is firmly glued to the orifice of the side tube. Shielded wires are used to take the electrical connections directly from the microphone. Entire system is then fixed inside a cylindrical hollow block of aluminium, leaving half the thickness of the acrylic disk outside the aluminium holder. Solid samples having uniform surface quality can be easily stuck at the top of the sample chamber (open end) by using vacuum grease. On

the other hand, if the sample is very thin and requires more tight contact, then another identical acrylic disk with a 3mm hole at the centre can be used to press the sample in between the two disks.

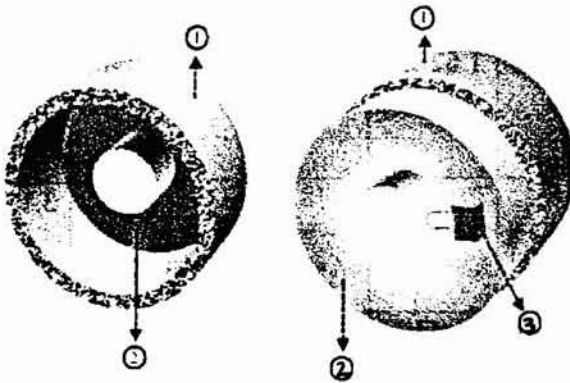


Figure 3. Open photoacoustic cell

1. Aluminium case 2. Perspex body 3. Microphone

### 3.5.3 Sample specifications

The investigations are carried out on green ceramic tapes obtained from CMET, Trichur. All the samples have a uniform thickness of 70 $\mu$ m. The green tapes contain a polymer network in which ceramic particles are embedded. Therefore no porosity is expected at green stage. Only after binder (polymer) burns out, porosity will appear. Specifications of the samples are given in table 1.

	SiC	PMN-PT	PZT	Al <sub>2</sub> O <sub>3</sub> / ZrO <sub>2</sub>	ZrO <sub>2</sub>	Barium titanate	Barium tin titanate
% ceramic	61.65	74.78	77.42	36.41	57.71	66.61	66.63
% binder (poly vinyl butyral- PVB)	2.57	1.62	1.37	21.5	3.09	2.00	2.45
% of plasticizer ( Pthalates and Glycoles)	2.8	2.17	1.78	3.33	4.11	3.18	3.55
%solvents	32.98	21.43	19.43	38.76	35.09	28.21	27.37

In the case of Al<sub>2</sub>O<sub>3</sub>/ZrO<sub>2</sub> ( Alumina- zirconia) the solvent is water and binder is polyvinyl alcohol(PVA).

Table 1

### 3.5.4. Thermal diffusivity measurements

The theory involved in the measurement of thermal diffusivity is given in section 3.3. The rear side illumination or the so-called heat transmission configuration is used for the present investigations. The ceramic tape sample is pasted on thermally thin aluminium foil using a thermal paste and is fixed to the top of the open photoacoustic cell (OPC) using vacuum grease at the edges. The cell is arranged such that the modulated laser beam falls on the aluminium foil. Photoacoustic signal phase is measured as a function of modulation frequency. The same experiment is repeated with aluminium foil alone.

Difference in phase readings of the two observations gives the phase for the sample under investigation corresponding to a modulation frequency.

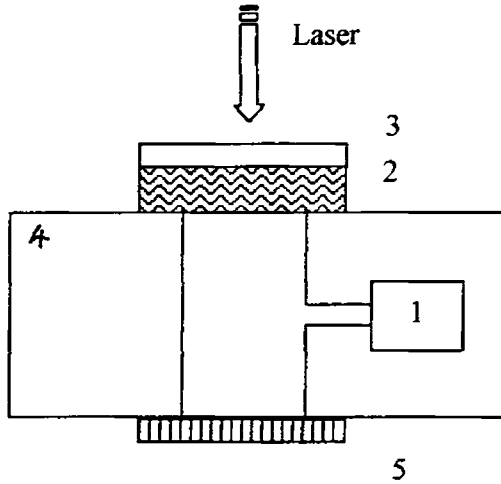


Figure 4. Cross sectional view of OPC geometry for the measurement of thermal diffusivity

1. Microphone 2. Sample 3. Aluminium foil 4. Acrylic body 5. Glass window

Since the phase of PA signal changes linearly with  $b\sqrt{f}$ , where  $b = l_s \sqrt{\frac{\pi}{\alpha_s}}$ , slope of phase difference vs square root of frequency plot gives the value of 'b'. Knowing sample thickness  $l_s$ , thermal diffusivity ( $\alpha_s$ ) is calculated from the slope.

### 3.5.5. Thermal effusivity measurements

Same ceramic tape samples and the same open photoacoustic cell are used for thermal effusivity measurements. In this investigation the reflection mode geometry is employed. Sample is pasted on to aluminium foil and the sample aluminium foil combination is mounted on the PA cell so that the free surface of the sample faces the ambient. Irradiation is made through the front glass window and thermal waves are generated from the aluminium-gas interface.

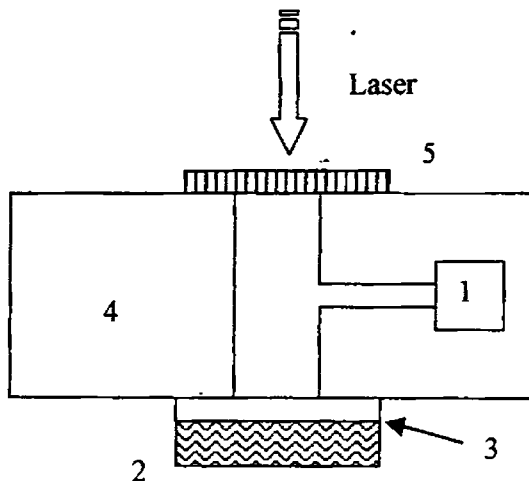


Figure 5. Cross sectional view of OPC geometry for the measurement of thermal effusivity

1. Microphone 2. Sample 3. Aluminium foil 4. Acrylic body 5. Glass window

Thermal effusivity is evaluated from the slope of the signal amplitude ratio (ratio of amplitudes corresponding to aluminium foil alone and sample+aluminium foil combination) vs square root of frequency plot.

### 3.6. Results and discussion

The variation of phase difference in the photoacoustic signal (difference in the phases corresponding to aluminium foil alone and ceramic tape pasted on aluminium foil ) as a function of modulation frequency under the heat transmission configuration for the samples under investigation is shown in figures 6 to 12.

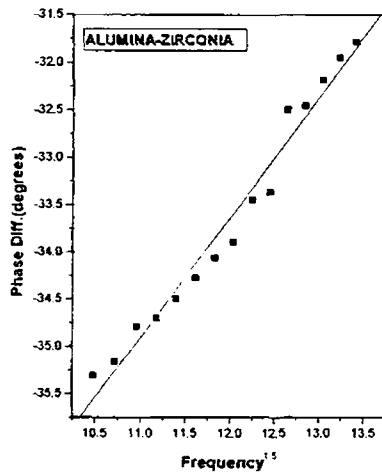


Figure 6. Variation of PAS phase difference as a function of modulation frequency for alumina-zirconia sample.

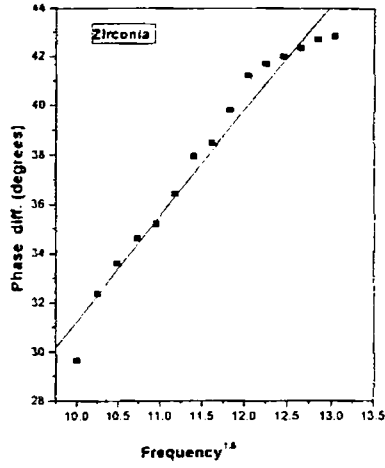


Figure 7. Variation of PAS phase difference as a function of modulation frequency for zirconia sample.

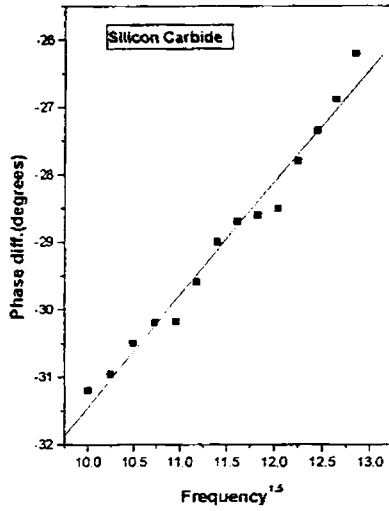


Figure 8. Variation of PAS phase difference as a function of modulation frequency for Silicon carbide sample

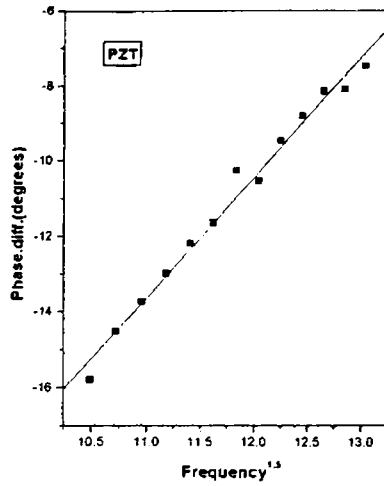


Figure 9. Variation of PAS phase difference as a function of modulation frequency for lead zirconate titanate (PZT) sample.

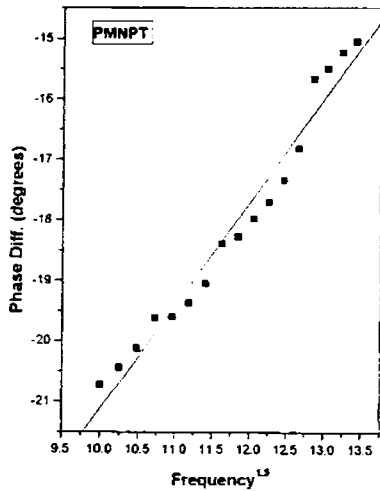


Figure 10. Variation of PAS phase difference as a function of modulation frequency for lead magnesium niobate titanate (PMNPT) sample

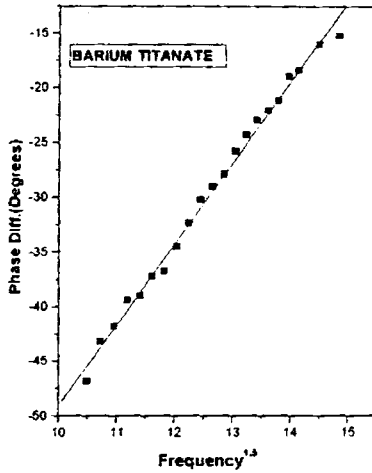


Figure 11. Variation of PAS phase difference as a function of modulation frequency for Barium Titanate sample

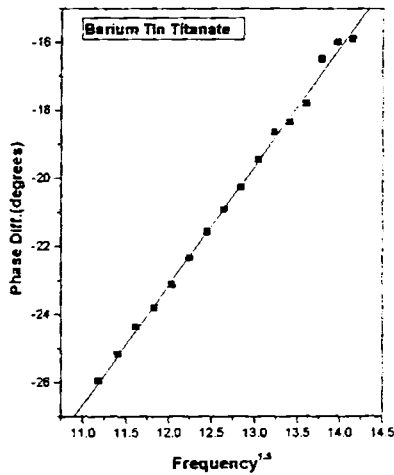


Figure 12. Variation of PAS phase difference as a function of modulation frequency for Barium Tin Titanate sample

Thermal diffusivities of the samples are calculated from the slopes of the straight-line graphs and are tabulated in table 2. Literature values (42-47) of the thermal diffusivities of pure ceramics and ceramic films are also included for comparison. Since tape casting is a batch process, there may be changes in the thermal parameters from batch to batch and will depend on the presence of additives and binders, which are added during the tape casting process. Values of thermal parameters of ceramic tapes are not available. However, it is seen from the table that the thermal diffusivity values calculated using the photoacoustic technique are of the same order of magnitude as that of the literature values. It is found that addition of certain materials changes the thermal diffusivity of the compound. Alumina has a higher thermal diffusivity compared to zirconia ( $\sim 0.1 \text{ cm}^2/\text{s}$ ). Thermal diffusivity of alumina-zirconia compound is greater than that corresponding to zirconia. The enhancement in thermal diffusion of the compound sample will be due to the presence of alumina. The same effect has been observed in the case of tin doped barium titanate also. Thermal diffusivity of barium tin titanate is found to be higher than that of barium titanate. The enhancement in thermal diffusivity might be due to the presence of tin in the compound. This shows that ceramic tapes with required intermediate values of thermal parameters can be prepared by mixing appropriate amounts of different materials. Difference in actual value can be attributed to the presence of materials other than ceramics.

Figures 13-19 show the variation of ratio of photoacoustic signal amplitude between sample attached to aluminum foil and aluminium foil alone as a function of modulation frequency. Thermal diffusivities are calculated from the slopes of the straight line fits.

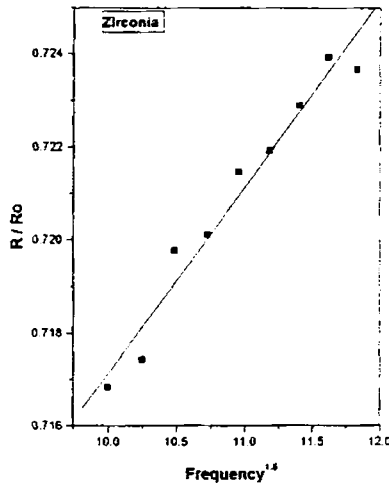


Figure 13. Variation of ratio of PAS amplitudes as a function of modulation frequency for zirconia sample.

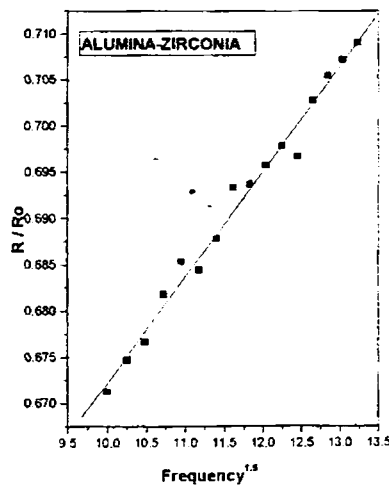


Figure 14. Variation of ratio of PAS amplitudes as a function of modulation frequency for Alumina-zirconia sample.

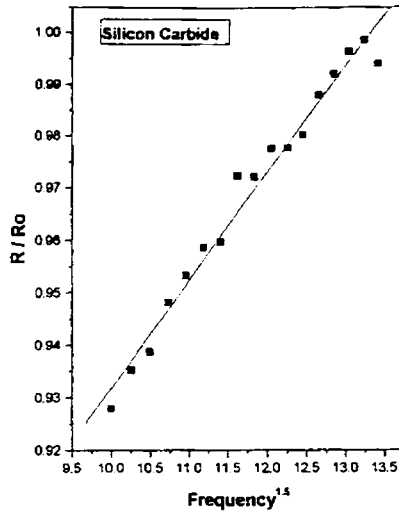


Figure 15. Variation of ratio of PAS amplitude as a function of modulation frequency for Silicon carbide sample

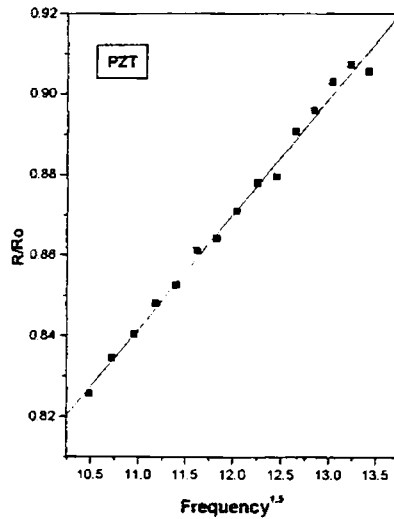


Figure 16. Variation of ratio of PAS amplitudes as a function of modulation frequency for lead zirconate titanate (PZT) sample

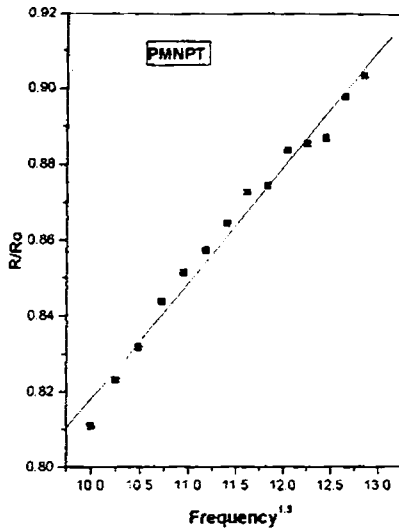


Figure 17. Variation of ratio of PAS amplitude as a function of modulation frequency for lead magnesium niobate titanate(PMNPT)

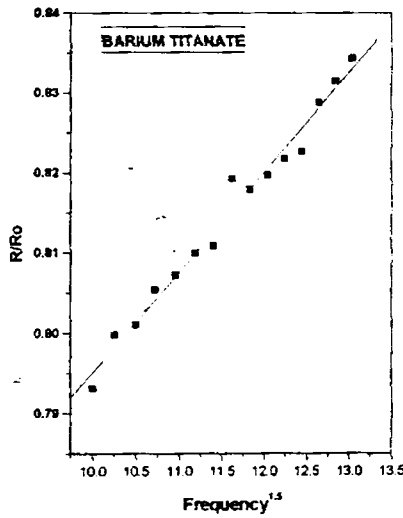


Figure 18. Variation of ratio of PAS amplitude as a function of modulation frequency for Barium Titanate sample

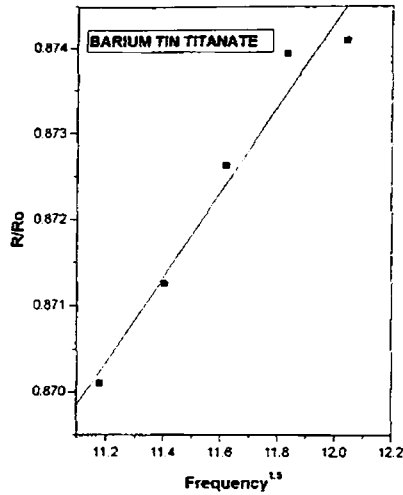


Figure 19. Variation of ratio of PAS amplitude as a function of modulation frequency for Barium Tin Titanate sample

Calculated values of thermal diffusivity, thermal effusivity and thermal conductivity values are tabulated in table 2. As a laser operating in the light mode is used for irradiation, the incident power is stable. Uncertainty of  $\sim \pm 0.0005$  can be expected in the calculations because of the variations that may occur in tape thickness from the expected value.

Sample	Thermal diffusivity of tapes ( $\text{cm}^2/\text{s}$ )	Thermal conductivity of tapes ( $\text{w/cmK}$ )	Effusivity of tapes ( $\text{ws}^{1/2}/\text{cm}^2\text{K}$ )	Thermal diffusivity( $\text{cm}^2/\text{s}$ ) of thin films (literature (43-48))
Zirconia	0.0044	0.049	0.74	0.002- 0.005
Alumina-Zirconia	0.055	0.061	0.26	Between 0.1 & 0.002
Silicon carbide	0.076	0.039	0.15	0.08
Lead Zirconate Titanate(PZT)	0.0078	0.011	0.12	Of the order of $10^{-3}$
PMNPT (lead magnesium niobate titanate)	0.029	0.017	0.1	Not available
Barium Titanate	0.0016	0.00941	0.24	0.0015
Barium Tin Titanate	0.0066	0.048	0.6	Not available

Table 2

---

### 3.7. Conclusions

The present study clearly shows that the photoacoustic technique is an effective tool for the thermal characterization of ceramic samples. Details of investigations carried out on the thermal parameters of seven different ceramic (green) tape samples and the results obtained are presented. Analysis of results shows that the thermal diffusivity values depend on the constituents of the medium. Mixing one ceramic with another changes the effective thermal parameters of the sample. In general, addition of plasticizers and binders is found to change the thermal diffusivity values of ceramic tapes compared to pure thin film samples.

### References

1. M.J. Adams, B.C. Beadle, G.F. Kirkbright, K.R. Menon, *Appl. Spectrosc.* **32**, 43 (1978)
2. C. A. Bennett and R.R. Patty, *Appl. Opt.*, **20**, 911 (1981)
3. G. Busse, *Appl. Opt.*, **21**, 107 (1982).
4. H. Coufal, P. Korpiun, P. Luscher, E. Schneider and R. Tilgner, "Photoacoustics- Principles and Applications" (H. Coufal, ed.) Vieweg Verlag, Braunschweig.
5. F. Lepoutre, G. Louis and J. Taine, *J. Chem. Phys.*, **70**, 2225 (1979).
6. C.K.N. Patel and A.C. Tam, *Appl. Phys. Lett.*, **36**, 7 (1980).
7. A.C. Tam and H. Coufal, *Appl. Phys. Lett.*, **42** (1983).
8. R.R. Sanches et al., *J. Braz. Chem. Soc.*, **10**, 97 (1999)
9. "Photoacoustic and Thermal Wave phenomena in smiconductors" A.Mandelis(Ed.) (North Holland, Amsterdam), (1987).
10. H.Varga and L.C.M.Miranda, *Phys. Rep.*, **161**, 4 (1988).

- 
11. J.A. Balderas Lopez and A. Mandelis, *J. Appl.Phys.*, **88**, 6815( 2000).
  12. M. J. Adams and G.F. Kirkbright, *Anal. Chem.*, **51**, 508( 1979)
  13. D.M. Todorovic, P.M.Nikolic, D.G. Vasseljevic and M.D. Dramicanin, *J. Appl.Phys.*, **76**,1( 1994).
  14. D.M. Todorovic, P.M.Nikolic, *Procee.twentieth Int. Conf. on Microelectronics (MIEL '95)*, 1, NIS, Serbia( 1995).
  15. S.Sankararaman, V.P.N.Nampoori , C.P.G.Vallabhan, G.Ambadas and S.Sugunan, *Appl.Phys. Lett.*, **67**, 20(1995).
  16. G.Gutierrez, M. Vergas-Luna et al, *Rev. of Sci. Instruments*, **74**, 845(2003)
  17. A. Bouguerra, A. Ledhem, J.P. Laurent, M.B. Diop and M. Queneudec, *J. Appl.Phys.*, **31**, 2184( 1998)
  18. A.M.Mansanares, H.Vargas, F. Galembeck, J. Buijs and D. Bicanic, , *J. Appl.Phys.*,**70**,7046 (1991)
  19. A.M.Mansanares, H.Vargas, A.C. Benta, N.F. Leite and L.C.M. Miranda, *Phys. Rev.B*, **42**, 4477 (1990).
  20. I. Deigadilio, A. Calderon and L.C.M.Miranda,*Opt. Eng.*, **36**, 343 (1997).
  21. G. Amato, G. Bendetto, L.Boarino, M.Maringelli and R. Spagnoto, *IEE Proc.-A*, **139**, 4( 1992).
  22. W.L.Sheppard,Jr., *Chem. Engg.***24**, 59-67 (1988)
  23. D.W.Richardson, *Chem. Engg.*,12-14(1982)
  24. Mel Schwartz, *Handbook of Structural Ceramics*
  25. A. Roosen, *Basic requirements for tape casting of ceramic powders*
  26. E.P.Hyatt, *Ceram. Bull.*, **68**,869 (1989)
  27. J.D. Cawley, *NASA Tm-87078 ( N85- 32333: NSP )*(1987).
  28. M Schwartz, *Hand book of structural ceramics ( Mc Graw-Hill)*
  29. J.S. Reed, *Introduction to the Principles of Ceramic processing*, Wiley, new York, pp486(1988).

- 
30. R. Morrell, *Hand book of Properties of technical and Engineering Ceramics*, Natl. Physical La., HMSO, London, 1985.
  31. H.S. Carslaw and J.C. Jaeger, *Conduction of heat in solids* (Oxford Press)
  32. H.S. Carslaw, *Introduction to the mathematical theory of the conduction of heat in solids* (McMillan).
  33. D. Fournier, C. Boccara, A. Skumaniach and N.M. Amer, *J. Appl. Phys.*, **59**, 787 (1986).
  34. M. Bertolotti, R.L. Votti, G. Liakhou and C. Sibila, *Rev. Sci. Instrum.*, **64**, 1576 (1993).
  35. G.D. Sajan, P. Radhakrishnan, V.P.N. Nampoori and C.P.G. Vallabhan, *J. Phys. D: Appl. Phys.*, **36**, 990 (2003).
  36. U. Zammit, M. Marinelly, R. Pizzoferrato, F. Scudieri and S. Martelluci, *J. Phys. E: Sci. Instrum.*, **21**, 935 (1988).
  37. A. Rosencwaig, *Photoacoustic and photoacoustic spectroscopy*, (John Wiley & Sons, New York), 1980
  38. A. Rosencwaig and A. Gersho, *J. Appl. Phys.*, **47**, 64 (1976).
  40. L.F. Perondi and L.C.M. Miranda, *J. Appl. Phys.*, **62**, 2955 (1987).
  41. A.M. Mansanares, H. Vergas, F. Galembeck, J. Buijs and D. Bicanic, *J. Appl. Phys.*, **70**, 7046 (1991)
  42. P. Charpentier, F. Lepoutre and L. Bertrand, *J. Appl. Phys.*, **53**, 608 (1982)
  43. *Measurement Sci. & Technol.* **12**, 2058 (2001).
  44. *National Physical Lab. TPAC News 7*
  45. *Microstructure develop. and thermal parameters (internet)*
  46. G.E. Youngwood et al, *Pacific North West National Lab (Internet)*
  47. N.P. Bansal, D. Zhu, *NASA/TM 212896*, 2003
  48. Y.G. Yoon, R. Car, D.J. Srolovitz, S. Scandolo, *Phys. Rev. B*, **70**, 012302, (2004).

## *Chapter 4*

### **Photoacoustic studies on dye mixtures**

#### **Abstract**

Laser induced photoacoustic technique is used in the study of photostability of polymethyl methacrylate (PMMA) films doped with Rhodamine 6G-Rhodamine B dye mixture system. Energy transfer from a donor molecule to an acceptor molecule in a dye mixture affects the emission output of the dye mixture. Details of investigations on the role of laser power, concentration of the dye, modulation frequency and the irradiation wavelength on the photosensitivity of the dye mixture doped PMMA films are presented in this chapter. Photosensitivity is found to change with changes in donor acceptor concentrations. Dye mixture doped PMMA samples are found to be more photosensitive when the dyes are mixed in the same proportion.

## 4.1 Introduction

Dye doped polymers find applications as active laser media and in the modern photonic technology (1-7). High-density information storage is an important technological objective. A large number of optical storage media have been reported. They include both inorganic and organic media. Current interests are in the write-once optical media and compact disk recordable media. The modification of the dye is necessary for writing and reading at short wavelengths. The promising candidates for information storage are organic dyes. One area that may be revolutionized by the use of organic luminophores in plastics is the flat screen monitor industry. Current flat screens typically use expensive, delicate plasma technology. Organic emitters doped in a polymer layer offer an inexpensive, malleable and easy-to-produce alternative. Organic dyes are also of interest for sensors, optical amplifiers and fiber optics. If organic fluorescent molecules are to be effectively used in such applications, they must be able to withstand repeated excitations and the large amounts of energy that will be cycled through them. Unfortunately upon repeated absorption, the dye molecules begin to photo-oxidize. This permanently destroys the dye, thereby limiting applications of such organic materials under exposure to high optical intensities. A nonlinear absorber of light has the unique property that its optical absorption can be altered by introducing changes in the intensity of radiation incident upon it. Different types of organic molecules undergo optical bleaching (8-10) when subjected to high intensity radiation and are useful as passive Q switches for lasers and as recording media (11,12). A number of techniques have been used

---

to study photoinduced changes in laser dyes (13-19). Photochemical changes induced in a medium can be monitored either by optical methods or photothermal methods. In optical methods the radiative relaxation or optical absorption (or transmission) is investigated whereas in photothermal technique, the energy liberated as a result of nonradiative relaxation is measured.

Spectroscopic studies based on photothermal effects, like photoacoustic spectroscopy (PAS)(20) and photothermal deflection spectroscopy (PDS)(21) offer powerful techniques to study absorption of highly fluorescent dyes and gives complementary information to fluorescence spectroscopy through the detection of non-radiative relaxation processes. The dominant feature of laser heating is that a large amount of energy may be absorbed in a short interval of time. Photothermal methods measure a signal, which is directly related to the amount of electromagnetic energy absorbed by the sample, which is converted into heat. These methods present the additional advantage of being much less sensitive to the light scattered by surface roughness and volume inhomogeneties (22). The photoacoustic technique has already been used by many researchers to study the energy transfer mechanisms in a number of dye systems (23-28).

Embedding a dye in solid matrices can modify the non-linear optical properties of it. Although both inorganic glasses and polymeric materials have been successfully used as host matrices for lasing dyes, polymers offer a number of advantages both from the technical and economical point of view, which include high optical homogeneity (29), better chemical compatibility with organic dyes, control over medium polarity and viscosity in a way similar to conventional solvents (30), and adaptability to inexpensive fabrication

---

techniques. Synthetic polymer hosts have additional advantages compared to other matrices because these polymers exhibit good compatibility with organic dyes permitting miniaturization and low cost integrated optical system designs. One of the important advantages of transparent polymers compared to traditional optical materials (inorganic glasses and crystals) is that it is possible to introduce organic dyes that play the role of active components into polymers, which appreciably changes the characteristics of the polymer matrix. Suitable materials for different applications can be prepared by properly selecting the type of solid matrix and the dye incorporated into it. Intermolecular energy transfer between two molecular species separated by a distance in the condensed phase has been observed in numerous molecular systems (31-45). Main mechanisms involved in the electronic energy transfer in molecular systems are radiative transfer, non-radiative transfer and excitation migration. Non-radiative transfer of electronic energy involves the simultaneous de-excitation of the donor and the excitation of the acceptor, a one step process that does not involve the intermediacy of a photon. A necessary condition for non-radiative energy transfer between two molecules is that the distance between the donor and the acceptor must be very small. The energy transfer mechanism results in the quenching of absorption of the donor molecule. Through suitable selection of dye combinations, absorption characteristics and the photostability of the mixture can be changed.

Different organic polymers can be used as solid host material and the basic requirements imposed on a polymeric host for lasing dye molecules are good optical transparency at both pump and lasing wavelengths, good solubility of the dye in the material, and resistance to pump laser radiations. Most frequently used polymeric materials are based on methylmethacrylate

---

(MMA), such as polymethyl methacrylate (PMMA) or compositions of the methacrylate co-polymers like HEMA:MMA etc. PMMA is the most frequently used host for lasing dyes due to its excellent optical transparency in the visible region and its relatively high laser damage resistance. The low solubility of majority of the conventional laser dyes in PMMA causes some limitations. Good solubility of dyes is achieved by introducing modifying additives, which also enhances laser damage resistance (46). Ethyl alcohol is chosen as an additive because it combines good solubility for xanthene dyes and enhancement of host laser damage resistance.

## 4.2 Materials

### 4.2.1 Rhodamine 6G- Rhodamine B Systems

Present work in the dye-doped polymer has been carried out with dyes of the xanthene family. Xanthene derivatives, Rhodamine 6G and Rhodamine B, with fluorescence emission in the yellow-red region of the electromagnetic spectrum are well known for their excellent laser performance in liquid solutions as well as in solid matrices. For the present investigations rhodamine 6G chloride (  $C_{28}H_{31}ClN_2O_3$ , LOBA Chemie, GR, molecular weight 479.02 ) and rhodamine B (  $C_{28}H_{31}ClN_2O_3$ , Merck,GR, molecular weight 479.02 ) are used as received. Structures of the two dyes and that of PMMA are shown in figure 1. Eventhough rhodamine6G and rhodamineB have the same molecular formula, their molecular structures are different.

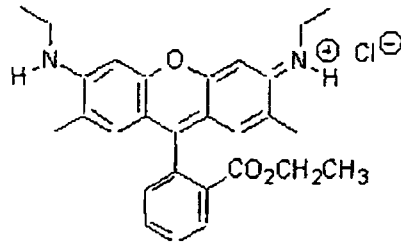


Figure 1a. Structure of Rhodamine 6G

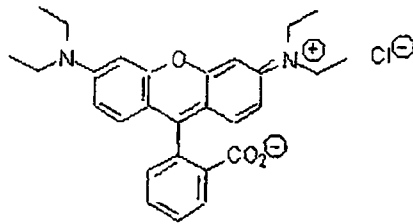


Figure 1b. Structure of Rhodamine B

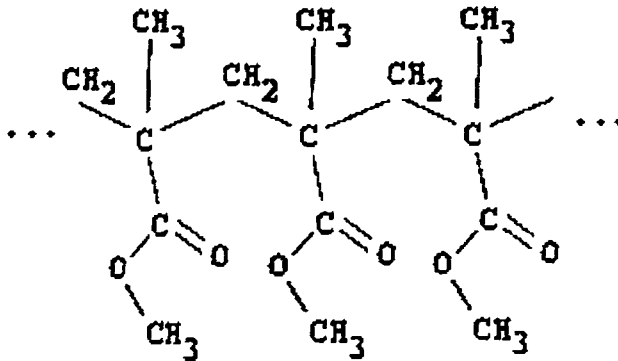


Figure 2 Structure of PMMA

#### 4.2.2 Preparation of dye doped polymer samples

Methyl methacrylate (MMA)(CDH Chemicals) is washed three times with 2% sodium hydroxide solution to remove foreign inclusions and then with distilled water till the solution is clear. Few pellets of anhydrous calcium chloride are added to the MMA and kept for 24 hours. The dry MMA is then filtered. Since Rhodamine dye has limited solubility in the monomer MMA, ethyl alcohol (Merck) is used as a solvent. The addition of ethanol as a plasticizer has also been reported to increase the laser damage threshold of PMMA (46). Accurately weighed dyes are dissolved in ethanol to prepare stock solutions of the two dyes from which solutions of different concentrations are prepared. For the preparation of different dye doped samples, the monomer MMA is mixed with the respective dye dissolved ethyl

---

alcohol in the ratio 4:1. Solutions of monomer –alcohol mixture with different volume ratios of the two dyes and at different dye concentrations for a fixed volume ratio are prepared. 1gm of benzoyl peroxide per 100ml of the solution is used as an initiator for polymerization. The monomer-alcohol mixture containing the dye and the initiator, taken in a glass test tube is kept in a constant temperature bath maintained at 50°C for polymerization. Care is taken to see that the dye is homogeneously distributed in the polymer matrix. After 24 hours completely polymerized sample is taken out of the water bath. Placing the dye doped polymer mixture drops on clean microscopic glass slides results in thin coatings (spot casting) of the sample. The slides coated with the samples are kept at room temperature for one week to dry. Perfect drying is necessary to avoid shrinkage of the sample.

### **4.3 Experimental details.**

Photothermal methods measure the photon energy that has been converted into heat. A continuous wave (CW) laser induced photoacoustic technique is used to investigate the photo-induced degradation of the dye doped polymer samples. The experimental set-up and the open photoacoustic cell used for the present investigation are same as that discussed in the previous chapter. For the photoacoustic (PA) signal measurements the reflection mode geometry of the PA cell is employed (figure1). The excitation source used is a highly stabilized Argon ion laser (Liconix 5000) and its different emission lines are used for the study. The CW laser emission is intensity modulated using a mechanical chopper (Ithaco HMS 230).

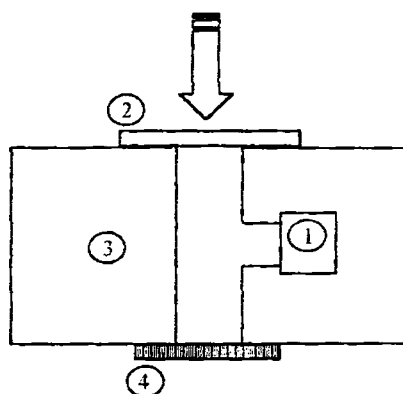


Figure 3. Reflection mode geometry of the photoacoustic cell.

1. Microphone 2. Glass window 3. Acrylic body of the cell 4. Sample

The modulated light beam at specific power levels is allowed to fall on the sample kept within the non-resonant photoacoustic cell. The photoacoustic signal detected by the microphone is amplified using a digital lock-in amplifier (Stanford Research Systems SR 830). Laser lines of wavelengths 488nm, 496nm and 532nm are used for the investigations. Influence of the excitation light on the rate of dye photodegradation is studied at power levels of 20mW, 30mW and 40mW. Other parameters that are varied are the dye concentration and the laser modulation frequency.

#### 4.4 Results and discussions

The process of photoacoustic signal generation in condensed media has already been experimentally established and a satisfactory theoretical explanation has been given by Rosencwaig and Gersho(20). The complex amplitude of the PA signal produced is given by the relation,

$$Q = \frac{-i\beta\mu^2\gamma P_0 I_0}{4\sqrt{2T_0}l_g a_g k}$$

where  $\beta$  is the optical absorption coefficient of the sample and  $\mu$  is the thermal diffusion length in the medium;  $\gamma$  is the ratio of specific heat capacities for air,  $P_0$  and  $T_0$  are the ambient pressure and temperature respectively.  $I_0$  is the intensity of incident light,  $l_g$  and  $a_g$  are the length of the gas column inside the cavity and the thermal diffusion length in the gas respectively and  $k$  is the thermal conductivity of the sample. Hence, by any means, if the absorption coefficient value changes, then the PA signal amplitude will also vary accordingly. Any kind of photochemical reaction will result in a change in the number density or concentration of the original species and this, in turn, will result in a change in the optical absorption properties of the sample. Doping of an organic dye in a solid matrix will not alter the thermal properties of the host(30). So when a dye doped polymer is investigated using photoacoustic technique, any change in the PA signal amplitude is essentially a measure of the rate of photodecomposition of the dye. Results of the studies carried out to

investigate the rapidity with which an optical dye in a solid host irreversibly degrades when it is illuminated by visible light are presented here.

The absorption spectra for mixtures of Rh 6G and Rh B are shown in figure(4). Absorption peak of Rh6G doped PMMA is around 520nm and that of RhB doped PMMA is at 550nm. Absorption of RhB doped PMMA is very low compared to that of Rh6G doped PMMA in the wavelength range selected for investigations. It is observed that the addition of RhB dye decreases the effective absorption of the mixture at 520nm.

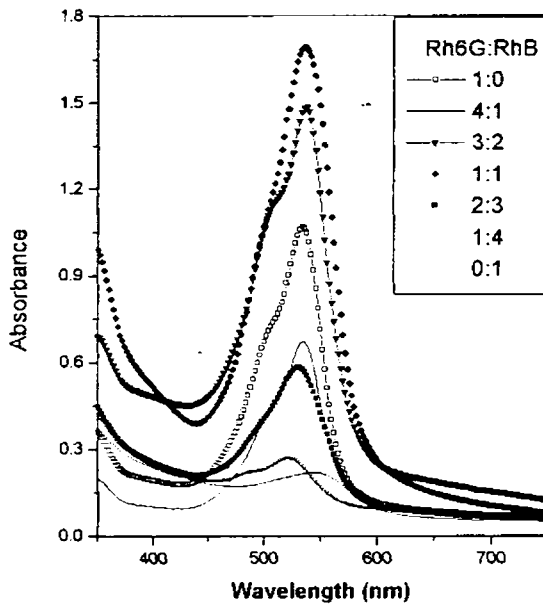


Figure4. Absorption spectra of different samples

Initial investigations are carried out on dye doped PMMA samples with varying volume ratios of the constituent dyes, Rhodamine 6G and Rhodamine B. The variation of PA signal amplitude as a function of time for the different samples is shown in figure5

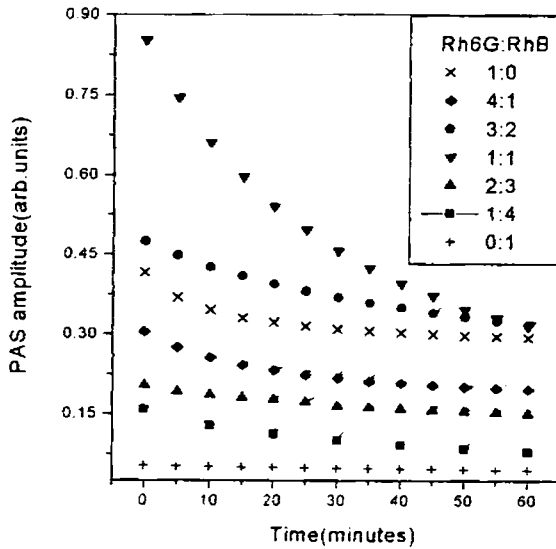


Figure 5. PA signal amplitude versus irradiation time plot for different volume ratios of Rhodamine 6G and Rhodamine B doped polymer samples

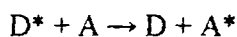
Concentration of Rhodamine 6G = 1mM

Concentration of Rhodamine B = 1mM

P=30mW  $\lambda = 488\text{nm}$   $f=80\text{Hz}$

---

From the plot it is clear that PA signal degradation rate change from sample to sample. Plots are shown shifted from each other for the sake of clarity. All the samples containing Rh6G exhibit signal degradation and then saturation on continued irradiation. This indicates that on irradiating the dye doped PMMA sample with strong laser beam, photodegradation of the dye molecules take place and the resultant product does not absorb in the spectral region where the original dye molecules absorb. The reduction in absorbance is evident in the absorption spectrum (Figure 6). Therefore the observed decrease in PA signal amplitude is due to the gradual decomposition of the dye molecules. The time taken to attain saturation is found to vary from sample to sample. This clearly shows the photosensitivity of the dye doped PMMA samples. As RhB has very low absorption at the irradiation wavelength, the photo-reaction is more for Rh6G. The PMMA sample doped with RhB alone does not show considerable change in PA signal on continuous irradiation whereas samples with Rh6G exhibit signal degradation. From this it can be deduced that RhB doped PMMA is photochemically stable at this particular concentration. Addition of RhodamineB changes the photosensitivity of Rhodamine6G. The reduction in photochemical reaction of Rh6G can be attributed to the enhancement in energy exchange to RhB. Non-radiative energy transfer from an excited state donor ( $D^*$ ) molecule can occur due to coulombic or electron exchange interaction between  $D^*$  and the acceptor (A) molecule. Non-radiative transfer of electronic energy involves the simultaneous de-excitation of the donor and the excitation of the acceptor, a one-step process that does not involve the intermediacy of a photon.



---

This type of energy transfer occurs when the energies involved in  $D^* \rightarrow D$  and  $A \rightarrow A^*$  transitions are same, the excitation transfer being the simultaneous occurrence of the two coupled or resonant transitions.

As the amount of RhB in the mixture is increased, the RhB- light interaction increases while that of Rh6G decreases. Samples with small amounts of RhB shows gradual photodegradation in the early stages followed by saturation . In these cases the influence of rhodamine 6G is maximum. As the volume ratio of RhB is increased above that of Rh6G, somehow changes are introduced in the energy exchange process so that signal degradation is very slow. This indicates that the presence of RhB stabilizes the sample against damage. The sample with the two dyes mixed in 1:1 ratio takes a long time for photodegradation and takes more than one hour to attain saturation. The PA signal magnitude is also found to be maximum for this particular combination. This may be because of the fact that the energy exchange between the two dyes is maximum for this particular combination and it reduces the rate of photochemical reaction.. Further investigations are carried out on samples with dyes mixed in the same ratio. Even though a large number of studies have been reported in the field of dye doped polymers, the exact mechanism responsible for the photodegradation of laser dyes in polymers is not yet fully brought out.

In order to investigate the influence of irradiation wavelength on the photodegradation of the dye system doped PMMA, photoacoustic studies are carried out at different wavelengths. 532nm, 496nm and 488nm lines of the argon ion laser are used for investigations and the PA signal amplitude is plotted as a function of irradiation time(figure7).

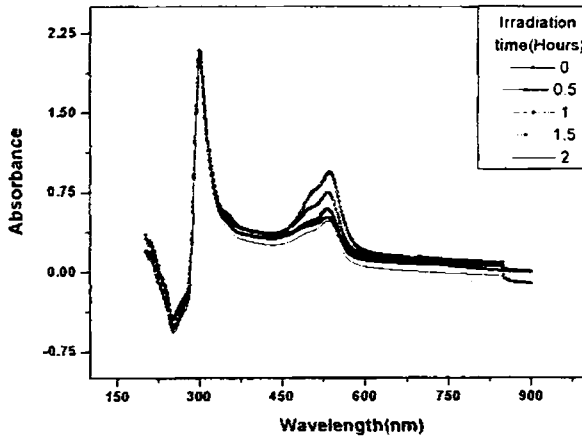


Figure6. Absorption spectra of the sample before and after irradiation

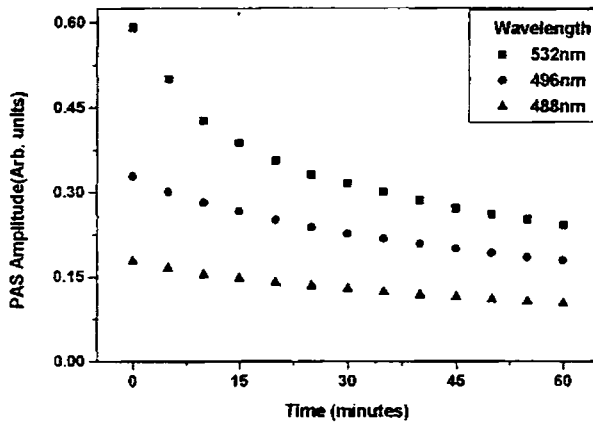


Figure7. PA signal versus time plot for different wavelengths (dyes of same concentration(1mM) are mixed in the ratio 1:1)  
Laser power = 30mW Modulation frequency = 80Hz

The photodegradation rate is found to increase as the irradiation wavelength increases from 488nm to 532nm. This is understandable as the absorption of Rh6G is maximum at around 520nm. The PA signal amplitude also increases as the irradiation wavelength approaches the peak absorption wavelength. Even though higher wavelengths give higher values of PA signal, investigations are carried out using 488nm because of the steady operational conditions for longer time durations at this wavelength.

The variation in PA signal amplitude for PMMA samples doped with Rhodamine 6G and Rhodamine B in the same volume ratio for a constant concentration of Rh6G and different concentrations of RhB is given in figure8.

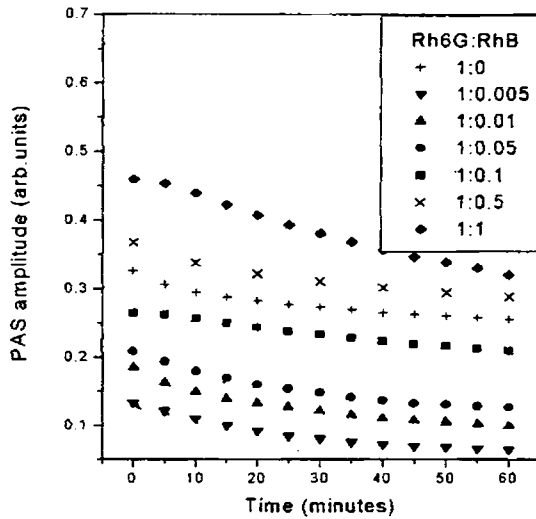


Figure 8 . PA signal amplitude versus irradiation time plot for PMMA doped with rhodamine6G-rhodamineB systems. Rhodamine6G concentration is fixed at 1mM and rhodamineB concentration(mM) is changed.

Laser power= 30mW  $\lambda = 488\text{nm}$  Modulation frequency = 80Hz

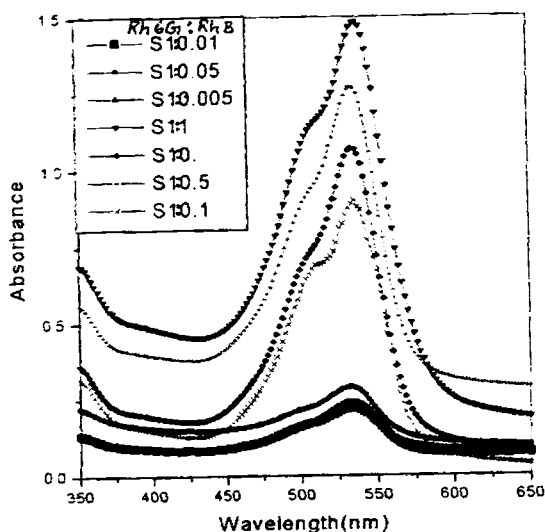


Figure 9 Absorption spectra of dye mixture doped PMMA samples for constant Rh6G and different RhB concentrations

In all the cases it is found that during the initial few (~5) minutes the PA signal is fluctuating and after that the signal is almost steady with a variation of around 10 microvolts. From the plot it is clear that the decay time is more for the PMMA film in which dyes are doped in the ratio 1:1. As equal amounts of both the dyes are present in the mixture, photons are equally shared between the two. In the case of films with low concentrations of RhB (0.005 mM and 0.1 mM) PAS signal is found to be lower than that corresponding to Rh6G alone. Here the presence of RhB effectively decreases the non-radiative relaxation processes which in turn reduces the PA signal

amplitude. Energy exchange is taking place between Rh6G and RhB molecules. When the concentration of RhB is increased above 0.1mM, PA signal is found to be more than that corresponding to PMMA doped with Rh6G alone and is maximum for 1:1 ratio with equal concentrations.

The absorption spectra of the samples also show maximum absorption for the sample in which dyes are mixed in same proportion (figure 9). For lower concentrations of RhB, signal degradation is not appreciable whereas for higher concentrations, signal degradation is gradual and it takes longer time for signal saturation. Presence of small amounts of Rhodamine B stabilizes the dye mixture against photodegradation.

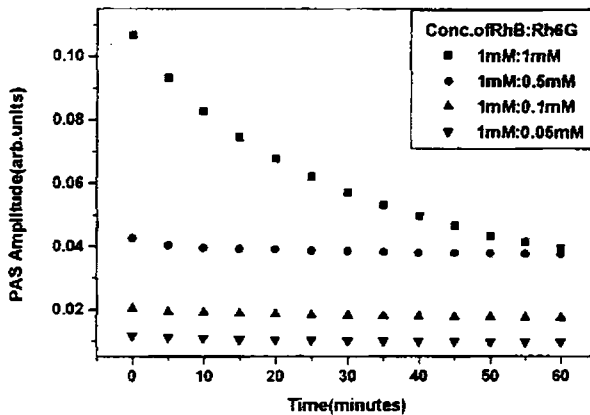


Figure 10 . PA signal amplitude versus irradiation time plot for PMMA doped with Rhodamine 6G-rhodamine B systems. Rhodamine B concentration is fixed at 1mM and rhodamine6G concentration is changed.

Laser power= 30mW  $\lambda = 488\text{nm}$  modulation frequency,  $f = 80\text{Hz}$

The variation in PA signal amplitude for PMMA samples doped with Rhodamine 6G and Rhodamine B in the same volume ratio for constant concentration of RhB and different concentrations of Rh6G is given in figure10.

Rhodamine B dye has lower absorbance than Rhodamine 6G at 488nm. When the concentration of Rh6G in the system is very low, the influence of RhB will be predominant and the signal is almost stable under continuous irradiation. As the concentration of Rh6G is increased to 0.5mM, PAS signal increases and degradation is visible. Signal saturation occurs within a short time. The presence of Rhodamine6G is found to enhance the photosensitivity of rhodamineB and hence bleaching.

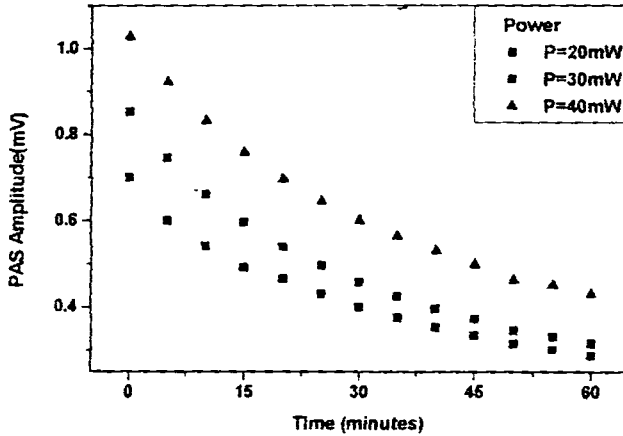


Figure 11. PA signal amplitude versus time plot for dye system doped PMMA at different irradiation intensities (dyes of same concentration (1mM) are mixed in the ratio 1:1)

$$f = 80\text{Hz} \quad \lambda = 488\text{nm}$$

From figure 11 it is clear that PA signal degradation increases with increase in pump power. These plots show that degradation rate is not uniform throughout. Initial degradation occurs at a faster rate followed by slower decay, which is more visible at lower pump levels.

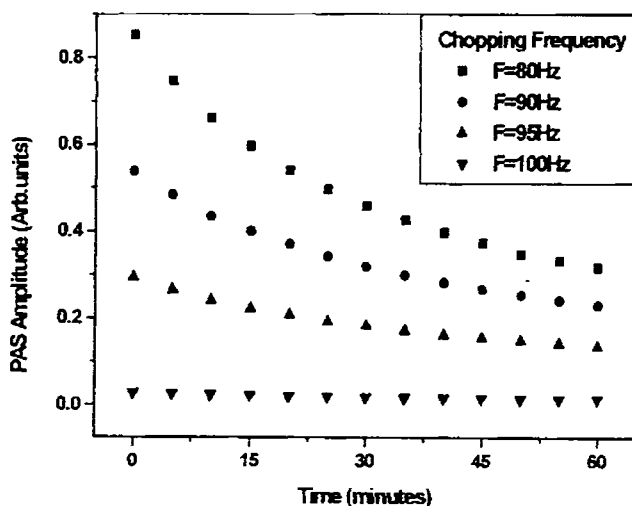


Figure 12. PA signal amplitude versus time plot for dye system doped PMMA for different modulation frequencies (dyes of same concentration(1mM) are mixed in the ratio 1:1)

$$\text{Laser power} = 30\text{mW} \quad \lambda = 488\text{nm}$$

The photoacoustic signal decreases with increase in modulation frequency. If ' $f$ ' is the modulation frequency, the number of light pulses falling on the sample in ' $t$ ' seconds will be ' $f t$ '. With increase in the value of either

---

frequency or irradiation time, number of photons falling on the sample and hence absorbed by it will increase. This increased absorption results in faster photodegradation. At higher modulation frequencies the degradation will be complete within a short time so that no change in PA signal can be observed. At lower frequencies photochemical changes take place at a slow rate and decrease in PA signal amplitude is gradual. The plot (figure12) also reveals that signal degradation is slow at low chopping frequencies. Changing the frequency of modulation can change the bleaching rate.

## **4.5 Conclusions**

The photoacoustic technique has been implemented successfully to investigate the bleaching of organic dye molecules embedded in PMMA matrix. From the observations it can be concluded that the bleaching rate of dye mixture doped PMMA matrix is directly proportional to the incident laser power and can be controlled by changing the modulation frequency. Addition of another dye into the system to form donor-acceptor combination can change the photostability of a dye doped polymer matrix. Adding Rhodamine B can enhance photostability of Rhodamine6G and photosensitivity of Rhodamine B can be enhanced by adding Rhodamine6G. When the dye doped polymeric material is to be used as an active medium for laser operations, the life-time of stable operation can be increased through proper selection of dye combinations and their concentrations. The dye doped PMMA can also be used as an optical recording medium. Through suitable selection of dye combinations and proper choice of concentrations of individual dyes, the time

---

for optical recording can be adjusted. Additional tuning is possible by the adjustment of pump power and modulation frequency.

## References

1. H.Franke, *Appl.Opt.*,**23**, 272(1984).
2. D.J.Welker and M.G.Kuzyk, *Appl.Phys.Lett.*, **69**, 183( 1996).
3. A.Suzuki, T.Ishii and Y.Maruyama, *J.Appl.Phys.*, **80**, 131( 1996).
4. M.A.Diaz-Garcia, F.Hide and B.J.Schwartz, *App.Phys.Lett.*,**70**, 3191, (1997).
5. I.Riess and D.cahen, *J.Appl.Phys.*, **82**, 3147( 1997).
6. S.Berleb, W.Brutting, M.Schwoerer, R.Wehrmann and A.Elschner, *J.Appl.Phys.*, **83**, 4403( 1998).
7. A.Magda and El-Shahawy, *Polymer testing*, **19**, 821 (2000)
8. G.N.Lewis, D.Lipkin and T.T.Magel, *J.Am.Chem.Soc.*, **63**, 3005(1941).
9. P.F.Gires and F.Combaudo, *J.Phys.D*, **26**,325( 1965).
10. C.R.Giuliano and L.D. Hess, *Appl. Phys. Lett.*, **9**, 19(1966).
11. W.E.Moerner, *Persistent spectral hole burning-science and applications* (Springer, Berlin, 1989)
12. K.K.Sharma, K.D.Rao, and G.R.Kumar, *Opt.Quantum Electron.*, **26**, 1, (1994).
13. G.Somasundaram and A. Ramalingam, *J.Photochemistry and Photobiology A: Chemistry*, **125**, 93(1999)
14. G.Somasundaram and A. Ramalingam, *J.Luminescence*, **90**, 1( 2000)

- 
15. G.Somasundaram and A. Ramalingam, *Chemical Phys. Letters*, **324**, 25, (2000)
  16. D.Tomic and A. Mickelson, *Applied Optics*, **38**, 3893 (1999)
  17. L.Carretero et al., *Applied Optics*, **37**, 4496 (1998)
  18. G.Wang, L.Hou and F.Gan, *Materials science and Engineering B* **65**, 75, (1999)
  19. B.P.Singh, G.R. Kumar and K.K.Sharma, *Chemical Physics letters*, **237**, 485(1995).
  20. A.Rosencwig and A.Gersho, *J.Appl.Phys.*, **47**, 64(1976).
  21. W.B.Jackson, N.M. Amer, A.C. Boccara and D. Fournier, *Appl. Optics*, **20**, 1333(1981).
  22. Z.A.Yasa, W.B.Jackson and N.M.Amer, *Appl. Optics*, **21**, 21(1982).
  23. M.S.A. Abdel-Mottaleb et al; *Chem Soc., Faraday Trans.*, **2**, 1779, (1989)
  24. M.S.A. Abdel-Mottaleb, S. negm and H. Talaat, *Photoacoustic and Photothermal Phenomena III*, D.Bicanic (Ed.), *Springer-Verlag Series in Optical Sciences*, **69**,283(1991)
  25. J.Szurkowski, *Photoacoustic and Photothermal Phenomena III*, D.Bicanic (Ed.), *Springer-Verlag Series in Optical Sciences*, **69**,155, (1991)
  26. K. Driss-Khodja, A. Gheorghiu and M.L. Theye, *Optics Communications*, **55**, , 169(1985).
  27. P.Sathy, R.Philip, V.P.N.Nampoori and C.P.G.Vallabhan, *J.Phys.D,Appl.Phys.*, **27**, 2019(1994).
  28. A. Kurian, N.A.George, B.Paul, V.P.N.Nampoori and C.P.G. Vallabhan, *journal of Laser Chemistry*, **00**,2(2002).

- 
29. F.J.Duarte, *Appl. Opt.*, **33**, 3857( 1994).
  30. A. Costela, I.Garcia Moreno, J.M..Figuera, F. Amat-Guerri and R. Sastre, *Recent Res. Devel. In Physical Chem.*,**1**, 125( 1997).
  31. L.N.M.Duyens, *Nature*, **168**, 548,(1951).
  32. E.J.Bowen and R.Livingston, *J.Am.Che.Soc.*, **76**, 6300( 1954).
  33. R.Livingston, *J.Phys.Chem.*, **61**, 860, (1957).
  34. R.Hardwick, *J.Chem Phys.*, **26**, 323( 1957).
  35. R.G.Bennet, *J.Chem.Phys.*, **41**, 3037( 1964).
  36. C.Lin and A.Dienes, *J.Appl.Phys.*, **44**, 5050(1973).
  37. J.Cox and B.K.Matise, *Chem Phys. Lett.*, **76**, 125( 1980)
  38. E.G.Marason, *Opt.Commun.*, **40**, 212( 1982).
  39. S.Muto, H.Nagashima and C.Ito, *Electr. And Commun. Jap.*, **66-c**, 104, (1983).
  40. M.Terada and Y.Ohba, *Jap. J. Appl.Phys.*, **22**, 1392( 1983).
  41. M.I.Savadatti, S.R.Inamdar, N.N.Math and A.D.Mulla, *J.Chem.Sco.*, **82**, 2417( 1986).
  42. B. Panoutsopoulos, M.Ali and S.A.Ahmed, *Appl.Opt.*, **31**, 1213( 1982).
  43. J.R.Coppetta and C.B.Rogers, *Am.Inst.Aeronautics and Astronautics*, (1994)
  44. J.R.Coppetta and C.B.Rogers, *Am.Inst.Aeronautics and Astronautics*, (1995).
  45. K.M.Dyumaev, A.A. Manenkov, A.P.Maslyukov, G.A.Matyushin, V.S.Nechitalio and A.M.Prokhorov, *Opt. Soc. Am.B*, **9**(1), 143,( 1992).
  46. K.M.Dyumaev, A.A.Manenkov, A.P.Maslyukov, G.A.Matyushin, V.S.Nechitailo and A.S.Tsaprilov, *Sov. J.Quantum Electronics*, **12**, 838, (1982)

## *Chapter 5*

# **Photoacoustic measurements on multilayer dielectric systems**

### **Abstract**

The application of photoacoustic (PA) technique to the non-destructive analysis of layered samples is demonstrated experimentally. This technique makes use of a laser source, a photoacoustic cell, a mechanical chopper and a lock-in amplifier. Multilayer stack of  $\text{SiO}_2$  and  $\text{TiO}_2$  is used as the absorbing medium. Frequency modulated laser beam is allowed to fall on the sample placed in the photoacoustic cell. The acoustic signal generated in the PA cell as a result of the periodic absorption of the multilayer sample is detected using a microphone and the resulting output is processed by a lock-in amplifier. The amplitude and phase of the signal are measured as a function of the chopping frequency. Striking step- like variations are observed in the phase-frequency plot, which clearly reveals the different layers present in the multilayer structure. Defect in the structure of a multilayer stack is also clearly brought out by the investigations.

## **5.1. Introduction**

The photoacoustic effect has been proven to be an effective and sensitive tool in the study of optical and thermal properties of solids, liquids and gases (1-13). By using the PA technique one can obtain quantitative information on the sample properties such as the thermal diffusivity, optical absorption coefficient or thickness of a thin film specimen. In addition, by changing the chopping frequency of the incident radiation, it is also possible to obtain a depth profile analysis of some of these properties. At high chopping frequencies, information about the sample near the surface is obtained while at low chopping frequencies, sample properties from deeper within becomes accessible. This is a feature unique to the PA technique. Another important aspect of the technique is its capability to measure the optical absorption of opaque samples.

Multilayer films are widely used in science and industry for the control of light. Periodic multilayer stack with films of two refractive indices in each period have been widely used as narrow band filters, broadband reflectors, high efficiency anti-reflection coatings, laser mirrors etc. The photoacoustic method has been widely adopted for studying multilayered media and thin films deposited on dielectric and conducting base materials (14-18). The depth profiling capability of the photoacoustic technique has been exploited advantageously to study multilayer dielectric thin films coated on a substrate. Ageing of multilayers will, sometimes, destroy the quality of the films due to interlayer diffusion. The PA technique can be used to determine the number of layers in a multilayer stack

or it can be used to check the reduction in the effective number of layers due to interlayer diffusion.

For the optimal performance of laser mirrors, absorbance  $A$  should be minimum and reflectance  $R$  and transmittance  $T$  should have specific values. The transmittance  $T$  can be measured with an accuracy of about 0.01% using the commercial spectrophotometer. The measurement of reflectance  $R$  with the same accuracy is very difficult with commercial equipments. The PA signal is a measure of the amount of heat energy absorbed by the sample. The high sensitivity of the photoacoustic technique can be used for the calculation of absorbance of even highly reflecting specimen. Using the PA technique, absorbance can be measured with an accuracy of 0.01%. Once the transmittance is evaluated,  $R$  can be calculated with an accuracy of 0.01%.

## 5.2. Theoretical background

According to the general theory of photoacoustics given by Rosencwaig and Gersho (14), the actual physical pressure variation  $\delta P(t)$  in the gas column in contact with the sample surface in the photoacoustic cell is given by,

$$\delta P(t) = Q_1 \cos(\omega t - \pi/4) - Q_2 \sin(\omega t - \pi/4)$$

or

$$\delta P(t) = q \cos(\omega t - \psi - \pi/4)$$

where  $Q_1$  and  $Q_2$  are the real and imaginary part of the complex envelope of the sinusoidal pressure variation ( $Q$ ) and  $q$  and  $\psi$  are the magnitude and phase of the acoustic pressure wave produced in the cell by the photoacoustic effect. PAS magnitude and phase from a layered structure can be derived from the equations given by Rosencwaig and Gersho (14). In the case of a two layer structure with thin non-absorbing top layer and an optically and thermally thin bottom layer, the photoacoustic signal is given by(15),

$$q \approx \left( \frac{\beta I_0}{C \rho \omega \mu} \right) e^{(-x/\mu)} \cos\left(\omega t - \frac{x}{\mu} - \frac{\pi}{4}\right) \quad (1)$$

where  $I_0$  is the incident monochromatic light flux,  $\beta$  is the absorption coefficient of top layer,  $\rho$  density,  $C$  specific heat,  $\omega$  chopping frequency,  $\mu$  thermal diffusion length of bottom layer and  $x$  thickness of top layer. Thermal diffusion length ( $\mu$ ), thermal diffusivity ( $\alpha$ ) of the medium and modulation frequency ( $\omega$ ) are connected through the equation

$$\mu = \sqrt{\frac{2\alpha}{\omega}} \quad (2)$$

From equation (1) it can be seen that the presence of a top layer decreases the photoacoustic signal amplitude and introduces a phase lag denoted by,

$$\psi = \frac{x}{\mu} \quad (3)$$

---

The additional phase lag  $\psi$  in the photoacoustic signal will depend on the thickness of the top layer and the phase of the signal is quite sensitive to the presence of a boundary in a layered structure. In all the reported studies number of layers employed is very few.

Depth profiling aspect of PA technique has been used by many scientists and a number of theoretical models have also been reported (16-24). Depth profiling can be performed in several ways. By changing the wavelength of the incident light, the depth of optical penetration, and thus the depth at which the photoacoustic signal is generated, can be changed. The thermal diffusion length in a medium is inversely proportional to the modulation frequency of the incident light. Hence it is possible to alter the penetration depth by changing the frequency of modulation. By changing the modulation frequency, the photoacoustic signal can be made to originate from different depths in the sample. An important application of the depth profiling capability of the photoacoustic technique is the measurement of thin film thickness. Such measurements can be performed by analyzing the magnitude and/ or phase of the PA signal as a function of the modulation frequency. Full range depth profiling requires operation over a broad frequency range.

### **5.3 Multilayer dielectric films**

Multilayer films find applications as beam splitters, reflection coatings, antireflection coatings, laser mirrors etc. Opaque metal films are used as mirrors for maximum reflectance only in the infrared. In the case of semitransparent films

the absorbance reaches a maximum if  $R \approx T$ . Semitransparent metal films can therefore be used as beam splitters with high absorbance(27). Semitransparent films are not suitable as output mirrors for a laser system. Dielectric films possess uniform thickness and refractive index and are assumed to be homogeneous in the direction of light propagation. In general, the absorption in dielectric films is assumed to be negligible(28). Because of these properties they give rise to interference and most applications of thin dielectric films make use of the interference effect. By using more than one layer, improved optical characteristics can be achieved. Most applications of thin films are based on the use of multilayer coatings. There are large variety of designs for multilayer coatings that can be used for laser applications and the most important among them is a quarter-wave stack. The simplest design of a multilayer structure is a stack of alternating films of equal optical thickness corresponding to one quarter of the design wavelength, but of two different refractive indices. Design of quarter-wave stack on glass can be represented as glass-LHLHLHLH-air where L and H represent low refractive index and high refractive index layers. Such a stack exhibits high reflectance at the centre wavelength region, where the effective optical thickness is equal to  $\lambda/4$ . The reflectance increases with increasing number of quarter-wave films in discreet steps.

In the case of semitransparent films, reflectance R, transmittance T and absorbance A are related through the equation,

$$R + T + A = 1 \quad (4)$$

Laser mirrors should have a well defined reflectance, mostly high reflectance, and they should exhibit extremely low losses. These requirements can

be fulfilled by multilayer stacks of dielectric materials. Laser mirrors normally possess low transmittance  $T$  and high reflectance  $R$ . By knowing  $R$  and  $T$  one can calculate the absorbance  $A$  and the value of  $A$  is a measure of the quality of the mirror. For the optimal performance of a certain laser type,  $A$  should be a minimum and  $R$  and  $T$  should correspond to specified values. So the accurate measurement of reflectance is very important in the case of laser mirrors. The photoacoustic signal is a measure of the amount of heat energy absorbed by the sample. Using the PA technique, absorbance  $A$  can be measured with an accuracy of 0.01%. Once the transmittance is evaluated,  $R$  can be calculated with an accuracy of 0.01%.

Multilayer stacks selected for the present studies are quarter-wave stacks ( $\lambda/4$  thick at 632.8nm) of  $\text{SiO}_2$  and  $\text{TiO}_2$ .

#### **5.4. Design and fabrication of a photoacoustic cell**

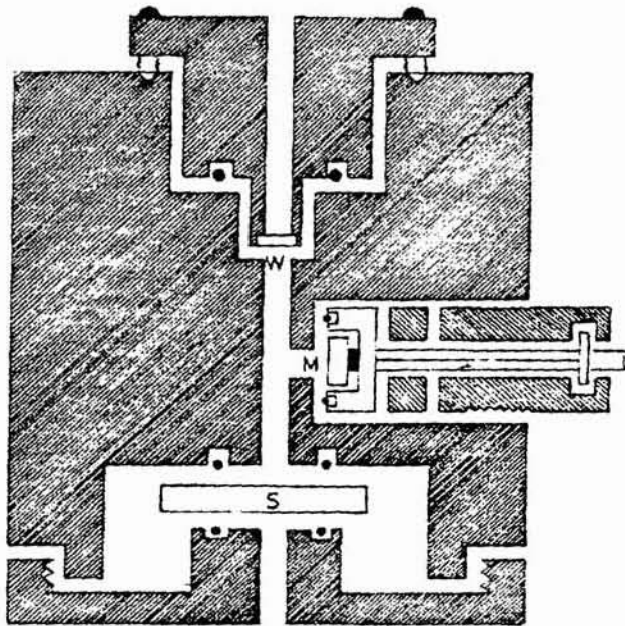
For the study of solid samples, a simple and sensitive photoacoustic cell is designed and fabricated. In the case of a conventional photoacoustic cell the sample is placed inside a chamber which is provided with a single window. Such PA cells can be used only in the reflection mode geometry. However, the non resonant PA cell fabricated for the present studies allows one to use it in both reflection mode geometry and transmission mode geometry. Illumination is possible from both sides. The microphone (Knowles 1834) is kept in the side chamber and is acoustically coupled to the main chamber through a small cylindrical cavity. The cross-sectional view of the cell is shown in figure 1. In the

---

reflection mode geometry, the sample is irradiated through the glass window and in the transmission configuration irradiation has to be made from the rear side of the sample.

The photoacoustic cell is designed in such a way that its walls have good acoustic impedance and the cell is acoustically isolated. In order to minimize the PA signal generation from the walls due to the absorption of incident radiation, the thermal mass of materials used for the fabrication of PA cell should be quite large. The cell is made out of an aluminium rod of diameter 8cm and length 6cm. Aluminium is selected as the core material for cell fabrication because of its high thermal mass. The acoustic chamber is made by drilling a bore of diameter 5mm along its length at the centre of the rod. A glass window is fixed on one end, well inside the aluminium block and perfect sealing is achieved using neoprene O ring. The other end of the cylindrical hole is left open. Another fine bore of diameter 1.5mm pierced at the middle of the main chamber and perpendicular to it serves as the acoustic coupler between the main chamber and the microphone. The microphone is placed in the side chamber. Shielded wires are used to take the electrical connections directly from the microphone. The open end of the cell is covered with the sample to be studied. Another aluminium disc having the same diameter as the cell is pressed to the rear surface of the sample to ensure its proper positioning and acoustic isolation. This backing disc of aluminium has a hole of diameter 5mm drilled through it which allows for rear surface illumination of the sample. If the sample is irradiated through the glass window, cell functions as a conventional PA cell in reflection geometry and if the illumination is through the

bore in the backing aluminium disc, the cell functions as an open cell in transmission geometry.



- M - Microphone
- W - Window
- S - Sample

Figure 1 Cross-sectional view of the photoacoustic cell.

## 5.5. Experimental

A schematic diagram of the experimental set-up is given in figure 2. The photoacoustic cell used here has provisions to illuminate the sample either from the rear side or from its front side. The cell is used in the reflection mode geometry for the present investigations. The experimental set-up consists of an Argon ion laser (Liconix 5000 series), a mechanical light beam chopper (Ithaco model 230), a lock-in amplifier (EG & G 5208) and a non resonant photoacoustic cell in which the sample and the microphone are kept.

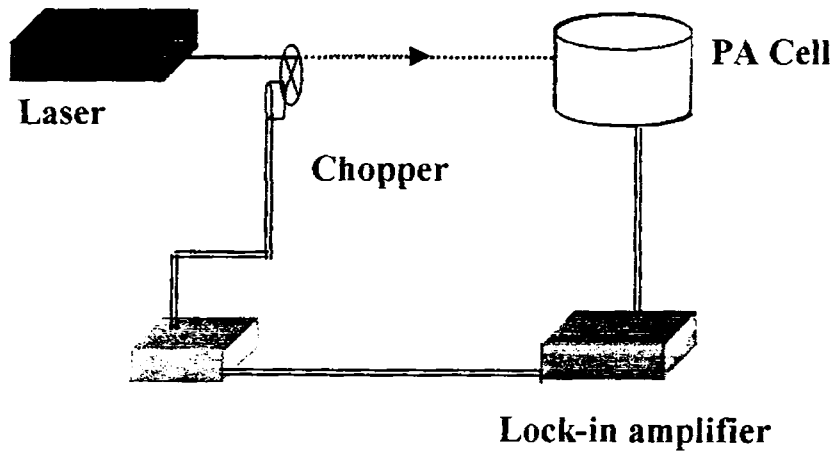


Figure 2 Schematic of the experimental setup used for investigations

## 5.6. Results and discussions

The response of the PA cell to the incident radiation is evaluated using carbon black as the sample. The PA signal amplitude plot (Figure 3) for the carbon black film shows an  $\omega^{-1}$  dependence as per the theoretical prediction of Rosencwaig and Gersho for a thermally thin carbon black. The phase plot (figure 4) doesn't show any anomalous behavior. The cell has uniform response over a large frequency range.

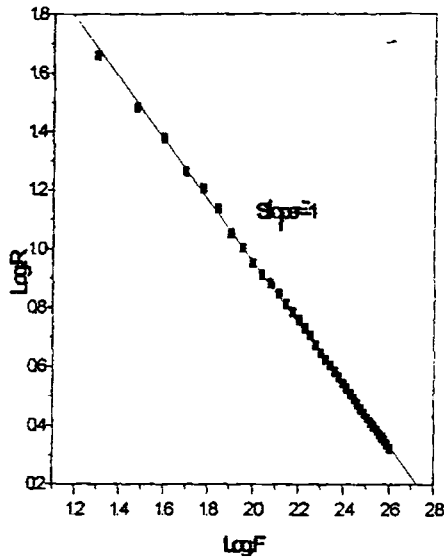


Figure 3 Log Amplitude vs log frequency plot for carbon black

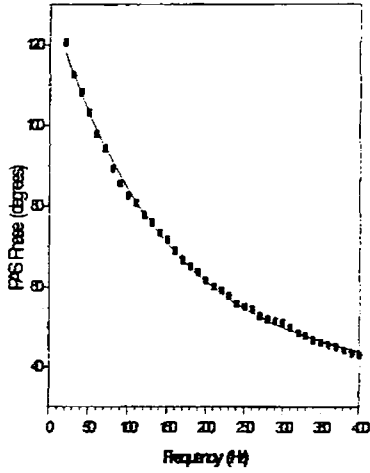


Figure 4 Phase frequency plot for carbon black

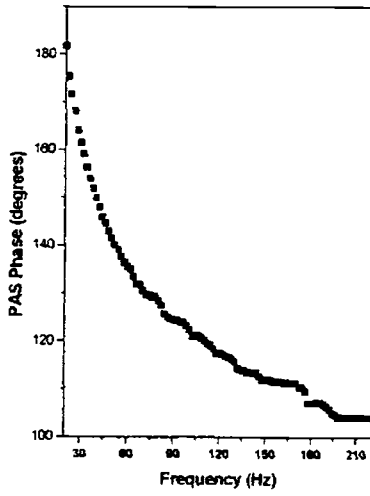


Figure 5.a Variation in phase with frequency for a 7 layer SiO<sub>2</sub> /TiO<sub>2</sub> system (phase measured using EG &G 5208 lock-in amplifier)

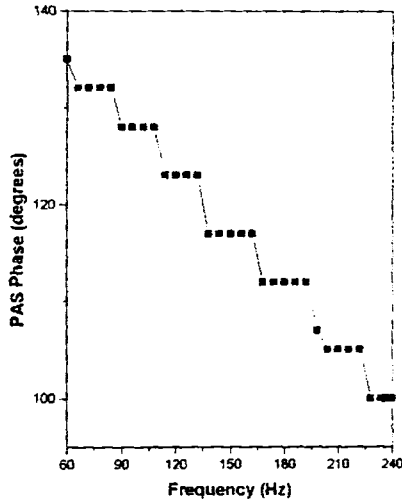


Figure 5.b Variation in phase with frequency for a seven layer SiO<sub>2</sub> / TiO<sub>2</sub> system (phase measured using EG &G 5101 lock-in amplifier)

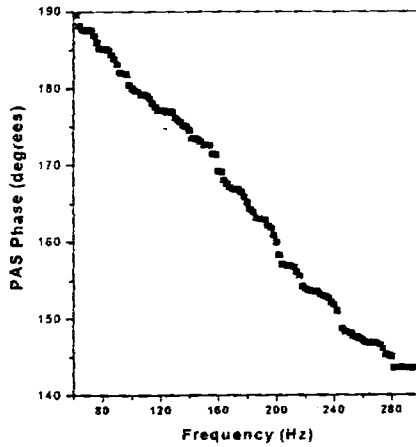


Figure 6.a Variation in phase with frequency for a 13 layer SiO<sub>2</sub> / TiO<sub>2</sub> system (phase measured using EG &G 5208 lock-in amplifier)

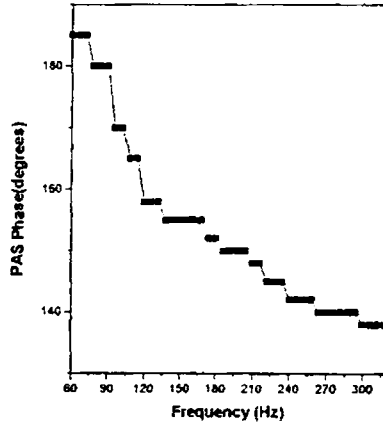


Figure 6.b Variation in phase with frequency for a 13 layer SiO<sub>2</sub> / TiO<sub>2</sub> system (phase measured using EG &G 5101 lock-in amplifier)

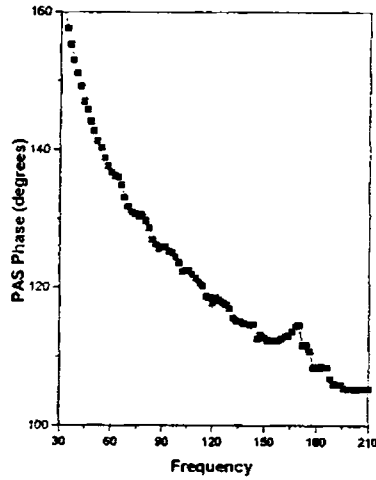


Figure 7 Variation in phase with frequency for a defective seven layer SiO<sub>2</sub> / TiO<sub>2</sub> system

---

Eventhough the phase and amplitude of the PA signal contains clear signature of the properties of the specimen, phase data is more reliable since the amplitude data depends on many external parameters such as sample surface quality and detector response at different wavelengths. Figures 5 and 6 show the dependence of the phase of the photoacoustic signal with modulation frequency of the laser beam for two multilayer stacks of 7 and 13 layers. Striking discontinuities in the phase plot due to phase lag at layer boundaries are clearly seen . Step like discontinuities are clearly brought out (figures 5.b and 6.b) when the measurements are done using a low resolution analogue lock-in amplifier (EG & G 5101). The abrupt changes in thermal and optical properties at the interfaces of the multilayer stack leads to abrupt discontinuities in the phase plot. It is observed that the number of discontinuities in the phase plot exactly matches with the number of layers in the thin film structure. However, the relationship between the film thickness and phase lag need not be of the simple form given in equation (3) due to the complexity of signal generation in multilayer films. The periodic heat flow in the material is a diffusive process , producing a periodic temperature distribution which is called a thermal wave. These waves will reflect and scatter from features beneath the surface which have different thermal characteristics from their surroundings. It is already established (25) that the multibeam interference of light waves within layers essentially change the mechanism of photoacoustic signal formation. Multiple reflections occurring in the thin film sublayer greatly enhance the effective optical absorption taking place in each layer and consequently one can no longer treat the sublayers as optically thin . The thermal wave that is very long will get reflected many times between

---

boundaries of a thermally thin sample before getting damped. The effects of multiple reflections and interference of thermal waves (26) also have to be taken into account to obtain a correct theoretical picture of the actual phase lag produced from the multilayer structure. If the sample is thin enough, thermal wave interference will affect the photoacoustic response. Only a detailed theoretical treatment of the photoacoustic effect in multilayer structure can throw light on actual phase dependence on thickness.

PA studies on a 21 layer  $\text{SiO}_2 / \text{TiO}_2$  structure have also been carried out. In the higher modulation frequency range, the phase variation is very low and we could identify only 18 irregularities/steps in the phase plot.

Figure 7 shows the frequency dependence of the photoacoustic signal phase from the seven layer  $\text{SiO}_2 / \text{TiO}_2$  structure at a different point of irradiation. The plot is similar to figure (5) except for an abnormal change in the phase corresponding to higher frequency region. The relative increases in phase in the frequency range 150-180 Hz corresponding to sixth and seventh layers can be attributed to structural defects or surface damages in these layers.

Figure 8 gives the reflectance of the seven layer sample calculated using photoacoustic technique. Absorbance and transmission measurements are carried out by employing a 10mW He-Ne laser. 632.8nm radiation from the He-Ne is used for this study as film is designed to have maximum reflection at this wavelength. From these measurements, the reflectance of the sample is evaluated using equation 4. The average value of the reflectance obtained at various modulation frequencies, (98.48 %) is in close agreement with the value (98.8%) measured using conventional techniques. However, the results obtained from PA

measurements will be more accurate due to its higher sensitivity. This proves the sensitivity of the PA detection technique in the optical characterization of highly reflecting samples.

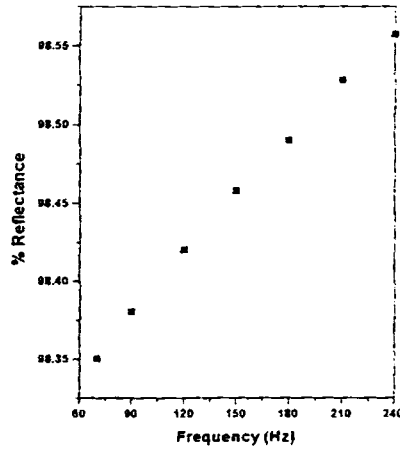


Figure 8. % Reflectance for a seven layer multilayer system

### 5.7 Conclusions

The feasibility of the photoacoustic technique for the characterization of a multilayer system has been demonstrated and the results are presented in this chapter. As the PA signal generation in multilayer dielectric coatings is a complex process, usual photoacoustics theories are not applicable. Even though actual evaluation of physical and thermal parameters are not possible using the existing

theories , PA signal phase data reveals the number of layers in a multilayer structure. The phase plot also reveals the defects in a thin film multilayer stack. Thus the present study demonstrates the feasibility of PA technique to precisely probe layered structures .

## References

1. A. Rosencwaig, *Science*, **181**,657 (1973)
2. A. Rosencwaig, *Opt. Commun.*, **7**,305 (1973)
3. A. Rosencwaig, *Physics Today*, **28**, 23 (1975)
4. A. Hardwik and Scholssberg, *Appl. Optics*, **16**, 101 (1975).
5. A. Rosencwaig and S.S.Hall, *Anal. Chem.*, **47**,548 (1975)
6. C.K.N. Patel, *Science*, **220**, 157 (1978)
7. R.G. Bray and M.J. Berry, *J. Chem. Phys.*, **71**, 4909 (1979)
8. T.H.Vansteenkiste, F.R.Foxvog and D.M.Roessler, *Appl. Spectrosc.*, **35**, 194 (1981)
9. H. Vargas and L.C.M. Miranda, *Phys.Rep.* **161** , 43-101 (1988)
10. A.M.Mansanares, A.C. Bento ,H. Vergas, N.F.Leite and L.C.M.Miranda, *Phys. Rev. B*, **42**,7 (1990)
11. G.Amato, G.Benedetto, I.Boarino, M.maringelli and R.Spagnolo, *IEE Proc.* **139**,4(1992)
12. D.M.Todorovic, P.M.Nokolic, D.G.Vasiljevic and M.D.Dramicanin, *J.Appl.Phys.*, **76**,7(1994)
13. R.L.Thomas,*Anal.Sci.* **17**,1, (2001)

- 
14. A. Rosencwaig and A. Gersho, *J. Appl. Phys.*, **47**, 64 (1976).
  15. M.J. Adam and G.F. Kirkbright, *Analyst*, **102**, 678 (1977)
  16. J. Baumann and R. Tilgner, *J. Appl. Phys.*, **58**, (1982)
  17. P. Helander, I. Lundstrom and D. McQueen, *J. Appl. Phys.* **52**, 1146 (1981)
  18. G. Busse, *Appl. Phys. Lett.*, **35**, 759 (1979)
  20. A. Mandelis, Y.C. Teng and B.S.H. Royce, *J. Appl. Phys.*, **50**, 7138 (1979)
  21. A. Mandelis, S.B. Peralta, J. Thoen, *J. Appl. Phys.*, **70**, 3 (1991)
  22. J. Bauman and R. Tilgner, *J. Appl. Phys.*, **58**, 5 (1985)
  23. C. Saloma, A.J. de Vera, *Appl. Optics*, **30**, 17 (1991)
  24. T.C. Ma, M. Munidasa, A. Mandelis, *J. Appl. Phys.*, **71**, 12 (1992)
  23. H. Endoh, S. Sugawara, Y. Hiwatashi, T. Hoshimiya; *Jpn. J. Appl. Phys.*, **38**, 3191 (1999)
  24. H. hu, X. Wang, X. Xu, *J. Appl. Phys.*, **86**, 7 (1999)
  25. G.S. Mityurich, V.P. Zeylny and A.N. Serdyukov, -167, pp165, *Photoacoustic and photothermal phenomena* (Springer Verlag), 1991
  26. J. Opsal and A. Rosencwaig, *J. Appl. Phys.*, **53**, 4240 (1982)
  27. E. Ritter, *Optical coatings and thin film techniques, Laser devices and techniques*
  28. Fowles, *Introduction to modern optics.*

## *Chapter 6*

# **Investigations on photobleaching of cresyl violet in polyvinyl alcohol**

### **Abstract**

Bleaching of cresyl violet (CV) in polymer matrix due to irradiation by a laser beam is investigated using photoacoustic technique. The linear dependence of the photoacoustic signal amplitude on the optical absorption coefficient of the sample is made use of in these measurements. Cresyl violet dye doped polyvinyl alcohol (PVA) films are deposited on glass substrates. Investigations are carried out at different dye concentrations, modulation frequencies and incident wavelengths. The photobleaching rate is found to decrease with increase in dye concentration and increase with increase in modulation frequency. In all these cases it is found that photodegradation of CV-PVA film is a slow process. Experimental details and results of the investigations are discussed in this chapter.

## 6.1. Introduction

Development of materials for fast optical switching and high efficiency holographic recording has attracted much attention (1-20). Laser dyes, which form the active media of several kinds of dye lasers, are compounds having a strong absorption generally in the visible and ultraviolet regions of the spectrum and fluorescence emission from the first excited singlet state at Stoke shifted wavelengths. Photo sensitive dye films have been successfully used as write-once-read many (WORM) type optical data storage materials. The suitability of a film for these applications is judged by its non-linear response to optical radiation (1). Because of the increased luminescence quenching resulting from a strong interaction of excited state dye molecules, it is not feasible to use the dye directly as solid-state cast films (2-5). This molecular quenching mechanism leads to suppression of stimulated emission in pure dye films. If the dye molecules are spatially separated by incorporating them as guest molecules in host materials, quenching due to molecular interaction can be minimized (6-9). A non-linear absorber of light has the unique property that its optical absorption can be altered by changes in the intensity of radiation incident upon it. Several different types of organic molecules undergo optical bleaching when subjected to high intensity radiation and are useful as saturable absorbers. Saturable absorbers show a typical nonlinear response for optical absorption and can be employed in a variety of devices like optical bistable elements, optical memory components etc. Cresyl violet (CV) is one of the well-known laser dyes which can be used as a saturable absorber. The phenomenon of saturable absorption is one of the first detected

non-linear optical effects and has been widely used for passive Q switching and mode -locking of lasers (10, 11).

The non-linear optical properties of a dye can be modified by embedding it in solid matrices such as gelatin, polyvinyl alcohol, glasses etc. One of the most promising approaches to optical limiting applications is the development of solid guest-host systems (11-16). Typically the solid host is a transparent polymer or an epoxy compound and the guest is an organic dye. Real time effects of exposure on a number of materials have already been studied (17). It has been shown that dyes like eosin or rose bengal , once incorporated in solid matrices, can be used as optical phase conjugators (18,19). The non-linear response of the dye can either be fast (nano seconds to microseconds) or very slow (milliseconds and sometimes hours). The former type of response is suitable for fast optical switching, while the latter is useful in recording and optical information storage. It has been shown that in dichromated gelatin (DCG) films the real time effects are caused by absorption modulation. Real time bleaching of methylene blue and thionine sensitized gelatin are reported (17). The laser marking of thin organic films by monitoring the reflectance variation as a function of time has also been reported (20).

Apart from the use as active laser media, dye doped polymers find many applications in the modern photonic technology. Even though the photodegradation of the dye is a disadvantage when these materials are used as a laser medium, the dye degradation can be made use of in many other applications such as holographic recording. Suitable materials for different applications can be prepared by proper selection of the type of solid matrix and the dye incorporated

into it. In all these applications a thorough knowledge of the photostability of the dye incorporated in a solid matrix is necessary. Several theoretical models have been developed to explain photobleaching of the dye under pulsed and continuous wave irradiation (21-23). However, these models are generally found to be valid only at low pump powers.

## 6.2. Methods to measure dye photodegradation

The photodegradation of organic dyes in a solid matrix is essentially due to a photo-induced reaction. Since the primary photo-process is absorption of a photon to create a photo-excited molecule, photochemistry and spectroscopy are intimately related. In a quantitative study, therefore, a radiation source of known intensity and wavelength and an appropriate detector are necessary to detect a photochemical reaction or any other photo-induced changes.

A molecule excited to a higher energy state must return to the ground state, unless it undergoes a chemical change. In condensed systems there exist a number of ways for the excited molecules to dissipate the excess energy. Out of these different paths, commonly occurring and most important channels are radiative relaxation (fluorescence and phosphorescence), non-radiative relaxation (usually thermal relaxation) and excited state chemical reaction. (23-27).

In the case of a photo-excited molecule, any of the above mentioned relaxation mechanisms are possible. Irrespective of whether the dye molecules are in a solution form or embedded in a solid matrix, the amount of energy liberated via radiative or non-radiative relaxation mechanisms is determined by the number of original dye molecules in the ground state as well as those in the excited state.

Any kind of a photochemical reaction will result in a change in the number density of the dye molecules. Consequently, the optical absorption as well as the amount of energy liberated through the radiative or non-radiative channels may change. Hence, by measuring either of these quantities or both, one can easily make a quantitative evaluation of the photochemical processes that the sample undergoes. Another way to monitor a photochemical change is the analysis of the resultant products.

Photochemical processes can be induced using continuous wave light source or pulsed optical radiation and the reaction rate can be monitored either by optical methods or by photo-thermal methods. In optical methods the radiative relaxation or optical absorption (or transmission) is investigated whereas in photo-thermal technique, the energy liberated as a result of non-radiative relaxation is measured.

Photo-thermal methods are a group of highly sensitive techniques used to measure optical absorption and thermal characteristics of a sample. The fundamental principle of a photo-chemical method is the photo-induced change in the thermal state of a sample. Sample heating is a direct consequence of optical absorption and hence the photothermal signal depends directly on the quantity of the light absorbed. Scattered and reflected waves do not produce photo-thermal signal. So photo-thermal technique is more sensitive in the measurement of optical absorption in scattering solutions, solids and interfaces.

In photo-chemical processes, generally, intermediate species (radicals) are created and eventually the free radicals will be converted into some other products. Usually these intermediate steps are associated with non-radiative

energy transfer which in turn produce the thermal effects. Hence, photo-thermal methods are more suitable for detecting these fast processes (28-35). They can also be used to detect the photo-chemical changes that occur during a steady state excitation of the molecule. As in the case of thermal and optical characterization of materials, almost all the photo-thermal methods can be employed to investigate the photo-chemical processes. Though many of the photo-thermal methods are used in the photo-chemical study of gases and liquids, they are not widely employed in solid samples such as dye doped polymers. Photo-thermal interferometry, photoacoustics, thermal lens, photo-thermal beam deflection, transient grating etc. are some of the most useful photo-thermal methods that can be used to investigate photo-degradation of organic materials.

### **6.3. Experimental details**

#### **6.3.1. Preparation of the sample**

##### **6.3.1a. Cresyl violet dye**

Laser dyes are organic compounds that relax radiatively after optical excitation, emitting in the visible or infrared region. Cresyl violet is one of the commonly used laser dyes. Cresyl violet (C H N O Cl), technically known as 5,9diaminobenzo[a] phenoxazoniumperchlorate (or oxazine 9 for short) and commonly referred to as LC6700 or CV670 is an efficient emitter at far red wavelengths (36). It is stable under ambient conditions, with minimal power saturation even at peak intensities as high as  $100\text{mW/cm}^2$  (37). It has a molecular weight of 361.74. Cresyl violet has very low fluorescence quantum efficiency so

that the non-radiative relaxation is the major channel by which molecules relax to the ground state (38, 39).

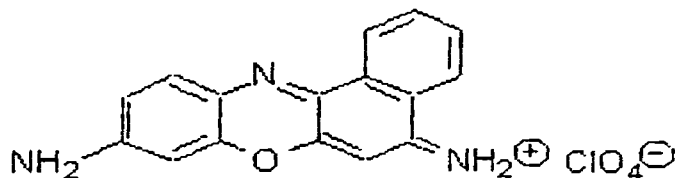


Figure 1 Chemical structure of cresyl violet perchlorate

### 6.31b. Film deposition

Laser dyes have a range of practical applications when rigidized in a polymer host. The basic requirements imposed for laser dye molecules in a polymeric host are its good optical transparency at pump laser wavelengths, good solubility of the dye in the material and resistance to pump laser radiation. Polyvinyl alcohol is employed for a variety of purposes such as adhesives, binders, holographic recording materials etc. Poly vinyl alcohol has been most frequently used as a host medium for laser dyes due to its excellent optical transparency in the visible region and its relatively high laser damage resistance.

---

Polyvinyl alcohol (PVA) (Aldrich make, Molecular weight  $\approx 14,000$ ) is dissolved in hot water to form a viscous solution. Cresyl violet 670 dye – perchlorate (Exciton make, molecular weight = 361.74) is added to the PVA solution and stirred thoroughly to ensure uniform distribution of the dye molecules in the host medium. The dye /PVA mixture is placed drop wise on cleaned microscopic glass slides (spot casting) and are kept at room temperature for one week for drying. Perfect drying is necessary to avoid shrinkage of the sample. Careful examination (including absorption spectrum) of the polymerized samples confirmed that the dye is homogeneously dispersed in the host matrix.

### 6.3.2. Experimental setup used for the photoacoustic study

The experimental setup used for the present investigation is schematically shown in figure 2. The excitation source used is a highly stabilized Argon ion laser (Liconix 5000 series). The continuous wave laser emission from the  $\text{Ar}^+$  laser is intensity modulated using a mechanical chopper (Ithaco HMS 230). The sample in the form of a thin film, deposited on glass substrate, is placed inside the non-resonant photo-acoustic cell. The schematic of the non resonant photo-acoustic cell used for the present investigation is given in figure 3. The same cell as that given in the previous chapter, in its reflection mode geometry, is used to carry out investigations. The modulated light beam is allowed to fall on the sample. A highly sensitive electret microphone (Knowles BT 1834), kept in the microphone chamber of the PA cell, is used to detect the periodic pressure variations generated in the air column in contact with the sample. The microphone

converts these periodic pressure variations into electrical signal. Finally, the PA signal is processed using a digital lock-in amplifier (EG & G 5208). Variation in photoacoustic signal is noted as a function of irradiation time. Influence of the excitation light intensity on the rate of dye photodegradation is studied at 30mW, 40 mW and 50mW. Influences of dye concentration and modulation frequency on photo-bleaching rate are also studied.

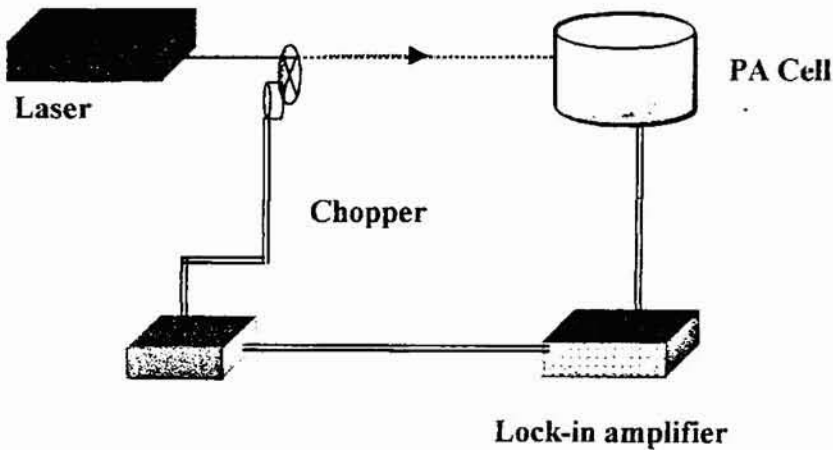


Figure 2. Schematic diagram of the experimental setup for photo-degradation studies

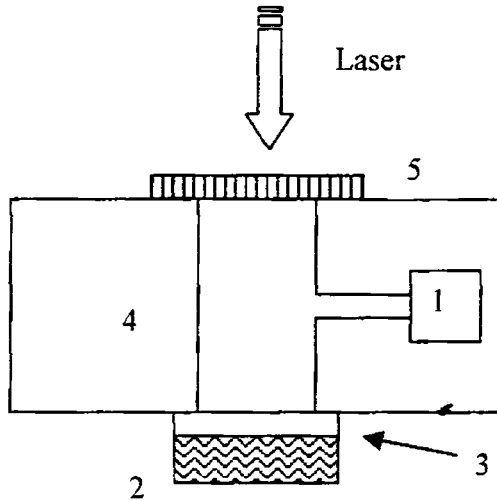


Figure3. Schematic of the non-resonant photo-acoustic cell

1.Microphone 2.Glass substrate 3.Sample 4.Acrylic body 5.Glass window

## 6.4. Results and discussion

The process of photoacoustic signal generation in condensed media has already been experimentally established and a satisfactory theoretical explanation has been given by Rosencwaig and Gersho. The complex amplitude of the PA signal produced is given by the relation (40),

$$Q = \frac{-i\beta\mu^2\gamma P_0 I_0}{4\sqrt{2T_0} l_g a_g k}$$

where  $\beta$  is the optical absorption coefficient of the sample,  $\mu$  is the thermal diffusion length in the medium,  $\gamma$  is the ratio of specific heat capacities for air,  $P_0$  and  $T_0$  are the ambient pressure and temperature respectively.  $I_0$  is the intensity of incident light,  $l_g$  and  $a_g$  are the length of the air column inside the cavity and the thermal diffusion length in the air respectively and  $k$  is the thermal conductivity of the sample. Hence, by any means, if the absorption coefficient value changes, then the PA signal amplitude will also vary accordingly. Any kind of photochemical reaction will result in a change in the number density or concentration of the original species and this, in turn, will result in a change in the optical absorption properties of the sample. Doping of an organic dye in a solid matrix will not alter the thermal properties of the host (12). So when a dye doped polymer is investigated using photoacoustic technique, any change in the PA signal amplitude is essentially a measure of the photo-decomposition of the dye.

The present studies show a decrease in PA signal amplitude with irradiation time. In other words, increase in exposure (light intensity x irradiation time) causes decrease in optical absorption of the sample, essentially due to photo-decomposition of the dye molecule (photo-bleaching). It takes more than two hours to complete the saturation effect indicating that the bleaching effect is a slow process. The photo-degradation of the molecules causes the violet coloured samples to turn colourless. Transmission measurements and PA measurements of the bleached area of the sample does not show any appreciable variation even after one month. The fact that the bleaching effect is a slow process, as far as CV

in PVA is considered, indicates the suitability of CV-PVA film as a holographic recording medium.

The effect of laser power on photo-bleaching rate of the dye molecules is investigated at three different pump powers. The variation of PA signal amplitude as a function of time for different pump powers is shown in figure (4). From this it is clear that degradation is fast during the initial stages followed by saturation. This indicates a decrease in absorption coefficient at the irradiation wavelength. The saturation in the PA signal corresponds to the complete photo-degradation of the dye molecules from their original state. The optical absorption spectrum of the sample (Figure (5)) also shows decrease in absorbance with increase in exposure. It is also observed that dye degradation rate increases with increase in pump power. For high pump powers, faster bleaching and hence saturation of PA signal is observed within shorter irradiation time.

The variation of photobleaching with concentration of the dye molecules is studied at three different concentration values viz. 0.5mM/litre, 1mM/litre and 2mM/litre. In all these measurements, the laser power is fixed at 40mW and the wavelength used is 488nm. The observed PA signal variation with time for different concentration values is shown in figure (6). It can be seen that there is a considerable increase in the photobleaching rate with decrease in dye concentration. As the dye concentration is increased, the number of available absorption centres also increases. So higher incident powers are necessary to obtain faster bleaching. The experimental result that the bleaching rate decreases with increase in concentration for the same pump power, also establishes this conclusion.

The dependence of photodegradation rate on modulation frequency is also studied. The observed PA signal variation with time for different modulation frequencies is shown in figure (7). It is observed that the bleaching rate changes with increase in chopping frequency. For higher modulation frequencies the bleaching is so fast that saturation is attained within a few seconds. For low chopping frequencies, quantity of energy falling on the sample per second is small, resulting in low absorption rate and slow degradation. Thus by adjusting the modulation frequency, rate of photo-degradation can be adjusted.

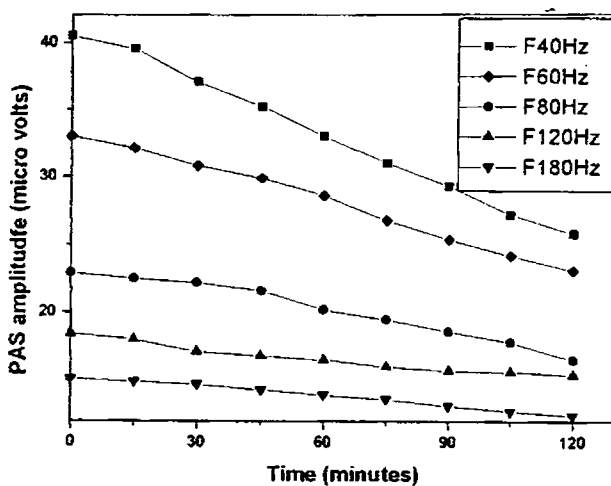


Figure 7 PA signal versus irradiation time plot for different modulation frequencies ( $\lambda = 488\text{nm}$ , concentration of the dye =  $1\text{mM}$ )

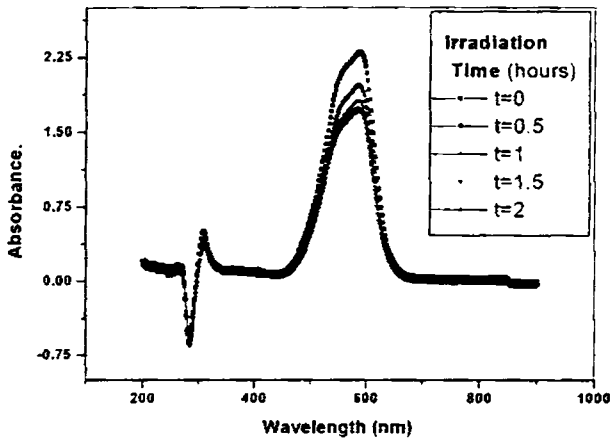


Figure 5. Absorption spectrum of the CV-PVA sample before and after exposure.

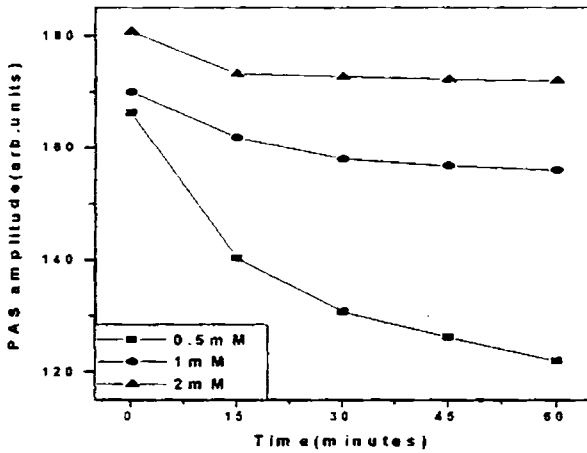


Figure 6 PA signal amplitude versus irradiation time plot for different dye concentrations ( $\lambda = 488\text{nm}$ , modulation frequency = 40Hz)

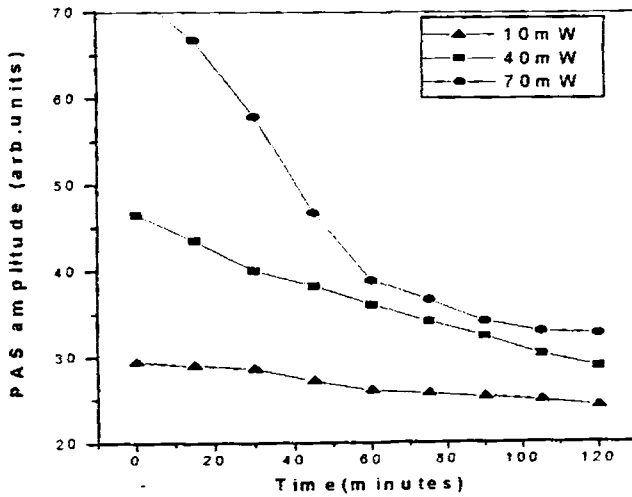


Figure 4. PA signal versus time graph for three pump powers

( $\lambda=488\text{nm}$ , chopping frequency = 40Hz)

## 6.5. Conclusions

The photoacoustic technique has been successfully made use of in the investigation of photo-stability of organic dye doped polymer films. The fact that the bleaching effect is a slow process in the case of CV – PVA films indicates the suitability of the medium as a low cost holographic recording medium. The speed of recording can be adjusted by changing the pump power. For a fixed pump power, recording rate can be further adjusted by changing the modulation frequency. By increasing the pump power, exposure time can be reduced. It is

observed that the rate of bleaching is directly proportional to the incident laser power and it decreases with increase in dye concentration.

Increase in dye concentration increases the optical density of the sample. The present study shows that by increasing the optical density of the sample, one can decrease the photodegradation rate.

Even though a large number of studies have been reported in the field of dye doped polymers, the exact mechanism responsible for photo-degradation of laser dyes in polymers is not yet fully understood.

## References.

1. O.V. Przhonska, J.H. Lim, D.J. Hagan and E.W. Van Stryland, *J.Opt.Soc.Am.B*, **15**, 2 (1998)
2. F.J. Duarte and L.W. Hillman, *Dye laser principles*, (Academic press, New York) (1990)
3. M. Maeda, *Laser dyes*, (Academic press, New York) (1984)
4. F.P. Schafer (edit.), *Dye lasers*, (Springer, Berlin) (1977)
5. M.W. Sigrist, *Laser* (1995)
6. B.H. Soffer and B.B. McFarland, *Appl.Phys.Lett.* **10**, 266 (1967)
7. O.G. Peterson and B.B. Snively, *Appl.Phys.Lett.* **12**, 238 (1968)
8. G. Kranzelbinder and G. Leising, *Rep.Prog.Phys.*, **63**, 729 (2000)
9. M. Rodriguez, A. Costela, I.G. Moreno, F. Florido, J.M. Figuera and R. Sastre, *Meas. Sci. Technol.*, **6**, 971 (1995)
10. J.A. Fleck, *Phys.Rev.B*, **1**, 84 (1970)

11. A. Kost, L. Tutt, M.B. Klein, T.K. Dougherty and W.E Elias, *Opt. Lett.* **18**, 334 (1993)
12. G.S.He, J.D. Bhawalker, C. F. Zhao and P.N.Prasad, *Appl.Phys. Lett.*, **67**, 2433-2435 (1995)
13. K.Mansour, P.Fuqua, S.R.Marder, B.Dunn and J.W.Perry, *Proc. SPIE*, **2143**, 239 (1994).
- 14.M.Brunel, M.Canva, A. Brun, F.Chaput and J.P. Boilet, *OSA Technical Digest*, **9**, 278, (1996)
15. O.V. Przhonska, M.V. Bondar and Y.A. Tikhonov, *Proc. SPIE*, **2143**, 289, (1994)
16. J.W. Perry, K. Mansour, Y.S. Lee et.al, *Science*, **273**, 1533-(1996)
17. K.P.B. Moosad, T.M.A. Rasheed and V.P.N. Nampoori, *Appl. Optics*, **29**, 449 (1990).
18. Capolla, R.A. Lessard, *Appl. Optics*, **30**, 1196 (1991)
19. K.P.B. Moosad, T.M.A. Rasheed and V.P.N. Nampoori, *Optical Engg.*, **29**, 47 (1990).
20. B.J. Bartholomeuz, M.C.Gupta, *Appl.Optics*, **31**, 4829 (1992).
21. K.M.Dyumaev, A.A.manenkov, A.P. Maslyukov, G.A.Matshin , V.S. Nechitailo and A.M. Prokhorov, *J.Opt.Soc.Am.B*, **9**,143 (1992)
- 22 J.C. Newell, L.Solymar and A.A. Ward, *Appl.Opt.*,**24**,4460 (1985)
23. D.S. Kilger, *Ultrasensitive laser spectroscopy*,( Academic press, New York) (1983).
24. K.K.R. Mukherjee, *Fundamentals of photochemistry*, New Age International Publishers, New delhi (1978).

25. J.D.Winefordner (edit.) *Chemical analysis ; A series of monographs on analytical chemistry and its applications*, (John Wiley & Sons, Inc.) (1996).
26. G.M.Hieftje, J.C.Travis and F.E.Lytle (Eds), *Lasers in chemical analysis* (Humana: Clifton, New Jersey) (1981).
27. W.West (edit.) *Chemical applications of spectroscopy, Vol.IX, Part 1* (John Wiley & Sons, New York) (1968).
28. K.Okamoto, N.Hirota, M.J.Terazima, *J.Chem.Soc.Farad.Trans.*, **94**, 185 (1998).
29. J.D.Simon and K.S.peters, *J.Am.Che.Soc.*, **105**, 5156 (1983).
30. K.Okamoto, N.Hirota, M.J.Terazima, *J.Phys. Chem.A*, **102**, 3447 (1998).
31. S. Yamaguchi, N.Hirota, M.J.Terazima, *Chem.Phys. Lett.*, **286**, 284 (1998).
32. H.Ooe, Y.Kimura, N.Hirota, M.J.Terzima, *J.Phys. Chem.A*, **103**, 7730 (1999).
33. D.Neckers, D.H. Volman, G.Bunau(eds), *Advances in photochemistry* (John Wiley, New York) (1998).
34. M.Terazima, *J.Chem.Phys.*, **110**, 7401 (1999).
35. T.Okazaki, N.Hirota, M.J.Terazima, *J.Chem.Phys.*, **110**, 11399 (1999)
36. A.T. Filho, N.F. Lete, L.C.M. Miranda and R.A. Stempniak, *J.Appl.Phys.*, **66**, 407 (1989)
37. F. Castelli, *Appl.Phys.lett.*, **26**, 18 (1975)
38. D. Magde et al., *J.Physical Chemistry*, **83**, 696 (1979).
39. C.A.Moore and C.D. Decker, *J.Appl.Phys.*, **49**, 47 (1978).
40. A.Rosencwaig and A. Gersho, *J. Appl. Phys.*, **47**, 64 (1976).

## *Chapter 7*

### **Summary and conclusions**

#### **Abstract**

A summary of the work presented in this thesis is given in this chapter. General conclusions arrived at and the future scope of experiments in this field are presented.

The photoacoustic investigations carried out on different photonic materials are presented in this thesis. Photonic materials selected for the investigation are tape cast ceramics, multilayer dielectric coatings, organic dye doped PVA films and PMMA matrix doped with dye mixtures. The studies are performed by the measurement of photoacoustic signal generated as a result of modulated cw laser irradiation of samples. The gas-microphone scheme is employed for the detection of photoacoustic signal. The different measurements reported here reveal the adaptability and utility of the PA technique for the characterization of photonic materials.

Ceramics find applications in the field of microelectronics industry. Tape cast ceramics are the building blocks of many electronic components and certain ceramic tapes are used as thermal barriers. The thermal parameters of these tapes will not be the same as that of thin films of the same materials. Parameters are influenced by the presence of foreign bodies in the matrix and the sample preparation technique. Measurements are done on ceramic tapes of Zirconia, Zirconia-Alumina combination, barium titanate, barium tin titanate, silicon carbide, lead zirconate titanate (PZT) and lead magnesium niobate titanate (PMNPT). Various configurations viz. heat reflection geometry and heat transmission geometry of the photoacoustic technique have been used for the evaluation of different thermal parameters of the sample. Heat reflection geometry of the PA cell has been used for the evaluation of thermal effusivity and heat transmission geometry has been made use of in the evaluation of thermal diffusivity. From the thermal diffusivity and thermal effusivity values, thermal conductivity is also calculated. The calculated values are nearly the same as the values reported

---

for pure materials. This shows the feasibility of photoacoustic technique for the thermal characterization of ceramic tapes.

Organic dyes find applications as holographic recording medium and as active media for laser operations. Knowledge of the photochemical stability of the material is essential if it has to be used for any of these applications. Mixing one dye with another can change the properties of the resulting system. Through careful mixing of the dyes in appropriate proportions and incorporating them in polymer matrices, media of required stability can be prepared. Investigations are carried out on Rhodamine 6G-Rhodamine B mixture doped PMMA samples. Addition of RhB in small amounts is found to stabilize Rh6G against photodegradation and addition of Rh6G into RhB increases the photosensitivity of the latter. The PA technique has been successfully employed for the monitoring of dye mixture doped PMMA sample. The same technique has been used for the monitoring of photodegradation of a laser dye, cresyl violet doped polyvinyl alcohol also.

Another important application of photoacoustic technique is in non-destructive evaluation of layered samples. Depth profiling capability of PA technique has been used for the non-destructive testing of multilayer dielectric films, which are highly reflecting in the wavelength range selected for investigations. Eventhough calculation of thickness of the film is not possible, number of layers present in the system can be found out using PA technique. The phase plot has clear step like discontinuities, the number of which coincides with the number of layers present in the multilayer stack. This shows the sensitivity of PA signal phase to boundaries in a layered structure. This aspect of PA signal can be utilized in non-destructive depth

---

profiling of reflecting samples and for the identification of defects in layered structures.

In general, the versatility and utility of photoacoustic technique for the evaluation of thermal and physical properties of certain photonic materials like ceramic tapes, dye doped polymer samples and multilayer reflecting coatings, has been experimentally demonstrated.

Scope for future studies:

There are different areas where further investigations can be carried out.

Some of them are:

1. The effect of electric field on the thermal parameters of ceramic tapes has not been investigated. As these materials are used in the preparation of microelectronic components, knowledge of the electric field effect will be an added advantage.
2. The theory of photoacoustic signal generation in dielectric multilayer coatings has not been developed.
3. Development of dye doped polymer matrices is an active area where investigations can still be carried out.

